PUCRS

FACULDADE BIOCIÊNCIAS
PROGRAMA DE PÓS-GRADUAÇÃO EM BIOLOGIA CELULAR E MOLECULAR
DOUTORADO EM BIOLOGIA CELULAR E MOLECULAR

FERNANDA CRISTINA DE MESQUITA

EFEITO DA LIRAGLUTIDA SOBRE A FIBROSE HEPÁTICA E CÉLULAS ESTRELADAS ATIVADAS

Porto Alegre
2017

PÓS-GRADUAÇÃO - *STRICTO SENSU*

Pontifícia Universidade Católica
do Rio Grande do Sul

PONTIFÍCIA UNIVERSIDADE CATÓLICA DO RIO GRANDE DO SUL
FACULDADE DE BIOCIÊNCIAS
PROGRAMA DE PÓS-GRADUAÇÃO EM BIOLOGIA CELULAR E MOLECULAR
DOUTORADO EM BIOLOGIA CELULAR E MOLECULAR

EFEITO DA LIRAGLUTIDA SOBRE A FIBROSE HEPÁTICA E CÉLULAS ESTRELADAS ATIVADAS

Tese apresentada ao Programa de Pós-Graduação em Biologia Celular e Molecular da Pontifícia Universidade Católica do Rio Grande do Sul como requisito parcial para a obtenção do grau de Doutora em Biologia Celular e Molecular.

FERNANDA CRISTINA DE MESQUITA

ORIENTADOR: Prof. Dr. Jarbas Rodrigues de Oliveira

Porto Alegre
2017

Ficha Catalográfica

M582e Mesquita, Fernanda Cristina de

Efeito da liraglutida sobre a fibrose hepática e células estreladas ativadas / Fernanda Cristina de Mesquita . – 2017.
88 f.
Tese (Doutorado) – Programa de Pós-Graduação em Biologia Celular e Molecular, PUCRS.

Orientador: Prof. Dr. Jarbas Rodrigues de Oliveira.

1. Cirrose. 2. Hipertensão portal. 3. Células hepáticas estreladas. 4. Liraglutida. 5. GLP-1. I. Oliveira, Jarbas Rodrigues de. II. Título.

Elaborada pelo Sistema de Geração Automática de Ficha Catalográfica da PUCRS com os dados fornecidos pelo(a) autor(a).

“THE MIND THAT OPENS UP TO A NEW IDEA NEVER RETURNS TO ITS ORIGINAL SIZE.” – ALBERT EINSTEIN

Dedico à minha mãe, que dividiu comigo as vitórias e obstáculos desta jornada.

AGRADECIMENTOS

Durante o doutorado percebi o quão importante são as relações pessoais e o quanto cada pessoa ao nosso redor contribui para o andamento da nossa vida profissional e claro, pessoal. Este trabalho só foi possível pelo esforço de muitas pessoas que me auxiliaram durante esses quatro anos. Ele vem de importantes contribuições que recebi durante este período e que foram fundamentais para essa construção.

Primeiramente, gostaria de agradecer a todos do Laboratório de Biofísica. Ao Professor Jarbas Rodrigues de Oliveira, obrigada por ser meu orientador durante 9 anos, desde a iniciação cientifica até o doutorado, pelo incentivo e pelos momentos de sabedoria. Agradeço também aos amigos, Leonardo, Eduardo e Gabriela por todos os momentos de ajuda e apoio. E muito obrigada a todos os colegas do laboratório que foram fundamentais durante essa jornada, pelo companheirismo e por tornarem o ambiente de trabalho tão alegre e descontraído.

Agradeço também aos meus orientadores espanhóis, Dr. Jordi Gracia-Sancho, Dr. Jaume Bosch e Dr. Jose Luis Rosa que me receberam na Espanha durante um ano e foram incansáveis na realização e finalização deste trabalho. Agradeço aos colegas Sergi e Anabel pelo esforço para que eu terminasse o trabalho e também aos amigos Taiane e Mónica pelo apoio.

Um agradecimento ao Programa de Pós-Graduação em Biologia Celular e Molecular e à CAPES pela bolsa de estudos no Brasil e na Espanha que possibilitou a realização deste trabalho e um crescimento profissional incrível.

Por fim, agradeço à minha mãe Leni, ao meu namorado Paulo e a todos os meus amigos que compartilharam minhas tristezas e sorrisos sempre dispostos a ajudar.

A todos vocês, que contribuíram para a realização de mais esta etapa, meu sincero agradecimento. Muito obrigada!

RESUMO

A fibrose hepática é a resposta cicatricial do fígado à lesões repetidas. Este processo inicia com o dano das células parenquimatosas e consecutiva inflamação, caracterizado pelo rompimento da arquitetura hepática associada ao aumento da expressão dos componentes da matriz extracelular. O desenvolvimento da fibrose hepática é baseado na ativação das células hepáticas estreladas (HSC) que sofrem mudanças fenotípicas e se caracterizam pela perda do depósito de vitamina A e aumento da proliferação celular, desencadeando disfunção microcirculatória hepática e fibrogênese nos pacientes com doença hepática crônica (CLD). A liraglutida é um análago do GLP-1 (glucagon-like peptide 1) bem estabelecido como fármaco antidiabético, mas que também possui propriedades antinflamatórias, além da efetividade para NAFLD (doença hepática gordurosa não alcoólica). Por essa razão, o objetivo deste estudo foi avaliar os efeitos da liraglutida sobre o fenótipo das HSC e a função microvascular hepática utilizando diversos modelos pré-clínicos de CLD. Os resultados obtidos demonstram que a liraglutida desativou o fenótipo das HSC humanas e de ratos através de um mecanismo independente do receptor GLP1. A liraglutida não afetou a viabilidade das HSC mas diminuiu a proliferação celular. Os ratos com CLD que receberam liraglutida apresentaram pressão portal significativamente menor (-20%) com consequente redução da resistência vascular intra-hepática. Houve também uma acentuada melhoria na função vascular hepática, fibrose, fenótipo das HSC e fenótipo endotelial sinusoidal. Os efeitos anti-fibróticos da liraglutida também foram confirmados em tecido hepático humano. Como conclusão, este estudo demonstra pela primeira vez que a liraglutida melhora o endotelio sinusoidal hepático em modelos experimentais clinicamente relevantes de cirrose, o que leva a melhora no quadro fibrótico e na hipertensão portal e, portanto, pode ser válido no tratamento da doença hepática crônica avançada.

Palavras-chave: cirrose, hipertensão portal, HSC, LSEC, GLP-1R, Liraglutida.

ABSTRACT

Liver fibrosis is the wound healing response to repeated injury of the liver. This process begins with the damage of the parenchymal cells and subsequent inflammation, characterized by the rupture of the hepatic architecture associated to the increase of the expression of the components of the extracellular matrix. The development of hepatic fibrosis is based on the activation of hepatic stellate cells (HSC) that undergo phenotypic changes and are characterized by loss of vitamin A deposition and increased cell proliferation, triggering hepatic microcirculatory dysfunction and fibrogenesis in patients with chronic liver disease (CLD). Liraglutide is a GLP-1 agonist (glucagon-like peptide 1) well established as an antidiabetic drug, but also has anti-inflammatory properties, in addition to the effectiveness for NAFLD (non-alcoholic fatty liver disease). Therefore, the aim of this study was to evaluate the effects of liraglutide on the HSC phenotype and liver microvascular function using diverse pre-clinical models of CLD. The results obtained demonstrate that Liraglutide de-activated human and rat HSC phenotype through a GLP1-Rindependent mechanism. Liraglutide did not affect the HSC viability but decreased cell proliferation. CLD-rats receiving liraglutide exhibited significantly lower portal pressure (-20%) with a consequent reduction in intrahepatic vascular resistance. There was also a marked improvements in hepatic vascular function, fibrosis, HSC phenotype and sinusoidal endothelial phenotype. The anti-fibrotic effects of liraglutide were confirmed in human liver tissue. In conclusion, this study demonstrates for the first time that liraglutide improves hepatic sinusoidal endothelium in clinically relevant experimental models of cirrhosis, which leads to improvement in fibrosis and portal hypertension, and therefore is valid in the treatment of advanced chronic liver disease.

Keywords: cirrhosis, portal hypertension, HSC, LSEC, GLP-1R, Liraglutide.

LISTA DE FIGURAS

CAPÍTULO I

CAPÍTULO III

LISTA DE ABREVIATURAS

ANVISA - Agência Nacional de Vigilância Sanitária

cAMP - Monofosfato cíclico de adenosina

CLD – *Chronic Liver Disease* / Doença Crônica do Fígado

DM2 – Diabetes Mellitus 2

DPP-IV – Dipeptidil peptidase IV

EMA - Agência Europeia de Medicamentos

ERO – Espécies Reativas de Oxigênio

FDA - *Food and Drug Administration*/ Administração de Comidas e Remédios

GLP-1 – *Glucagon-like peptide 1* / Peptídeo semelhante a glucagon 1

GLP-1R – Receptor do GLP-1

HBV – Vírus da hepatite B

HCV – Vírus da hepatite C

HSC – Célula estrelada hepática

IL1 – Interleucina 1

KC – Células de Kupffer

LPS - Lipopolissacarídeo

LSEC – Células endoteliais sinusoidais hepáticas

MEC – Matriz extracelular

NAFLD - Doença gordurosa hepática não-alcoólica

NF-κB – Fator nuclear kappa B

NO – Oxido nítrico

PDGFβR - Fator de crescimento derivado de plaquetas

PHA - Fitohemaglutinina

TGF-β – Fator de transformação do crescimento beta

TNF-α – Fator de necrose tumoral alfa

α-SMA - Actina do músculo liso alfa

SUMÁRIO

CAPÍTULO I

APRESENTAÇÃO

1. Introdução

1.1 Doença hepática crônica

A fibrose hepática é uma resposta cicatricial que ocorre em quase todos os pacientes com lesão crônica do fígado (1, 2). Este processo inicia com o dano das células parenquimatosas e consecutiva inflamação (3) e é caracterizado pela produção e deposição excessiva de matriz extracelular (MEC), principalmente colágeno tipo I (4).

Na maioria dos casos, a fibrose hepática acumula-se durante décadas, proveniente de uma lesão crônica (5), que é geralmente decorrente de infecção por vírus da hepatite C (HCV) ou hepatite B (HBV), abuso de álcool, obesidade e esteato-hepatite não alcoólica (4, 6). O prolongamento natural dessa resposta, em contraste com a progressão mais rápida da fibrose nos rins ou pulmões, é creditado à capacidade excepcional do fígado de regeneração, pois se sabe que deve haver uma redução de 80 a 90% da capacidade funcional do fígado para que ocorra falência hepática, tamanha a reserva funcional desse órgão (2, 7).

A cirrose hepática é considerada um estágio avançado de fibrose, constituindo-se em um dos maiores problemas de saúde mundial (2) e compreende todas as complicações da doença hepática no estágio final, que inclui hipertensão portal, ascite, encefalopatia e alterações no metabolismo, principalmente de lipídeos e da glicose (8). O maior determinante da cirrose hepática é a dificuldade em degradar a matriz fibrótica, o que provoca destruição da arquitetura do fígado, interrupção das funções hepáticas, acarretando em disfunção (2, 9-11).

1.2 Células hepáticas estreladas

As células hepáticas estreladas (HSC, do inglês, *Hepatic Stellate Cells*) são também chamadas de lipócitos, células armazenadoras de gordura, células armazenadoras de vitamina A, células intersticiais ou células de Ito (11, 12). Foram descobertas por Kupffer em 1876 e caracterizadas quase um século depois por Ito e Nemoto como células armazenadoras de gordura (13).

Estas células estão localizadas no espaço perissinusoidal de Disse. Classicamente este espaço define-se como uma zona limitada pelos hepatócitos e pela parede sinusoidal formada pelas células endoteliais sinusoidais (2, 12, 13). O espaço perisinusoidal de Disse contém fibras nervosas e componentes da MEC como fibras de colágeno dos tipos I e III e componentes da membrana basal (14).

As HSC constituem 5-8% do número total de células hepáticas considerando as parenquimatosas (hepatócitos), endoteliais (sinusoidais e vasculares), células de Kupffer (macrófagos hepáticos) e as células epiteliais da via biliar. As HSC manifestam dois fenótipos distintos: miofibroblástico (quando estão ativadas) e lipocítico (quando estão quiescentes), como demonstrado na figura 1. Quando expressam o fenótipo miofibroblástico estão essencialmente envolvidas com a produção da matriz extracelular (MEC) e controle da homeostasia do tecido conectivo hepático. O aumento do número e ativação dos miofibroblastos hepáticos está associado com fibrose e cirrose (14).

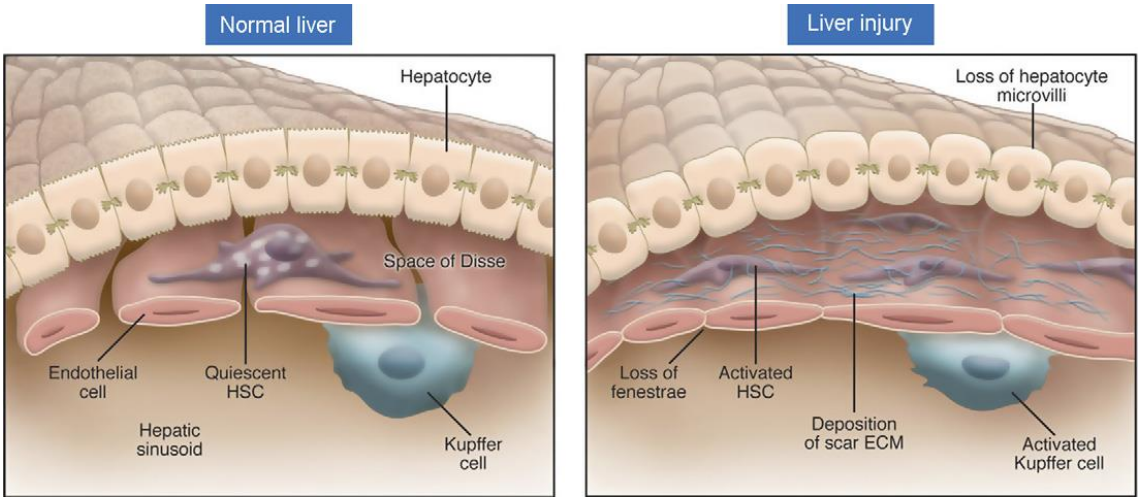

Figura 1 - Papel das células residentes do fígado na lesão hepática. As mudanças no espaço perisinusoidal de Disse durante o desenvolvimento da fibrose em resposta a alguma lesão no fígado incluem alterações tanto no comportamento celular quanto na composição da MEC. A ativação das HSC leva a síntese de colágeno e consequentemente a deposição de matriz fibrótica precedendo a falência hepática. A ativação das células de Kupffer tem ação parácrina sobre as HSC (10).

Expressando o fenótipo lipocítico, seu citoplasma se caracteriza por conter gotículas de gordura onde está a vitamina A (retinol) (2, 11, 12). Mais de 90% da vitamina A hepática (aproximadamente 80% do total do organismo) é captada, armazenada e metabolizada nas HSC, que podem ser identificadas pela autofluorescência desta vitamina (2, 13).

Em condições normais as HSC cumprem várias funções no fígado, entre elas as mais importantes são: armazenamento da vitamina A, controle da comunicação intercelular através da liberação de mediadores e remodelamento da MEC (13).

Além disso, alguns estudos relatam que as HSC têm um papel crucial no sistema imune hepático. Elas expressam receptores para os lipopolissacarídeos bacterianos (*Toll-like receptor 4* – TLR4), moléculas co-estimulatórias e citocinas necessárias para a modulação da resposta imune além de atuarem como células apresentadoras de antígenos (APCs) (13).

O desenvolvimento de fibrose hepática é baseado na ativação das HSC que sofrem mudanças fenotípicas características. Essa ativação é um processo patológico que se caracteriza pela perda das gotículas de gordura onde a vitamina A é armazenada, pelo aumento do número e tamanho celulares e pela diferenciação das HSC em células proliferativas, fibrogênicas, contráteis, muito similares aos miofibroblastos (2, 11).

A ativação das HSC consiste em duas subfases: iniciação e perpetuação, seguidas pela fase final chamada resolução, conforme pode ser observado na figura 2. A primeira fase está associada ao estímulo parácrino de células inflamatórias e hepatócitos lesados. As células de Kupffer podem estimular a proliferação, síntese de matriz, e perda dos retinóides pelas HSCs através da ação de citocinas como fator de transformação do crescimento β (TGF-β) e fator de necrose tumoral α (TNF-α) (15). A perpetuação resulta dos efeitos desses estímulos que mantêm o fenótipo ativado principalmente através do aumento da expressão de fatores de crescimento. Essa fase de ativação envolve no mínimo sete mudanças no comportamento celular: proliferação, quimiotaxia, fibrogênese, contratilidade, degradação da matriz, perda de lipídios e liberação de citocinas. Durante essa fase há liberação de estimulos pró-inflamatórios, pró-fibrogênicos e pró-mitogênicos que agem de forma autócrina e

parácrina, além do remodelamento acelerado da MEC (16). O marcador mais confiável dessa ativação é α-SMA (*alpha smooth muscle actin*), porque está ausente na forma lipocítica destas células e em outras células residentes no fígado. A proteína α-SMA é uma das seis isoformas de actina expressas em tecidos de mamíferos. A sua presença é típica de células de músculo liso vascular e miofibroblastos (17). Na resolução, as HSC podem sofrer apoptose, senescência ou podem também voltar a exibir um fenótipo quiescente, o que seria benéfico para o tecido hepático (13).

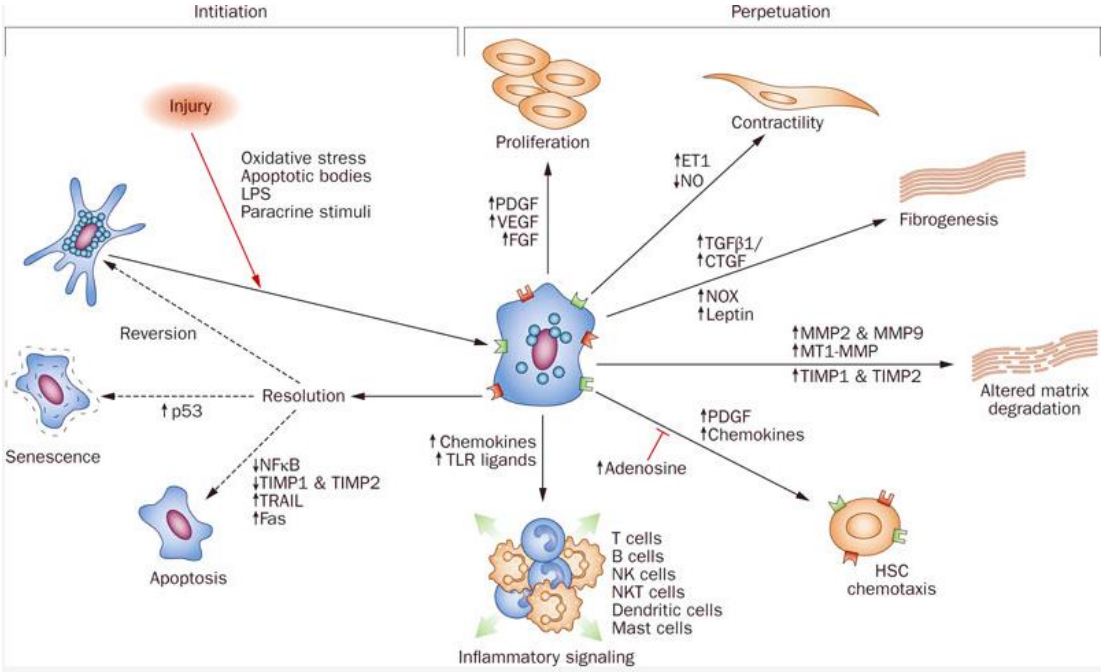

Figura 2 - Vias de ativação das HSC. As características da ativação de células estreladas podem ser distinguidas entre aquelas que estimulam a iniciação e aquelas que contribuem para a perpetuação. A iniciação é provocada por estímulos que incluem espécies reativas de oxigenio, substâncias apoptóticas, lipopolissacarídeos (LPS) e os estímulos parácrinos de células vizinhas, que incluem macrófagos e hepatócitos. A perpetuação que se segue é caracterizada por várias mudanças fenotípicas como proliferação, contratilidade, fibrogênese, alteração na degradação da matriz, quimiotaxia e sinalização inflamatória (2).

Além da ativação das HSC, atualmente tem ganho destaque o conceito de *crosstalk* celular, que se aplica ao endotélio hepático. O *crosstalk* é um processo pelo qual uma mensagem é transmitida dentro de uma célula individual (*crosstalk* intracelular) ou entre células diferentes (*crosstalk* intercelular) (18). O *crosstalk*

intercelular no microambiente do fígado é crítico para a manutenção das funções hepáticas normais e para que as células sobrevivam (19).

Alterações no *crosstalk* hepático normal causam disfunção microvascular progressiva no fígado cirrótico, aumento da resistência vascular hepática e favorece o desenvolvimento de cirrose e hipertensão portal. Todas as células sinusoidais fazem parte deste processo: elas se comunicam e adquirem um fenótipo vasoconstritor que é exacerbado em resposta a danos biomecânicos, patogênicos e infamatórios (18).

A reação fibrogênica é iniciada por duas principais vias de crosstalk intercelulares que são finalmente conectadas. Na presença de lesão hepática, as LSEC (*liver sinusoidal endothelial cells*) tornam-se rapidamente desreguladas e iniciam a diferenciação para um fenótipo capilarizado. Isto é acompanhado pela produção e liberação de fatores solúveis que vão rapidamente para células vizinhas afetando seu fenótipo (19) (figura 3). Paralelamente, a lesão hepática exógena modifica significativamente os programas transcricionais dos hepatócitos promovendo a sua proliferação e morte. A apoptose dos hepatócitos resulta na formação de corpos apoptóticos que, uma vez capturados pelas células não-parenquimatosas (HSC e KC), contribuem para a sua ativação (20-22). As HSC, por sua vez, começam a proliferar, contrair e depositar quantidades elevadas de fibras de colágeno e moléculas de matriz extracelular no parênquima hepático, contribuindo para o endurecimento do órgão , afetando todas as funções celulares. Curiosamente, a acumulação de colágeno no espaço de Disse pode contribuir para a perda de fenestras endoteliais, agravando a fibrose hepática (23). Assim, um ciclo de auto-perpetuação entre HSC ativada produtor de colágeno e LSEC capilarizada estimulam-se mutuamente, contribuindo ainda mais para a fibrose hepática.

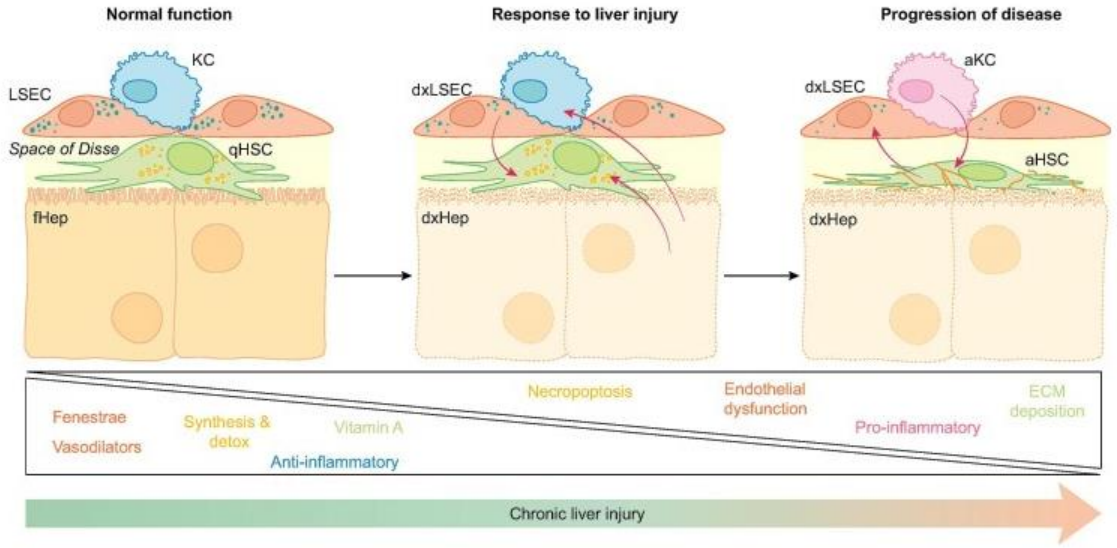

Figura 3 – Cross-talk sinusoidal durante a lesão hepática crônica. Devido a lesões hepáticas, a desregulação inicial em hepatócitos funcionais (fHep) e células endoteliais sinusoidais hepáticas (LSEC) iniciam interações complexas parácrinas (setas vermelhas) com células quiescentes estreladas hepáticas (qHSC) e células Kupffer (KC), criando um microenvolvimento sinusoidal disfuncional composto por LSEC disfuncionais (dxLSEC), HSC ativadas (aHSC), KC ativadas (aKC) e hepatócitos disfuncionais e necroptóticos (dxHep). As características fenotípicas de cada tipo de célula são progressivamente perdidas durante a progressão da doença hepática, e novas propriedades patológicas aparecem (18).

1.3 Hipertensão portal, cirrose e HSC

A hipertensão portal é uma grave consequência da cirrose hepática e resulta em complicações com elevada morbidade e mortalidade. De acordo com a lei de Ohm ($\Delta P = Q \times R$), a pressão venosa portal é proporcional ao fluxo sanguíneo e à resistência, onde ΔP é a mudança na pressão portal ao longo do vaso, Q é o fluxo sanguíneo portal e R é a resistência ao fluxo (24). No fígado normal, a resistência intra-hepática varia de acordo com mudanças no fluxo sanguíneo portal, mantendo assim a pressão portal dentro dos limites normais. No entanto, na cirrose, a resistência intra-hepática e o fluxo sanguíneo aumentam. A hipertensão portal é, portanto, a consequência de uma combinação de diminuição da complacência e aumento do fluxo sanguíneo portal (25).

O evento inicial na fisiopatologia da hipertensão portal é o aumento da resistência vascular ao fluxo portal, causado principalmente por alterações estruturais como tecido cicatricial fibrótico e nódulos regenerativos que comprimem as vênulas portal e central. Além disso, tem sido demonstrado que o inchaço dos hepatócitos e a capilarização dos sinusóides hepáticos (perda de fenestrações endoteliais e deposição de colágeno no espaço de Disse) fazem parte do aumento da resistência vascular. Vários aspectos estruturais e fisiológicos das HSC são semelhantes aos pericitos de outros órgãos, sugerindo que as HSC podem funcionar como pericitos específicos do fígado (26). De fato, tanto a localização anatômica das HSC como a capacidade de contrair ou relaxar em resposta a vários mediadores vasoativos sugerem que estas células possam desempenhar um papel na modulação da resistência vascular intra-hepática e do fluxo sanguíneo sinusoidal. Assim, as HSC tornaram-se alvos terapêuticos para tratar complicações das doenças hepáticas crônicas (25, 27).

1.4 Tratamento

A fibrose hepática e a sua fase final, a cirrose, foram consideradas irreversíveis por muitos anos, porém em 1979, pela primeira vez, este dado foi questionado. Atualmente já se sabe que mesmo a cirrose pode ser revertida, especialmente como consequência de uma terapia antiviral bem-sucedida (4, 28).

Nossa compreensão dos mecanismos subjacentes à fibrose tem avançado muito nos últimos 10 a 15 anos, e uma lista crescente de agentes estão sendo testados com potencial ação antifibrótica. No entanto, nenhum destes foi aprovado ainda para uso clínico. Uma seleção dos ensaios clínicos em andamento até o ano de 2016, inscritos no site *ClinicalTrials.gov* para "fibrose hepática" estão listados na Tabela 1 (28).

Quadro 1 – Seleção de ensaios clínicos antifibróticos registrados em *ClinicalTrial.gov* (28).

Drug	Mechanism	Subjects	Results	Year of start	Phase	NCT identifier (alternate name)
Control primary disease						
UDCA	Secondary bile acid	PBC	Delayed fibrosis progression	_____	4	[54]
Farglitazar	PPARγ agonist	HCV	No effect	2005	2	NCT00244751[55]
Pioglitazone/ Vitamin E	PPARγ agonist/ antioxidant	NASH	Improved NAS No progression in fibrosis	2003	3	NCT00063622 (PIVENS)[56]
Pioglitazone/ Vitamin E	PPARγ agonist/ antioxidant	NASH	Pending	2009	4	NCT01002547
GFT505	Dual PPARα/δ agonist	NASH	Pending	2012	2	NCT01694849
Obeticholic acid	FXR agonist	NASH	Improved NAS Improved fibrosis	2010	2	NCT01265498 (FLINT) [57]
Obeticholic acid	FXR agonist	PBC	Pending	2014	3	NCT02308111
Obeticholic acid	FXR agonist	NASH	Pending	2015	3	NCT02548351 (REGENERATE)
Liraglutide	GLP-1 agonist	NASH	Pending	2010	2	NCT01237119
Antagonize receptor ligand interactions and/or intracellular signaling						
Irbesartan	Angiotensin II type 1 receptor antagonist	HCV	Completed Results pending	2005	3	NCT00265642
Losartan	Angiotensin II type 1 receptor antagonist	NASH	Completed	2010	2	NCT01051219 (FELINE)
Pentoxifylline	TNFα inhibitor	NASH	Improved NAS No change in fibrosis	2007	2	NCT 00590161[58]
GR-MD-02	Galectin-3 inhibitor	NASH	Completed Results pending	2013	1	NCT01899859
GR-MD-02	Galectin-3 inhibitor	NASH	Pending	2015	2	NCT02421094
IDN-6556 (Emricasane)	Pan-caspase inhibitor	Posttransplant HCV	Pending	2014	2	NCT02138253
Cenicriviroc	CCR5 and CCR2 antagonist	NASH	Pending	2014	2	NCT02217475 (CENTAUR)
PRI 724	Wnt signaling inhibitor	HCV	Pending	2014	1	NCT02195440
Pirfenidone	TGFβ and HSP 47 inhibitor	HCV	Pending	2014	2	NCT02161952
Nintedanib	Tyrosine kinase inhibitor	Liver cirrhosis	Pending	2014	1	NCT02191865
GS4997/ Simtuzumab	Apoptosis signal-regulation kinase (ASK 1) inhibitor/ Anti-LOXL2 monoclonal antibody	NASH	Pending	2015	2	NCT02466516
Inhibit fibrogenesis						
FG-3019	Anti-CTGF monoclonal antibody	HBV	Pending	2010	2	NCT01217632

Table 1 (*Continued*)

Drug	Mechanism	Subjects	Results	Year of start	Phase	NCT identifier (alternate name)
ND-L02 second-201	Vitamin A-coupled liposome targeting HSP 47	Moderate to extensive fibrosis	Pending	2014	1/2	NCT02227459
Promote fibrosis resolution						
Simtuzumab (GS-6624)	Anti-LOXL2 monoclonal antibody	HIV and/or HCV	Pending	2012	2	NCT01707472
Simtuzumab (GS-6624)	Anti-LOXL2 monoclonal antibody	PSC	Pending	2012	2	NCT01672853

Abbreviations: CCR, chemokine receptor; CENTAUR, Combined Effects of Non-statin Treatments on Apolipoprotein A-I Up-Regulation (CENTAUR): A Feasibility Study; CTGF, connective tissue growth factor; FELINE, Anti-Fibrotic Effects of Losartan in NASH Evaluation Study; FXR, farnesoid X receptor; FLINT, The Farnesoid X Receptor (FXR) Ligand Obeticholic Acid in NASH Treatment Trial; GLP-1, glucagon-like peptide-1; HBV, hepatitis B virus; HCV, hepatitis C virus; HIV, human immunodeficiency virus; HSP, heat shock protein; LOXL2, lysyl oxidase-like molecule 2; NAS, NAFLD activity score; NASH, nonalcoholic steatohepatitis; PBC, primary biliary cirrhosis; PIVENS, Pioglitazone vs Vitamin E vs Placebo for Treatment of Non-Diabetic Patients With Nonalcoholic Steatohepatitis; PPAR, peroxisome proliferator-activated receptor; PSC, primary sclerosing cholangitis; REGENERATE, Randomized Global Phase 3 Study to Evaluate the Impact on NASH With Fibrosis of Obeticholic Acid Treatment; TGF, transforming growth factor; TNF, tumor necrosis factor; UDCA, ursodeoxycholic acid.

A caracterização dos mecanismos da fibrose identificou vias comuns à fibrose renal, pulmonar, cutânea e hepática. Estas novas abordagens antifibróticas nos tecidos levam a um ritmo acelerado de desenvolvimento de fármacos, que inclui também terapias de reaproveitamento de fármacos ou terapias de combinação.

Embora as principais vias de ativação das células estreladas hepáticas e fibrose sejam comuns a todas as etiologias da lesão crônica, foram descritas vias específicas da doença e padrões de progressão da fibrose. Independentemente de os alvos serem específicos da doença ou estarem presentes em todas as formas de lesão hepática, as terapias antifibróticas para doenças não-virais terão de ser eficazes em decorrência da lesão em curso, uma vez que, diferentemente dos doentes com hepatite viral, a etiologia primária pode não ser curável. Na figura 4 demonstramos os principais alvos terapêuticos dos agentes antifibróticos atualmente estudados, entre os quais seria importante destacar: o tratamento da causa da doença primária, o bloqueio das rotas de produção de colágeno e a promoção da degradação da MEC (28, 29).

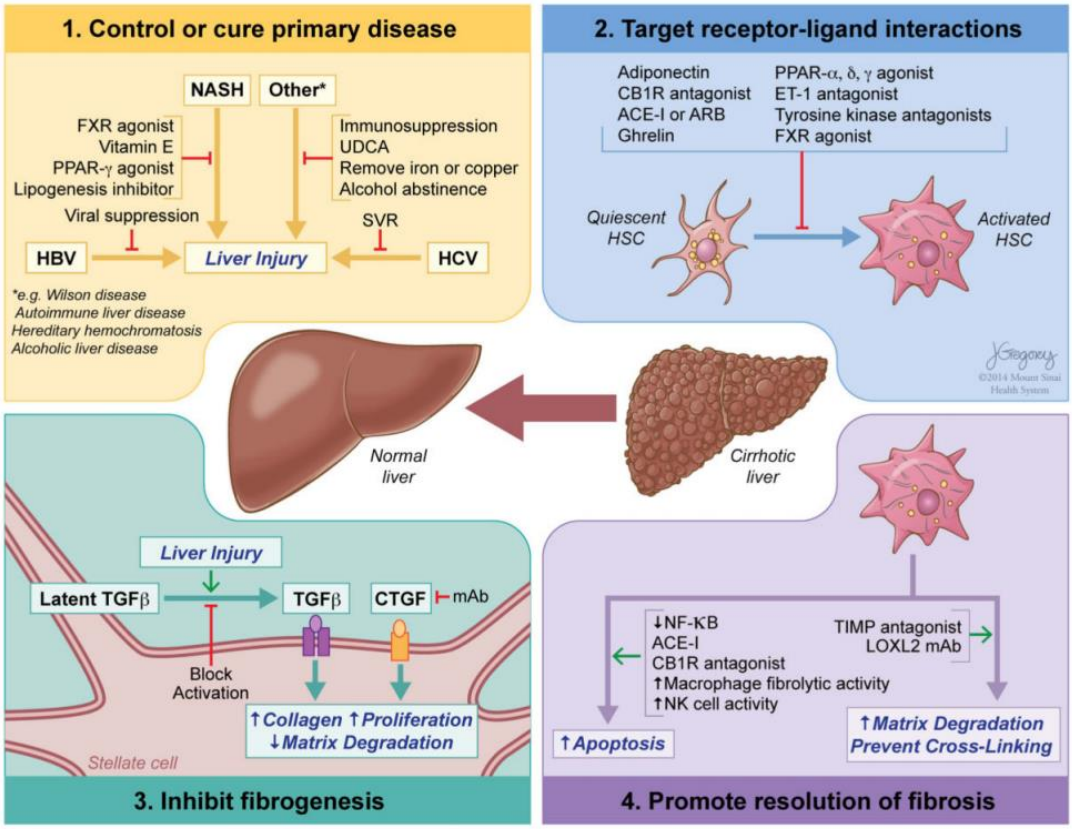

Figura 4 - Alvos terapêuticos dos agentes antifibróticos. O quadro para as estratégias antifibróticas incluem [1] terapias específicas que controlam ou curam a doença subjacente. [2] As interações receptor-ligante para atenuar a ativação das HSC reduzindo a fibrogenese. [3] A inibição das vias profibrogênicas mais potentes, por exemplo, impedir a ativação de TGFβ latente, ou bloquear a atividade de CTGF. [4] Promover a resolução da fibrose aumentando a apoptose das HSC ativadas ou aumentando a degradação da matriz extracelular (28, 29).

Além dos fármacos já em testes clínicos, existem inúmeras outras pesquisas buscando terapias antifibróticas ainda em fase pré-clínica (ou seja, em animais). Uma delas, que ganha destaque, é o uso das estatinas (inibidores da HMG-CoA redutase que reduzem o colesterol). As estatinas têm efeitos pleiotrópicos, incluindo funções anti-inflamatórias, antiproliferativas, antioxidantes e imunomoduladoras (30), e também promovem um efeito antifibrótico. O tratamento de ratos cirróticos com atorvastatina ou sinvastatina, levou a uma redução significativa da fibrose (31, 32) e efeitos antifibróticos também foram analisados no pulmão (33) e no coração (34). Ainda que sejam necessárias análises adicionais sobre os efeitos de estatinas

em modelos pré-clínicos e clínicos, as estatinas indicam resultados promissores no tratamento da fibrose hepática.

1.5 Liraglutida

A terapia baseada no hormônio GLP-1 (*Glucagon-like peptide 1*) atraiu recentemente a atenção como um novo tratamento de diabetes mellitus tipo 2 (DM2) em humanos (35). Agonistas do receptor do GLP-1 e inibidores da DPP-4 (*dipeptidil peptidase IV),* enzima que degrada o GLP-1, têm se mostrado eficazes no controle da glicemia em vários ensaios clínicos (35). Foi lançada então a liraglutida, um peptídeo análago do GLP-1, aprovado pela Agência Europeia de Medicamentos (EMEA) em julho de 2009, pelo *Food and Drug Administration* (FDA) em janeiro de 2010 e pela Agência Nacional de Vigilância Sanitária (ANVISA) em março de 2010. A ação da liraglutida é estimular a liberação de insulina pelo pâncreas, proporcional aos níveis de glicose através da ligação ao receptor de GLP-1 na superfície da membrana das células β. Após esta ligação ocorre a ativação da adenilciclase e o aumento dos níveis de cAMP, que é responsável pela liberação de insulina quando estimulada pela glicose (figura 5B) (36-38). Mas também pode reduzir o glucagon caso este esteja elevado, em relação inversa à glicose. Desta forma, caso a glicose esteja elevada, o fármaco irá estimular a secreção da insulina e inibirá o glucagon. (36, 37) No caso de hipoglicemia, o fármaco diminui a liberação de insulina e não afeta a liberação de glucagon, portanto, não afeta os níveis de glicose em pessoas não diabéticas (36, 37).

A vida plasmática do GLP-1 é extremamente curta (menor do que 3 minutos) devido à sua degradação pela enzima dipeptidilpeptidase 4 (DPP-4), então, tornou-se necessário a síntese de análogos do GLP-1 resistentes à inativação enzimática. A liraglutida é exatamente um desses compostos resistentes, sendo constituída por duas modificações na sequência de aminoácidos da molécula nativa e o acoplamento de um ácido graxo à cadeia peptídica (figura 5A). Seu mecanismo de atuação e seus efeitos são como o GLP-1, porém, com maior potência e maior vida média. Essa amplificação permite o uso clínico com apenas uma injeção subcutânea por dia (36, 37).

O hormônio GLP-1 possui efeitos múltiplos, incluindo a modulação da proliferação de células, apoptose e neogênese (39). Corroborando com estes dados, estudos demonstraram resultados benéficos do GLP- 1 sobre o miocárdio (39) e sobre a função endotelial (40, 41). Em um modelo experimental murino, a liraglutida reduziu o tamanho da área lesada pelo infarto do miocárdio (42). Além destes efeitos, estudos demonstram também que a liraglutida possui ações neuroprotetoras (43) e anti-inflamatórias (44) em modelos de doenças neurodegenerativas em camundongos. Análogos de GLP-1 tem mostrado reduzir mediadores pró-inflamatórias como IL-1β induzida por LPS (45) e o estresse oxidativo induzido por TNF-α em células endoteliais (35).

Os receptores GLP-1 (receptor acoplado a proteína G) estão presentes nas células pancreáticas e em muitos outros tecidos, entretanto sua expressão no fígado não é clara. Apesar da maioria dos estudos demonstrarem ausência deste receptor no fígado, em 2010 Gupta e colaboradores publicaram no periódico *Hepatology* a presença de receptores de GLP-1 no fígado (46, 47). Mesmo com estes dados controversos, é importante destacar que estudos recentes demonstraram a eficácia dos agonistas de GLP-1R em doenças que afetam o fígado, como por exemplo, na doença hepática gordurosa não alcoólica (NAFLD) (48, 49). As propriedades anti-inflamatórias e antioxidantes já descritas também são importantes para a resolução da doença hepática crônica (CLD). Os mecanismos subjacentes a estes diferentes efeitos ainda não são totalmente compreendidos. Porém, interessantemente, muitos destes efeitos foram evidentes em camundongos knockout para receptores de GLP-1, sugerindo que sejam efeitos independentes dos receptores de GLP- 1 já conhecidos (50-52).

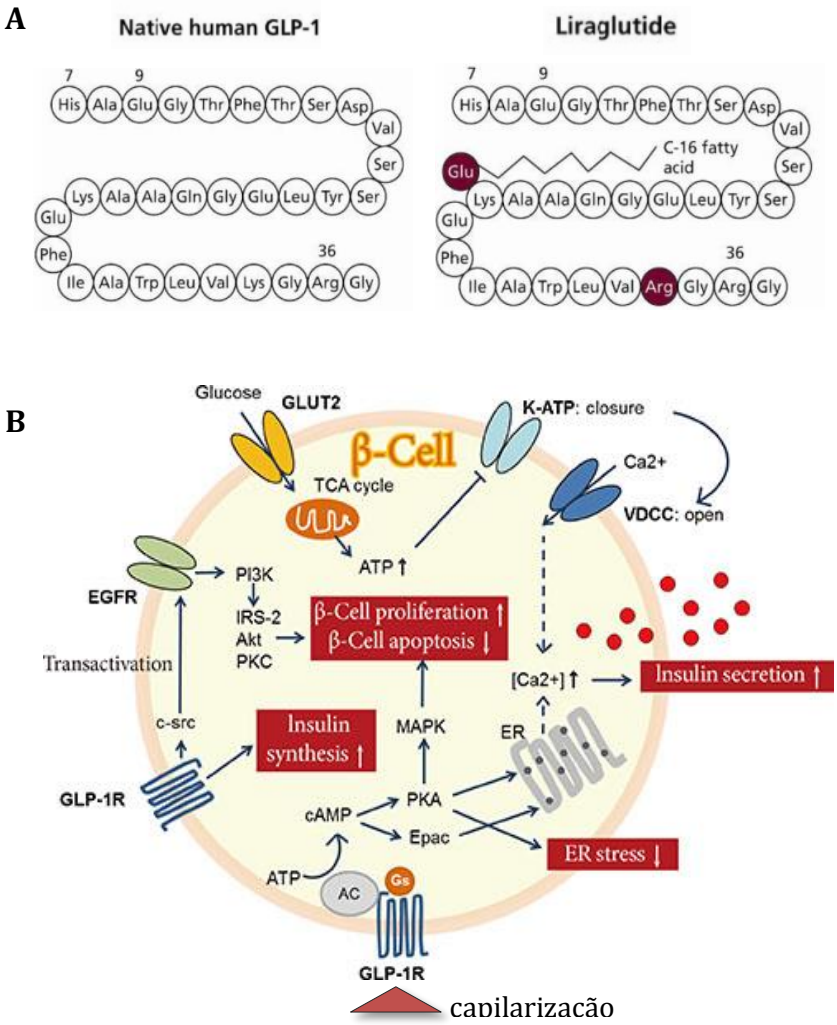

Figura 5 – Estrutura do GLP-1 e da liraglutida (A). Ação do GLP-1 na superfície da membrana das células β (B). GLP-1 promove o aumento dos níveis de cAMP, que é responsável pela liberação de insulina na presença de glicose (38).

2. Justificativa

As atuais opções de tratamento para doença crônica hepática (CLD) e a sua principal complicação, a hipertensão portal, ainda são limitadas e sem nenhuma terapia eficaz disponível para melhorar a fibrose hepática e a microcirculação hepática de pacientes com CLD (12, 16). Portanto, são necessárias novas estratégias terapêuticas baseadas em fármacos já aprovados por EMA/FDA/ANVISA e sem efeitos adversos sistêmicos para melhorar os tratamentos para pacientes com CLD. Além disso, estudos prévios relataram a propriedade anti-inflamatória da liraglutida em modelos celulares e animais (35, 53, 54) e efeitos benéficos na redução da doença hepática gordurosa não alcoólica (NAFLD) (48, 55). Sabendo que o processo de fibrose hepática envolve mediadores inflamatórios como citocinas e quimiocinas e que já foi descrito efeitos benéficos da liraglutida no fígado, é importante avaliar a efetividade deste fármaco no processo fibrótico hepático.

3. Objetivos

3.1. Objetivo geral

Avaliar o efeito *in vitro* e *in vivo* da liraglutida sobre a fibrose hepática.

3.2. Objetivos específicos

In vitro

▪ Determinar alterações de fenótipo de células HSC humanas e de ratos.

▪ Avaliar os marcadores de ativação de fenótipo, α-SMA, colágeno e TGF-β.

▪ Determinar a ação da liraglutida sobre a proliferação e viabilidade da células HSC.

▪ Avaliar a ação da liraglutida sobre a apoptose em HSC.

▪ Avaliar o efeito sinérgico da liraglutida com sinvastatina.

In vivo

▪ Avaliar a hemodinâmica hepática e microcirculação intra-hepática em ratos fibróticos tratados com liraglutida.

▪ Avaliar os marcadores bioquímicos de lesão e função hepática no soro de ratos fibróticos tratados com liraglutida.

▪ Avaliar a ação da liraglutida sobre o fenótipo das células sinusoidais.

▪ Realizar histologia no fígado dos animais tratados com liraglutida para avaliar a fibrose hepática.

▪ Verificar se a liraglutida atua através do receptor de GLP-1.

CAPÍTULO II

ARTIGO ORIGINAL

Liraglutide improves liver microvascular dysfunction in cirrhosis: Evidence from translational studies.*

*Os resultados do presente trabalho foram publicados em ***Scientific Reports*** e está formatado de acordo com as normas do periódico.

Fator de Impacto dos últimos 5 anos: 5.525

4. Artigo científico

: 19th April 17 12:19:35
: 19th April 17 12:19:35
: Redacted
: Redacted
: Scientific Reports: Decision letter for SREP-17-08836A
: Dear Dr Gracia-Sancho,

We are delighted to accept your manuscript entitled "Liraglutide improves liver microvascular dysfunction in cirrhosis: Evidence from translational studies." for publication in Scientific Reports. Thank you for choosing to publish your work with us.

You should have just received another email from scientificreports@nature.com with instructions for the next step, which is to complete your publication agreements. To continue with your publication agreements you will need to create a new account on this new system. Please complete these as soon as possible so we can start preparing your manuscript for publication. The agreements include the licence, which defines the terms of publication, and billing information for your Open Access article. Please see our FAQs page for further information about article processing charges.

After we've prepared your paper for publication, you will receive a PDF proof for checking. At that point, please check the author list and affiliations to ensure that they are correct. For the main text, only errors that have been introduced during the production process or those that directly compromise the scientific integrity of the paper may be corrected at this stage. Please ensure that only one author communicates with us and that only one set of corrections is returned. The corresponding (or nominated) author is responsible on behalf of all co-authors for the accuracy of all content, including spelling of names and current affiliations.

To ensure prompt publication, your proofs should be returned within two working days; please contact SciRep.Production@nature.com immediately if you wish to nominate a contributing author to receive the proofs on your behalf.

Acceptance of your manuscript is conditional on all authors' agreement with our publication policies (see http://www.nature.com/srep/policies/index.html). In particular, your manuscript must not be published elsewhere and there must be no announcement of this work to any media outlet until the publication date is confirmed. We will inform you by email as soon as your manuscript is scheduled for publication, which will be after we have received and approved your proof corrections. Advice about media relations is available from NPG's press office at press@nature.com.

Your article will be open for online commenting on the Scientific Reports website. You may use the report facility if you see any comments which you consider inappropriate, and of course, you can contribute to discussions yourself. If you wish to track comments on your article, please register for this service by visiting the 'Comments' section in the full text (HTML) version of your paper.

A form to order reprints of your article is available at http://www.nature.com/reprints/author-reprints.html. To obtain the special author reprint rate, orders must be made within a month of the publication date. After that, reprints are charged at the normal (commercial) rate.

We look forward to publishing your article.

Best regards,

Ruchi Bansal
Editorial Board Member
Scientific Reports

Editorial Board Member comments:

P.S. If appropriate, you may also consider uploading any biologically- or biomedically-related protocols used in this manuscript to the protocol exchange, part of our on-line web resource, nature.com/protocolexchange. By participating, you are enabling researchers to more readily reproduce or adapt the methodology you use. The protocol exchange is fully searchable, providing your protocols and paper with increased utility and visibility. Please submit your protocol to http://protocols.nature.com/manuscripts. After entering your nature.com username and password you will need to enter your manuscript number (SREP-17-08836A). Further information can be found at www.nature.com/protocolexchange.

Liraglutide improves liver microvascular dysfunction in cirrhosis: Evidence from translational studies.*

Fernanda Cristina de Mesquita[a,c,#], Sergi Guixé-Muntet[a,b,#], Anabel Fernández-Iglesias[a,#], Raquel Maeso-Díaz[a], Sergi Vila[a], Diana Hide[a], Martí Ortega-Ribera[a], José Luís Rosa[d], Juan Carlos García-Pagán[a,b], Jaime Bosch[a,b], Jarbas Rodrigues de Oliveira[c*], Jordi Gracia-Sancho[a*]

[a] Liver Vascular Biology Research Group, Barcelona Hepatic Hemodynamic Lab, IDIBAPS Biomedical Research Institute - CIBEREHD, Barcelona, Spain.

[b] University of Barcelona Medical School.

[c] Laboratório de Biofísica Celular e Inflamação, PUCRS, Porto Alegre-RS, Brazil.

[d] Departament de Ciències Fisiològiques, IDIBELL, Universitat de Barcelona, L'Hospitalet de Llobregat, Barcelona, Spain.

# These authorsequally contributed and share first authorship.

* Co-last authors.

Correspondence: Jordi Gracia-Sancho, PhD. Barcelona Hepatic Hemodynamic Laboratory. IDIBAPS Biomedical Research Institute. Rosselló 149, 4th floor. 08036 Barcelona, Spain. Tel: +34932275400 ext 4306.
Email: jordi.gracia@idibaps.org

Conflict of interest: None to declare (all authors). This study was not supported nor discussed with Novo Nordisk (owner of Liraglutide).

Abstract (200 words)

Hepatic stellate cells (HSC) play a key role in the development of chronic liver disease (CLD). Liraglutide, well-established in type 2 diabetes, showed anti-inflammatory and anti-oxidant properties. We evaluated the effects of liraglutide on HSC phenotype and hepatic microvascular function using diverse pre-clinical models of CLD. Human and rat HSC were *in vitro* treated with liraglutide, or vehicle, and their phenotype, viability and proliferation were evaluated. In addition, liraglutide or vehicle was administered to rats with CLD. Liver microvascular function, fibrosis, HSC phenotype and sinusoidal endothelial phenotype were determined. Additionally, the effects of liraglutide on HSC phenotype were analysed in human precision-cut liver slices. Liraglutide markedly improved HSC phenotype and diminished cell proliferation. Cirrhotic rats receiving liraglutide exhibited significantly improved liver microvascular function, as evidenced by lower portal pressure, improved intrahepatic vascular resistance, and marked ameliorations in fibrosis, HSC phenotype and endothelial function. The anti-fibrotic effects of liraglutide were confirmed in human liver tissue and, although requiring further investigation, its underlying molecular mechanisms suggested a GLP1-R-independent and NF-κB-Sox9-dependent one. This study demonstrates for the first time that Liraglutide improves the liver sinusoidal milieu in pre-clinical models of cirrhosis, encouraging its clinical evaluation in the treatment of chronic liver disease.

Introduction

Glucagon-like peptide-1 (GLP-1) receptor agonists (GLP-1RA) are a new class of anti-diabetic medications that mimic the effects of incretin hormones 1. As an incretin hormone, which is synthesized in response to food intake, GLP-1 can stimulate insulin release by pancreatic β-cells in a glucose-dependent manner and suppress glucagon secretion from α-cells 2. The favourable actions of GLP-1 on glucose homeostasis are mediated through GLP-1 receptors. However, native GLP-1 is rapidly degraded in circulation 3. Liraglutide, a synthetic GLP-1RA that shares 97% homology with the structure of human GLP-1, possesses a much longer circulating half-life, thereby making it a novel anti-diabetic drug suitable for once-daily injection 1. Apart from the pancreatic islets, GLP-1 receptors are present in many other tissues and, although its expression within the liver is not clear 4,5, recent studies demonstrated efficacy of GLP-1RA in liver diseases, such as NAFLD 6,7. In this regard, studies showed other beneficial properties for this type of drugs, including anti-inflammatory and antioxidant 8,9, which are also important for the resolution of chronic liver disease (CLD).

Cirrhosis is the end stage of CLD that starts with deregulations in the phenotype of all hepatic cells leading to parenchymal and sinusoidal dysfunction 10. In CLD, both architectural alterations of the liver parenchyma and sinusoidal microvascular dysfunction contribute to the development of portal hypertension 11. Architectural distortion of the cirrhotic liver is mainly due to excessive synthesis and deposition of extracellular matrix performed by deregulated fibrogenic cells mainly hepatic stellate cells (HSC) 12. Indeed, in response to liver injury, HSC gradually transdifferentiate to an activated α-SMA-positive phenotype with extensive proliferation, and high vasoconstrictive and proinflammatory properties 13,14. It is widely accepted that activation of HSC is a key factor in the pathogenesis of liver fibrosis, CLD and portal hypertension 15. Moreover, an intimate crosstalk between HSC and other sinusoidal cells further contribute to the development and aggravation of CLD 16.

CLD may improve in response to injury cessation, blockade of pro-fibrogenic mediators or drug-induced HSC inactivation 17. Unfortunately, current treatment options for CLD and its main complication portal hypertension are limited, and importantly there is no effective therapy available to efficiently ameliorate the hepatic microcirculation of CLD 18. Therefore, novel therapeutic strategies based on EMA/FDA approved drugs with no systemic adverse effects are required to improve treatments for patients with CLD. The primary purpose of the present study was to evaluate the effects of liraglutide on HSC phenotype, liver microvascular function and underlying mechanisms in pre-clinical models of CLD.

Results

Liraglutide improves the phenotype of Hepatic Stellate Cells

Effects of liraglutide on HSC phenotype were assessed in diverse pre-clinical models of CLD. After preliminary dose- and time-response experiments (Supplementary Fig. 1), we characterized liraglutide's effects promoting the deactivation of cirrhotic primary hHSC and in the prevention of activation of control primary hHSC undergoing 7-day plastic activation. Both conditions showed a marked down-regulation in the activation markers collagen I and α-SMA at a concentration of 50μM and after 72h of treatment (Fig. 1A left and middle panels). The anti-fibrotic effects of liraglutide were further validated in human precision-cut liver slices (PCLS) (Fig 1A right). In addition, the amelioration in hHSC phenotype in response to liraglutide was validated using a functional assay. As shown in Figure 1B, liraglutide significantly prevented the contraction of primary hHSC. The effects of liraglutide on activated HSC were further analyzed in LX-2, a widely-accepted human cell line mimicking activated HSC. These experiments indeed showed de-activation of LX-2 cells in response to liraglutide (Fig 2A), which was associated with significant reductions in the pro-inflammatory and pro-fibrogenic markers TNF-α and TGF-βR1 (Fig 2A). Interestingly, LX-2 cells treated with liraglutide showed no significant changes in

viability when compared to controls, as observed with the double staining with AO-PI (Fig 2B). Contrarily, using two different analysis of cell proliferation, the trypan blue exclusion assay and the expression of the proliferative marker PDGFRβ, we herein show the anti-proliferative effects of liraglutide in HSC (Fig 2C), which were accompanied with a marked reduction in their contraction ability (Fig 2D). Altogether, validating the global improvement in HSC phenotype in response to liraglutide. Similar beneficial effects of liraglutide were observed in rat primary HSC (Supplementary Fig 2).

Liraglutide improves HSC phenotype and portal hypertension in CLD-rats.

The potential beneficial effects of liraglutide as a new therapeutic strategy to improve CLD and portal hypertension were also analyzed in vivo. After 15 days of treatment, CLD-rats treated with liraglutide displayed lower expression of α-SMA and PDGFRβ (Fig 3A), accompanied by reductions in extracellular matrix synthesis and deposition as demonstrated by diminished collagen expression and hepatic fibrosis (Fig 3B). No significant differences in TIMPs and MMPs were observed, thus suggesting that the peak of fibrinolysis already occurred (Supplementary Fig 3). No effects on HSC viability (desmin expression) were observed, thus supporting the results obtained in vitro. Additional analysis of HSC phenotype in cells freshly isolated from CLD-rats treated with liraglutide, or vehicle, confirmed the marked beneficial effects of the drug promoting HSC deactivation (Fig 3C).

Possible beneficial effects of liraglutide on hepatic and systemic hemodynamic in CLD-rats were also analyzed. Table 1 shows the morphometric and hemodynamic data from these animals. As expected, CLD-rats treated with liraglutide exhibited a slight but significant reduction in body weight, which is in agreement with previous studies 19. Importantly, liraglutide-treated animals showed significantly lower portal pressure than vehicle-treated animals (11.6±0.8 vs. 9.3±1.0mmHg; -20%; p=0.03) without changes in portal blood flow, thus suggesting an improvement in the hepatic vascular resistance (9.5±1.8 vs.

5.7±1.3mmHg·mL·min-1·g-1; -23%; p=0.1). No effects of liraglutide on systemic hemodynamic or biochemical tests were observed.

Intrahepatic microcirculatory amelioration in response to liraglutide was further confirmed analyzing the hepatic microvascular phenotype. Indeed, LSEC from animals receiving liraglutide showed a significant reversal in their capillarization, as suggested by marked increments in fenestrae frequency and porosity (Fig 4A), and a trend to higher nitric oxide bioavailability (Fig 4B). In addition, characterization of the hepatic microvascular function *ex vivo* confirmed the global sinusoidal improvement, as demonstrated by reduction in HVR (Table 1) and improved liver vascular response to incremental doses of acetylcholine (Fig 4C).

Liraglutide has a complementary effect with simvastatin improving HSC

Treatment of LX-2 cells with liraglutide did not modify the expression of the simvastatin-inducible transcription factor KLF2 (Supplementary Fig 4 left). However, LX-2 treated with liraglutide or simvastatin showed reduced levels of α-SMA in the same magnitude. Interestingly, when both drugs were combined further reduced α-SMA (Supplementary Fig 4 right), altogether suggesting that liraglutide has a complementary effect to simvastatin improving the phenotype of activated HSC.

Liraglutide improves HSC phenotype and liver microcirculation probably through a GLP1-R independent mechanism

Analysis of GLP1-R expression in rat and human liver tissues and HSC showed no detectable mRNA expression (Supplementary Fig 5A), while a band corresponding to 53kDa (predicted GLP-1R molecular weight) was only detected in LX-2 and barely present in cirrhotic and NASH human livers, but not in control human or rat livers (either control or cirrhotic) (Supplementary Fig 5B). Accordingly, analysis of the GLP-1R secondary messenger PKA in rHSC and LX-2 treated with liraglutide did not show differences in its phosphorylation in

comparison to cells treated with vehicle (Supplementary Fig 5C), and incubation of LX-2 with the GLP-1R antagonist Exendin 9-39 did not affect the deactivation effects of liraglutide (Supplementary Fig 5D). Oppositely, liraglutide did repress the NF-κB molecular pathway (Supplementary Fig 6).

Discussion

The major findings of the current study are that liraglutide promotes a marked amelioration in the phenotype of activated HSC, which in a pre-clinical model of chronic liver disease leads to significant improvement in portal hypertension and liver fibrosis. Importantly, the de-activating effects of liraglutide are herein demonstrated in human primary HSC and human liver tissue. Liraglutide was developed as an anti-diabetic drug predictably acting on GLP-1R in pancreatic β-cells. Interestingly, different studies have demonstrated that these receptors may not be only limited to pancreatic β-cells. Considering the beneficial anti-inflammatory effects of GLP-1R agonists on cardiac fibrosis and NASH 20–22, we aimed the present study at analyzing the effects of liraglutide in chronic liver disease (CLD).

Liver cirrhosis is the end stage situation of CLD being the main triggering factor a complex multicellular response of all hepatic cells. Indeed, in front of a chronic injury both parenchymal and non-parenchymal cells undergo profound changes in their phenotype, becoming highly de-regulated and ultimately leading to fibrosis and microvascular dysfunction 16. The most relevant clinical consequence of sinusoidal cells de-regulation is the development of portal hypertension, which derives both from pathological increases in intrahepatic vascular resistance and in portal blood flow. Considering the importance of HSC in CLD progression and aggravation, many studies focused on liver-specific drugs capable of inactivating the HSC, however few studies have advanced to the clinical stage 23.

Our study is the first showing that liraglutide is able to improve the phenotype of HSC. Indeed, we performed dose- and time-dependent experiments indicating that liraglutide de-activates HSC as demonstrated by reduced expression of α-SMA and collagen. Similarly, we observed prevention of HSC activation in response to liraglutide, therefore suggesting possible beneficial effects of the drug when administered at early stages of CLD. Importantly, we planned this study as a bed to bench-side one, and not vice versa, therefore firstly evaluating the effects of liraglutide in human primary HSC, to latterly use different preclinical models of CLD to further study the molecular mechanisms of such ameliorations.

Hepatic stellate cells are activated in response to different liver injuries, or due to paracrine factors, promoting tissue repair. Their response includes cell mobilization, proliferation, migration towards the lesion, and production of extracellular matrix components. When continuous liver injury occurs, HSC become chronically activated, acquire high expression of pro-inflammatory, profibrogenic and proliferative markers like TNF-α, TGFβ and PDGFRβ, ultimately representing the main cell-type responsible for fibrosis deposition 24,25. In the present study, we show that improvement in HSC phenotype in response to liraglutide was accompanied by marked reductions in the expression of these cytokines and proliferation markers, without affecting cell viability. Altogether suggesting that liraglutide promotes the de-activation of HSC, reduces their proliferation but does not induce cell apoptosis. Such anti-inflammatory effects, which are potentially optimal for the resolution of liver fibrosis in vivo, are quite different from previous studies showing concomitant de-activation and apoptosis/necrosis of HSC in response to certain therapeutic strategies 26–28. Importantly, analysis of HSC was not limited to molecular markers, but also included the cell contraction functional assay, which further confirmed the global improvement of HSC phenotype in response to liraglutide.

Additionally, we tested the possible beneficial effects of liraglutide when administered to human liver tissue. Taking advantage of the precision cut liver slices technique, considered an excellent tool to analyze the effects of drugs within the liver 29, we observed marked reductions in the expression of α-SMA and collagen in response to liraglutide therefore corroborating the anti-fibrotic effects of the drug. Once the phenotype of HSC was characterized in vitro, we studied the effects of a physiological-relevant dose of liraglutide administered in vivo. Liraglutide treatment markedly improved both HSC and LSEC phenotypes. In fact, HSC activation markers collagen I, α-SMA and PDGFRβ were reduced in CLD rats receiving liraglutide, which was accompanied by amelioration in LSEC fenestrae and NO bioavailability. Although we herein demonstrate direct action of liraglutide on HSC, we do not rule out possible paracrine interactions between both sinusoidal cell types in response to the drug 16,30. Importantly, global

improvement in the sinusoidal phenotype led to regression of liver fibrosis, and to significant amelioration in the hepatic microvascular dysfunction. Indeed, liraglutide was able to reduce the PP in rats with CLD and portal hypertension. Such improvement in hepatic hemodynamics was mostly due to a significant improvement in the intrahepatic microvascular dysfunction, as demonstrated by the estimations of the in vivo and ex vivo HVR, and the analysis of the ex vivo vasodilatory capacity in response to incremental doses of acetylcholine. Importantly, liraglutide did not affect systemic hemodynamics. We next ascertained which could be the molecular pathway underlying liraglutide effects on HSC, and consequently on liver microcirculation and fibrosis. First, and considering that liraglutide was formulated to act on GLP-1 receptor, we analyzed the expression of this receptor both in HSC isolated from rat and humans, and also in liver tissues. Surprisingly, GLP-1R mRNA was not detected in whole liver homogenates, primary HSC or LX-2 cells using two different Taqman probes with PCR reactions going up to 60 cycles. At the protein level, western blot of hepatic samples using an antibody against GLP-1R showed signal in LX-2 lysates at the predicted GLP-1R molecular weight, but this signal was barely present in cirrhotic and NASH human tissue, while it was not detected in control human livers or rat liver tissue (either control or cirrhotic). These observations suggest that the beneficial effects of liraglutide in rat HSC and its effects in vivo would not be dependent on GLP-1R. Previous reports already showed contradictory results in terms of GLP-1R expression within the liver 4,5, and we are not totally convinced that the band detected by the antibody in human samples really corresponds to GLP-1R (as it is contradictory to the two specific mRNA TaqMan probes). In agreement, additional experiments showed lack of protein kinase A phosphorylation (marker of GLP-1R activation) 31,32 in response to liraglutide, and no differences in liraglutide-mediated HSC de-activation and proliferation when an antagonist of liraglutide on HSC were quite similar to those previously observed using statins 26,33–35. These experiments showed no up-regulation in response to the drug, moreover a synergistic effect of liraglutide and simvastatin de-activating HSC was observed, thus suggesting that they act by different

pathways and could be used in combination at the bedside. Lastly, we evaluated the NF-κB molecular pathway, which plays a major role in liver fibrosis 36 and is inhibited by liraglutide in the endothelium 37. Interestingly, liraglutide down-regulated the expression of NF-κB, and also of its target gene Sox9. With these results we cannot delineate the exact molecular mechanism driving liraglutide's beneficial effects, and represents a limitation of the study. Nevertheless, considering the main role of NF-κB and Sox9 modulating HSC phenotype 38,39, and the findings described above, we herein suggest that in the specific scenario of CLD liraglutide may improve HSC phenotype and liver microcirculation through a GLP-1R independent mechanism, being the NF-κB-Sox9 pathway a solid candidate to mediate, at least in part, these effects. Desirable future experiments, out of the scope of the present study, will clarify the specific receptor and the molecular mechanisms that mediate the beneficial effects of this drug in chronic liver disease.

In conclusion, the present study describes the anti-fibrotic effects of liraglutide both in rodent and, importantly, human pre-clinical models of chronic liver disease, therefore encouraging its application at the bedside as new therapeutic tool to improve cirrhosis and portal hypertension. Moreover, the potential results of the LEAN trial opens the possibility to use liraglutide not only to improve mild GLP-1R was used. Secondly, we analyzed the expression of the transcription factor Kruppel-like factor 2 (KLF2) in response to liraglutide since the effects of NASH 7, but promote regression of advanced chronic liver disease. Desirable future trials will clarify this promising therapeutic alternative.

Materials and Methods

Animal models of chronic liver disease (CLD)

The study was carried out in male Wistar rats (Charles River Laboratories, Barcelona, Spain). Animals were kept in environmentally controlled animal facilities. All procedures were approved by the Laboratory Animal Care and Use Committee of the University of Barcelona and were conducted in accordance with

the European Community guidelines for the protection of animals used for experimental and other scientific purposes (EEC Directive 86/609). The personnel who prepared and administered treatments and those that performed the experimental studies were different. Treatment's codes were not open for interpretation of the results until the inclusion of all animals.

Induction of CLD by thioacetamide (TAA)

TAA (Sigma Chemical Co) was dissolved in 0.9% normal saline approximately one hour before injection. Treatment groups received 200mg/kg of TAA twice per week for a total of 12 weeks while control groups received the same volume of 0.9% normal saline [18].

Induction of CLD by Carbon Tetrachloride (CCl_4)

Rats underwent inhalation exposure to CCl_4 (Sigma) and received phenobarbital (0.3g/L) in the drinking water. When rats developed ascites, toxicants administration was stopped [40].

HSC isolation, culture and treatments

Isolation and culture of HSC

HSC were isolated from human (hHSC: control or cirrhotic) and rat (rHSC: control, TAA-CLD or CCl4-CLD) livers as described 26 with minor modifications. Briefly, liver tissues were perfused with collagenase A, pronase and DNase (all Roche) in Gey's Balanced Salt Solution (GBSS; Sigma), and dispersed cells were fractionated by density gradient centrifugation using 11.5% Optiprep (Sigma). HSC were cultured in Iscove's Modified Dulbecco's Media (IMDM, Invitrogen, Gibco) supplemented with fetal bovine serum, glutamine, antibiotics and amphotericin B. Results using primary HSC derived from at least 3 independent isolations and 3 replicates.

Immortalized human-activated HSC LX-2 were cultured as described 11. Results using LX-2 derived from at least three replicates per experimental condition.

HSC treatments

HSC were incubated with liraglutide (Novo Nordisk), or its vehicle PBS, at different concentrations (1μM, 10μM, 50μM and 100μM) and for different periods of time (24h, 48h and 72h). *In vitro* dosing of liraglutide was based on previous literature 41. Considering that liraglutide exerted beneficial effects at 50μM and after 72h of treatment, all subsequent experiments were performed using these experimental conditions. Simvastatin was used in 10μM dose alone and in combination with liraglutide. Exendin fragment 9-39 (Sigma-Aldrich; 10nM - 1uM) was used as a GLP-1R antagonist 41.

Cell viability & proliferation

Equal number of LX-2 were seeded and after 72h of liraglutide or vehicle, floating and adhered cells were collected and counted using a hemocytometer with trypan blue dye exclusion (FLUKA).

Cell apoptosis

Cells were incubated with fresh medium containing 800ng/mL Acridine Orange (AO) and 5μg/mL Propidium Iodide (PI) for 10min at 37ºC and then washed with PBS. Fresh medium was added and cell death was examined using a fluorescence microscope (Olympus BX51, Tokyo, Japan) equipped with a digital camera (Olympus, DP72). AO is a metachromatic dye that stains both viable and apoptotic cells by intercalating into DNA and emits green fluorescence upon excitation at 480-490nm. Nevertheless, nuclear condensation that occurs during apoptosis glares a more intense fluorescence. PI is excluded by viable cells but can penetrate cell membranes of dying or dead cells due to necrosis, emitting red fluorescence. Positive controls (*in vitro* ischemia and reperfusion), and negative controls (without dye) were included 26.

Cell contraction

Contraction of HSC was performed as previously described with some modifications 42. Briefly, culture plates were incubated with 1% BSA-PBS and afterwards filled with a mix of collagen (2mg/mL) and human HSC (1-2x105 cells/mL). Once the gels were solidified, serum free IMDM with 50μM liraglutide or vehicle was added. After 24h,

contraction was induced by adding 10% FBS for 24h. Finally, the contraction area was digitalized and measured with ImageJ software. The results are expressed as % of contraction relative to the initial area of the gel.

Characterization of CLD-rats treated with liraglutide

Liraglutide administration

TAA-CLD-rats received by subcutaneous injections, twice a day, either liraglutide (0.5mg/kg/day; n=11) or vehicle (0.9% NaCl; n=11) during 15 days. The dose was selected based on a conversion calculation starting from the dose used in humans and agreed with previous publications 19,43,44. Administration of liraglutide to CLD-rats started one week after stopping the administration of TAA.

In vivo hemodynamics

Rats (n=8 per group) were anesthetized with ketamine hydrochloride (100mg/Kg; Merial Laboratories) plus midazolam (5mg/kg; Laboratorios Reig Jofré) intraperitoneally. A tracheotomy was performed and a polyethylene tube PE-240 was inserted into the trachea to ensure a patent airway. PE-50 catheters were introduced into the femoral artery to measure mean arterial pressure (MAP; mmHg) and into ileocolic vein to measure portal pressure (PP; mmHg). A perivascular ultrasonic flow probe (Transonic System) was placed around the portal vein, as close as possible to the liver to avoid portal-collateral blood flow, in order to measure portal blood flow (PBF; mL·min-1). Hepatic vascular resistance (mmHg·min·mL-1·g-1) was calculated as: PP/PBF. Blood pressures and flows were registered on a multichannel computer based recorder (Power Lab; AD Instruments). Temperature of the animals was maintained at 37 ± 0.5°C and hemodynamic data were collected after 20min stabilization 40,45. Blood serum and plasma samples were stored for biochemical analysis.

Liver microvascular function

Immediately after recording *in vivo* hemodynamics, rat livers were isolated and perfused with Krebs buffer as previously described (n=5 per group) 45,46. The perfused rat liver preparation was allowed to stabilize for 20min before vasoactive

substances were added. Intrahepatic microcirculation was preconstricted by adding the α1-adrenergic agonist methoxamine (Mtx; 10-4M; Sigma) to the reservoir, and liver microvascular function was assessed as concentration–response curves to cumulative doses of acetylcholine (Ach; 10-7 - 10-5M; Sigma). Liver tissue was snap-frozen for subsequent molecular analysis.

Evaluation of hepatic fibrosis

CLD-rat livers were fixed in 10% formalin, embedded in paraffin, sectioned, and stained with 0.1% Sirius Red, photographed, and analyzed using a microscope equipped with a digital camera. The red-stained area was measured using Axiovision software 26. Values are expressed as the mean of 8 fields per sample.

Sinusoidal characterization using Scanning Electron Microscope

In a sub-group of animals (n=3 per group), after obtaining *in vivo* hemodynamics, livers were perfused through portal vein with a solution containing 2.5% glutaraldehyde and 2% paraformaldehyde and fixed overnight at 4ºC. Samples were washed 3 times with 0.1M cacodylate buffer. Liver sections were fixed with 1% osmium in cacodylate buffer, dehydrated in ethanol, and dried with hexamethyldisilazane. Six randomly selected blocks from each animal were mounted onto stubs, and sputter coated with gold. 10 images per animal were acquired at a resolution of 15,000x using a Jeol 6380 Scanning Electron Microscope (JEOL Ltd, Tokyo, Japan). Liver sinusoidal fenestrations were quantified using ImageJ Software (NIH) 47.

Nitric Oxide bioavailability

Levels of cGMP, a marker of NO bioavailability, were analyzed in liver homogenates using an enzyme immunoassay (Cayman Chemical Co., Ann Arbor, MI) as previously described 48.

RNA isolation and quantitave PCR

RNA from cells and tissue were extracted using RNeasy mini kit (Qiagen) and Trizol (Life Technologies), respectively. RNA quantification was performed using a NanoDrop spectrophotometer. cDNA was obtained using QuantiTect reverse

transcription kit (Qiagen). Real-Time PCR were performed in an ABI PRISM 7900HT Fast Real-Time PCR System, using TaqMan predesigned probes for Col1A1 (Hs00164004_m1, Rn01463848_m1), α-SMA (Hs00426835_g1, Rn01759928_g1), PDGFRβ (Hs01019589_m1, Rn01491838_m1), GLP1-R (Hs00157705_m1, Hs01006326_m1), Sox9 (Hs00165814_m1, Rn01751070_m1) and GAPDH or 18S as endogenous controls. Results, expressed as 2-ΔΔCt, represent the x-fold increase of gene expression compared with the corresponding control group.

Western blot analysis

Cells were rinsed twice with PBS and lysed with Triton lysis buffer. Livers were homogenized in triton-lysis buffer for whole protein extraction. Aliquots from each sample containing equal amounts of protein were run on a sodium dodecylsulphate polyacrylamide gel, and transferred to a nitrocellulose membrane. After the transfer, blots were blocked with Tris buffered saline containing 0.05% Tween-20 and 5% non-fat dry milk or 3% albumin and subsequently incubated overnight at 4ºC with primary antibodies against collagen I (ABT123, Millipore), α-SMA (A2547, Sigma), TNF-α (sc-1351, Santa Cruz Biotechnology), TGFβR (sc-398, Santa Cruz Biotechnology), GAPDH (sc-32233, Santa Cruz Biotechnology), p-PKA (4781, Cell Signaling), NF-κB (6956, Cell Signaling) and IκB (4812, Cell Signaling), all at 1:1000 dilution. Then membranes were incubated with the appropriate horseradish peroxidase conjugated secondary antibody at room temperature. Protein expression was determined by densitometric analysis using the LAS4000 (GE Healthcare) and Image Studio Lite software (LI-COR). Quantitative densitometric values of all proteins were normalized to GAPDH.

Precision-cut liver slices of human livers (PCLS)

Fresh human liver biopsies were used to obtain 250μm slices using a Vibratome VT1000S (Leica Microsystems, Wetzlar, Germany). Samples were washed in PBS, soaked in 4% agarose solution (Ultrapure LMP Agarose, Invitrogen, Carlsbad, California, USA) for 20min, and then orientated, mounted and immobilized using cyanoacrylate glue. Tissue slices were placed on organotypic tissue culture plate inserts (Millicell®-CM; Millipore). Tissues were maintained at 37°C in a 5% CO2 humidified incubator using 1.1mL of Williams' Medium E supplemented with 1%

inactivated fetal bovine serum, 2mM LGlutamine, 50U/mL penicillin and 50µg/mL streptomycin. Tissue slices were incubated with 50µM liraglutide for 24h. Sections were then transferred to a 1.5mL tube and lysed for RNA isolation and qPCR 29.

Ethics information

Quiescent hHSC (for prevention of *in vitro* activation) and PCLS were obtained from remnants from partial hepatectomy. Livers were considered control, but exhibited fibrosis staging between F1 and F2. In all cases surgery was recommended to excise tumor metastasis from colon carcinoma. Cirrhotic hHSC (for *in vitro* de-activation) were isolated from remnant cirrhotic livers (all alcoholic aetiology) obtained after transplantation. The Ethics Committee of the Hospital Clinic de Barcelona approved the experimental protocol, samples manipulation and isolation procedures were carried out following good laboratory practices; in all cases patients signed the informed consent.

Statistical analysis

Statistical analysis was performed with the SPSS V.23.0 for Windows statistical package (IBM, Armonk, New York, USA). Results are expressed as mean ± s.e.m. Normality of samples was assessed using the Kolmogorov Smirnov test. For samples following a normal distribution, comparisons between groups were performed with the Student t test or analysis of variance, followed by a Bonferroni Post Hoc test when adequate. Otherwise, comparisons were assessed with the non-parametric Mann-Whitney U or Kruskal Wallis test when adequate. Differences were considered significant at a p value <0.05.

Acknowledgments: Authors are in debt with Drs Garcia-Valdecasas and Molina for providing human biopsies, Dr Bataller for providing LX-2 cells, and Bibiana Rius and Dr Clària for their expertise in PCLS.

Author contributions: F.C.dM., S.G.-M and A.F.-I. designed the research, conceived ideas, performed experiments, and wrote the manuscript. R.M.-D., S.V., D. H. and M. O.-R. performed experiments and analyzed data. J.L.R. and J.C.G.-P. critically revised the manuscript. J.B. critically revised the manuscript and obtained

funding. J.R.dO. conceived ideas and critically revised the manuscript. J.G.-S. designed the research, conceived ideas, wrote the manuscript, obtained funding and directed the study. All authors edited and reviewed the final manuscript.

Financial support: This work was funded by the Ministerio de Economía y Competitividad – Instituto de Salud Carlos III, FIS (PI14/00029 and PI13/00341), and the European Union (Fondos FEDER, “una manera de hacer Europa”). FCdM has a Fellowship from CAPES/Ciência sem Fronteiras - Brazil, and SG-M from the Fundació Catalana de Trasplantament. AF-I has a Sara Borrell contract from the Instituto de Salud Carlos III. CIBEREHD is funded by the Instituto de Salud Carlos III.

References

1. Nauck, M. A. Incretin-based therapies for type 2 diabetes mellitus: properties, functions, and clinical implications. *Am. J. Med.* **124,** S3-18 (2011).

2. Kazafeos, K. Incretin effect: GLP-1, GIP, DPP4. *Diabetes Res. Clin. Pract.* **93 Suppl 1,** S32-6 (2011).

3. Drucker, D. J. The biology of incretin hormones. *Cell Death Differ.* **3,** 153– 165 (2006).

4. Gupta, N. A. *et al.* Glucagon-like peptide-1 receptor is present on human hepatocytes and has a direct role in decreasing hepatic steatosis in vitro by modulating elements of the insulin signaling pathway. *Hepatology* **51,** 1584–1592 (2010).

5. Pyke, C. *et al.* GLP-1 Receptor Localization in Monkey and Human Tissue: Novel Distribution Revealed With Extensively Validated Monoclonal Antibody. *Endocrinology* **155,** 1280–1290 (2014).

6. Wang, X.-C., Gusdon, A. M., Liu, H. & Qu, S. Effects of glucagon-like peptide-1 receptor agonists on non-alcoholic fatty liver disease and inflammation. *World J. Gastroenterol.* **20,** 14821–14830 (2014).

7. Armstrong, M. J. *et al.* Liraglutide safety and efficacy in patients with nonalcoholic steatohepatitis (LEAN): a multicentre, double-blind, randomised, placebo-controlled phase 2 study. *Lancet (London, England)* **387,** 679–90 (2016).

8. McClean, P. L., Jalewa, J. & Hölscher, C. Prophylactic liraglutide treatment prevents amyloid plaque deposition, chronic inflammation and memory impairment in APP/PS1 mice. *Behav. Brain Res.* **293,** 96–106 (2015).

9. Shiraki, A. *et al.* The glucagon-like peptide 1 analog liraglutide reduces TNF-α-induced oxidative stress and inflammation in endothelial cells. *Atherosclerosis* **221,** 375–82 (2012).

10. Fernández-Iglesias, A. & Gracia-Sancho, J. How to face chronic liver disease: the sinusoidal perspective. *Front. Med.* **4,** 7 (2017).

11. Marrone, G. *et al.* The transcription factor KLF2 mediates hepatic endothelial protection and paracrine endothelial-stellate cell deactivation induced by statins. *J. Hepatol.* **58,** 98–103 (2013).

12. Pinzani, M. & Gentilini, P. Biology of hepatic stellate cells and their possible relevance in the pathogenesis of portal hypertension in cirrhosis. *Semin. Liver Dis.* **19,** 397–410 (1999).
13. Török, N. J. Recent advances in the pathogenesis and diagnosis of liver fibrosis. *J. Gastroenterol.* **43,** 315–21 (2008).
14. Soon, R. K. & Yee, H. F. Stellate Cell Contraction: Role, Regulation, and Potential Therapeutic Target. *Clin. Liver Dis.* **12,** 791–803 (2008).
15. Reynaert, H. Hepatic stellate cells: role in microcirculation and pathophysiology of portal hypertension. *Gut* **50,** 571–581 (2002).
16. Marrone, G., Shah, V. H. & Gracia-Sancho, J. Sinusoidal communication in liver fibrosis and regeneration. *J. Hepatol.* **65,** 608–17 (2016).
17. Kisseleva, T. *et al.* Myofibroblasts revert to an inactive phenotype during regression of liver fibrosis. *Proc. Natl. Acad. Sci. U. S. A.* **109,** 9448–9453 (2012).
18. Cerini, F. *et al.* Enoxaparin reduces hepatic vascular resistance and portal pressure in cirrhotic rats. *J. Hepatol.* **64,** 834–42 (2016).
19. Gao, H. *et al.* The Glucagon-Like Peptide-1 Analogue Liraglutide Inhibits Oxidative Stress and Inflammatory Response in the Liver of Rats with Diet-Induced Non-alcoholic Fatty Liver Disease. *Biol. Pharm. Bull* **694,** 694–702 (2015).
20. Gaspari, T. *et al.* Molecular and cellular mechanisms of glucagon-like peptide-1 receptor agonist-mediated attenuation of cardiac fibrosis. *Diabetes Vasc. Dis. Res.* **13,** 56–68 (2016).
21. Armstrong, M. J. *et al.* Glucagon-like peptide 1 decreases lipotoxicity in non-alcoholic steatohepatitis. *J. Hepatol.* **64,** 399–408 (2016).
22. Steven, S. *et al.* Gliptin and GLP-1 analog treatment improves survival and vascular inflammation/dysfunction in animals with lipopolysaccharideinduced endotoxemia. *Basic Res. Cardiol.* **110,** 6 (2015).
23. Schuppan, D. & Kim, Y. O. Evolving therapies for liver fibrosis. *J. Clin. Invest.* **123,** 1887–1901 (2013).
24. Weiskirchen, R. & Tacke, F. Cellular and molecular functions of hepatic stellate cells in inflammatory responses and liver immunology. *Hepatobiliary Surg Nutr* **3,** 344–363 (2014).
25. Trautwein, C., Friedman, S. L., Schuppan, D. & Pinzani, M. Hepatic fibrosis: Concept to treatment. *J. Hepatol.* **62,** S15–S24 (2015).

26. Marrone, G. *et al.* KLF2 exerts antifibrotic and vasoprotective effects in cirrhotic rat livers: behind the molecular mechanisms of statins. *Gut* **64,** 1434–43 (2015).
27. Klein, S. *et al.* Atorvastatin inhibits proliferation and apoptosis, but induces senescence in hepatic myofibroblasts and thereby attenuates hepatic fibrosis in rats. *Lab. Investig.* **92,** 1440–1450 (2012).
28. Wright, M. C. *et al.* Gliotoxin Stimulates the Apoptosis of Human and Rat Hepatic Stellate Cells and Enhances the Resolution of Liver Fibrosis in Rats. *Gastroenterology* **121,** 685–698 (2001).
29. Olinga, P. & Schuppan, D. Precision-cut liver slices: A tool to model the liver ex vivo. *J. Hepatol.* **58,** 1252–1253 (2013).
30. Xie, G. *et al.* Role of Differentiation of Liver Sinusoidal Endothelial Cells in Progression and Regression of Hepatic Fibrosis in Rats. *Gastroenterology* **142,** 918–927 (2012).
31. Laviola, L. *et al.* Glucagon-like peptide-1 counteracts oxidative stress dependent apoptosis of human cardiac progenitor cells by inhibiting the activation of the c-Jun N-terminal protein kinase signaling pathway. *Endocrinology* **153,** 5770–81 (2012).
32. Wang, L. *et al.* GLP-1 analog liraglutide enhances proinsulin processing in pancreatic β-cells via a PKA-dependent pathway. *Endocrinology* **155,** 3817–28 (2014).
33. Abraldes, J. G. *et al.* Simvastatin treatment improves liver sinusoidal endothelial dysfunction in CCl4 cirrhotic rats. *J. Hepatol.* **46,** 1040–6 (2007).
34. Trebicka, J. *et al.* Atorvastatin lowers portal pressure in cirrhotic rats by inhibition of RhoA/Rho-kinase and activation of endothelial nitric oxide synthase. *Hepatology* **46,** 242–253 (2007).
35. La Mura, V. *et al.* Effects of simvastatin administration on rodents with lipopolysaccharide-induced liver microvascular dysfunction. *Hepatology* **57,** 1172–1181 (2013).
36. Luedde, T. & Schwabe, R. F. NF-κB in the liver—linking injury, fibrosis and hepatocellular carcinoma. *Nat. Rev. Gastroenterol. Hepatol.* **8,** 108– 118 (2011).
37. Gaspari, T. *et al.* A GLP-1 receptor agonist liraglutide inhibits endothelial cell dysfunction and vascular adhesion molecule expression in an ApoE-/- mouse model. *Diabetes Vasc. Dis. Res.* **8,** 117–24 (2011).

38. Pritchett, J. *et al.* Osteopontin is a novel downstream target of SOX9 with diagnostic implications for progression of liver fibrosis in humans. *Hepatology* **56,** 1108–1116 (2012).
39. Martin, K. *et al.* PAK proteins and YAP-1 signalling downstream of integrin beta-1 in myofibroblasts promote liver fibrosis. *Nat. Commun.* **7,** 12502 (2016).
40. Gracia-Sancho, J. *et al.* Endothelial expression of transcription factor Kruppel-like factor 2 and its vasoprotective target genes in the normal and cirrhotic rat liver. *Gut* **60,** 517–24 (2011).
41. Cantini, G. *et al.* Effect of liraglutide on proliferation and differentiation of human adipose stem cells. *Mol. Cell. Endocrinol.* **402,** 43–50 (2015).
42. Perri, R. E. *et al.* Defects in cGMP-PKG pathway contribute to impaired NO-dependent responses in hepatic stellate cells upon activation. *Am. J. Physiol. Gastrointest. Liver Physiol.* **290,** G535-42 (2006).
43. Lu, N. *et al.* Glucagon-like peptide-1 receptor agonist Liraglutide has anabolic bone effects in ovariectomized rats without diabetes. *PLoS One* **10,** e0132744 (2015).
44. Hoang, V., Bi, J., Mohankumar, S. M. & Vyas, A. K. Liraglutide Improves Hypertension and Metabolic Perturbation in a Rat Model of Polycystic Ovarian Syndrome. *PLoS One* **10,** e0126119 (2015).
45. Hide, D. *et al.* Effects of warm ischemia and reperfusion on the liver microcirculatory phenotype of rats: underlying mechanisms and pharmacological therapy. *Sci. Rep.* **6,** 22107 (2016).
46. Gracia-Sancho, J. *et al.* Evidence Against a Role for NADPH Oxidase Modulating Hepatic Vascular Tone in Cirrhosis. *Gastroenterology* **133,** 959–966 (2007).
47. Hilmer, S. N. *et al.* Age-related changes in the hepatic sinusoidal endothelium impede lipoprotein transfer in the rat. *Hepatology* **42,** 1349–1354 (2005).
48. Hide, D. *et al.* A novel form of the human manganese superoxide dismutase protects rat and human livers undergoing ischaemia and reperfusion injury. *Clin. Sci. (Lond).* **127,** 527–37 (2014).

Figure legends

Figure 1. Amelioration of human primary HSC in response to liraglutide. (a) Expression of depicted proteins/genes after *in vitro* treatment with 50 μM liraglutide or vehicle in: 1-HSC isolated from cirrhotic human livers (left), 2- quiescent human HSC undergoing *in vitro* activation (middle), and 3-human precision-cut liver slices (PCLS) (right). **(b)** Effects of liraglutide, or its vehicle, on the contraction of primary human HSC. n=3 per experimental condition. *p<0.05 vs. vehicle.

Figure 2. Underlying effects of HSC deactivation due to liraglutide. After 72h of treatment with 50 μM liraglutide, LX-2 cells were assessed for markers of HSC activation **(a)**, cell viability by double staining with acridine orange (green dense nuclei: apoptosis, indicated by arrowheads) and propidium iodide (red cells: necrosis) **(b)**, HSC proliferation assessed by cell counting and expression of the proliferative marker PDGFRβ **(c),** and cell contraction **(d)**. n=3 per experimental condition. *p<0.05 vs. vehicle.

Figure 3. Analysis of HSC phenotype and liver fibrosis in CLD-rats treated with liraglutide. (a) Expression of HSC activation markers (α-SMA and PDGFRβ) and Desmin in livers from TAA-CLD-rats treated for 15 days with liraglutide or vehicle. **(b)** Analysis of hepatic fibrosis in rats described in A (collagen I expression and Sirius Red staining). **(c)** Analysis of the phenotype of HSC freshly isolated from rats described in **a**. *p<0.05 vs. vehicle. n=8 (**a** & **b**) and n=3 (**c**) per group. Results are indicated as mean ± s.e.m.

Figure 4. Effects of liraglutide on hepatic endothelial phenotype and microvascular function. (a) Liver sinusoidal fenestrae analysis by means of frequency (no. fenestrae/cell area) and porosity (fenestrae area/cell area) in TAA-CLD-rats treated with liraglutide or vehicle. **(b)** Hepatic nitric oxide (NO) bioavailability in rats described in A. **(c)** Hepatic microvascular function, calculated as the decrease in portal pressure in response to increasing doses of the endothelium-dependent vasodilator acetylcholine after vasoconstriction with methoxamine. *p<0.05 vs. vehicle. n=3 (**a**), n=8 (**b**) and n=5 (**c**) per group.

Supplementary figure 1. Analysis of LX-2 de-activation in terms of α-SMA expression in response to liraglutide administered at different doses and times. n=3 per experimental condition. *p<0.05 vs. vehicle.

Supplementary figure 2. Effects of 72h-liraglutide on the *in vitro* activation of primary quiescent HSC isolated from healthy rats **(a),** and in the amelioration of activated HSC isolated from TAA-CLD **(b)** and CCl4-CLD **(c)** rats. n=3 per group. *p<0.05 vs. vehicle.

Supplementary figure 3. Expression of TIMPs and MMPs in livers from TAACLD- rats treated for 15 days with liraglutide, or vehicle. n=8 per group.

Supplementary figure 4. (a) Expression of the transcription factor KLF2 in LX-2 cells treated with 50 μM liraglutide, or vehicle. **(b)** Expression of α-SMA in LX-2 cells treated with 50 μM liraglutide, or vehicle, in combination with 10μM simvastatin, or its vehicle. n=3 per experimental condition. *p<0.05 vs. vehicle.

Supplementary figure 5. (a) 60-cycle amplification charts of GLP-1R mRNA expression analyzed in human liver & cells samples using the human cell line SH-SY5Y as positive control. **(b)** Western blot of different hepatic samples using a GLP-1R antibody (Abcam ab189397). From left to right, brain tissue as positive control, LX-2 cells, human liver tissue (control, cirrhotic, NASH) and rat liver tissue (control, cirrhotic). **(c)** p-PKA protein expression in primary cirrhotic HSC from TAA-CLD (left), CCl4-CLD (middle) and in LX-2 cells (right) in response to 50μM liraglutide. **(d)** Effects of the GLP-1R antagonist exendin 9-39 on α-SMA mRNA expression (left) and proliferation (right) in LX-2 cells. n=3 per experimental condition. *p<0.05 vs. vehicle.

Supplementary figure 6. (a) Protein expression of NF-κB and its inhibitor IκB and **(b)** mRNA expression of Sox9 in livers from TAA-CLD-rats treated with liraglutide, or vehicle. n=8 per group.

Table 1

	Vehicle n=11	Liraglutide n=11	*p value*
PP (mmHg)	11.6 ± 0.8	9.3± 1.0	*0.03*
MAP (mmHg)	99.5 ± 7.2	89.9 ± 7.1	0.4
PBF (mL/min)	11.9 ± 1.0	11.5 ± 2.3	0.5
HVR (mmHg·min·mL^{-1}·g^{-1})	9.5 ± 1.8	5.7 ± 1.3	0.1
ex vivo HVR (mmHg·min·mL^{-1}·g^{-1})	1.6 ± 0.3	0.9 ± 0.04	0.07
Body weight pre-treatment (g)	289 ± 12	288 ± 7	0.5
Body weight post-treatment (g)	310 ± 9	274 ± 9	*0.03*
Liver weight (g)	8.4 ± 0.7	6.7 ± 0.4	0.1
AST (U/L)	105 ± 14	126 ± 14	0.3
ALT (U/L)	61 ± 10	67 ± 4	0.5
Albumin (g/L)	15.3 ± 1.3	16.3 ± 0.5	0.5
Cholesterol (mg/dL)	54.0 ± 8.3	44.6 ± 5.8	0.4
TG (mg/dL)	31.2 ± 5.6	26.8± 3.4	0.5
FFA (µmol/L)	506 ± 66	477 ± 55	0.7

Effects of Liraglutide on hepatic and systemic hemodynamic, and biochemical parameters in rats with chronic liver disease.

PP, portal pressure; MAP, mean arterial pressure; PBF, portal blood flow; HVR, hepatic vascular resistance; AST, aspartate aminotransferase; ALT, alanine aminotransferase; TG, triglycerides; FFA, free fatty acids.

Figure 1

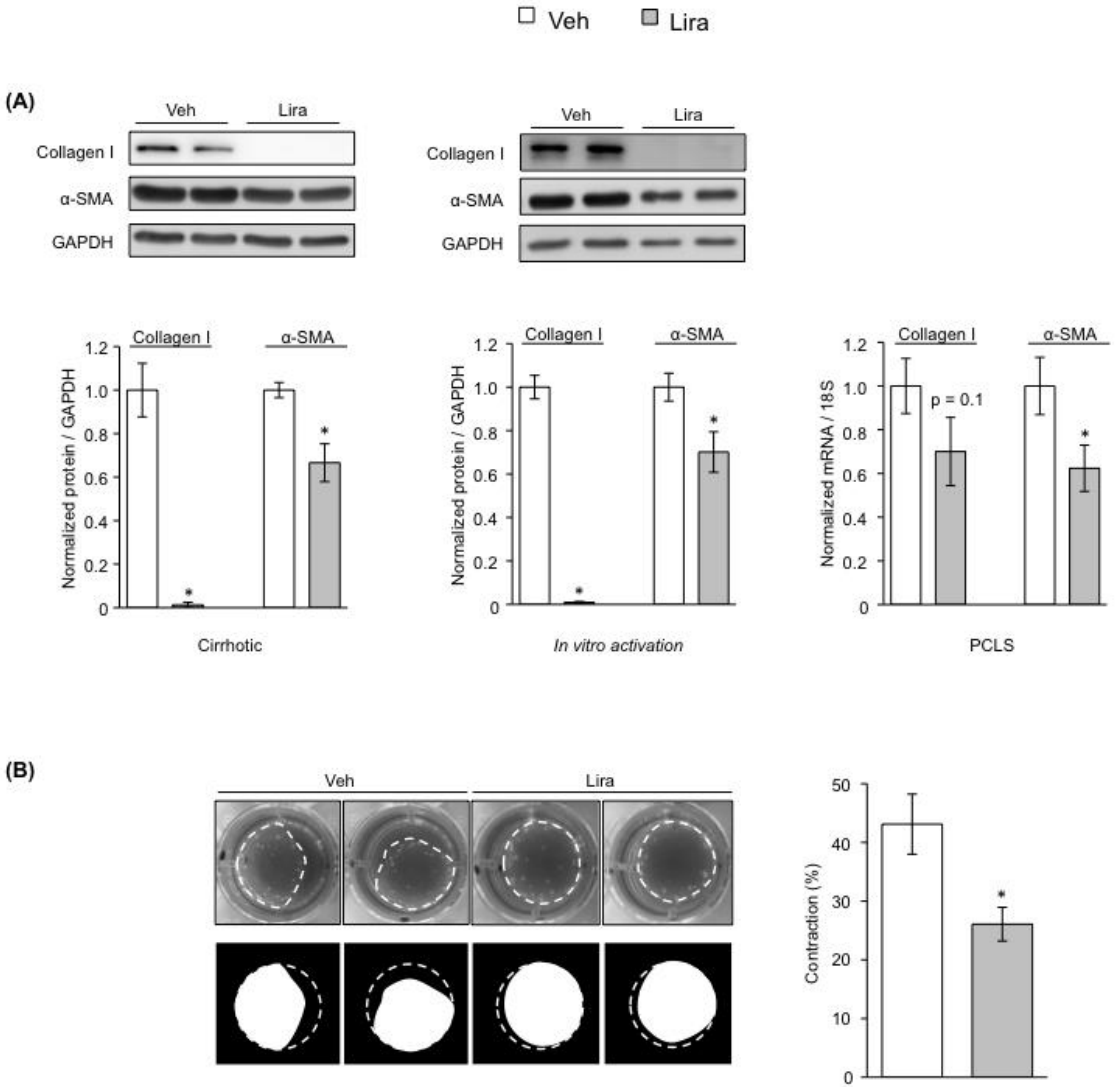
Veh
Lira
(A)
Collagen I
α-SMA
GAPDH
Normalized protein / GAPDH
Normalized mRNA / 18S
p = 0.1
Cirrhotic
In vitro activation
PCLS
(B)
Contraction (%)

Figure 2

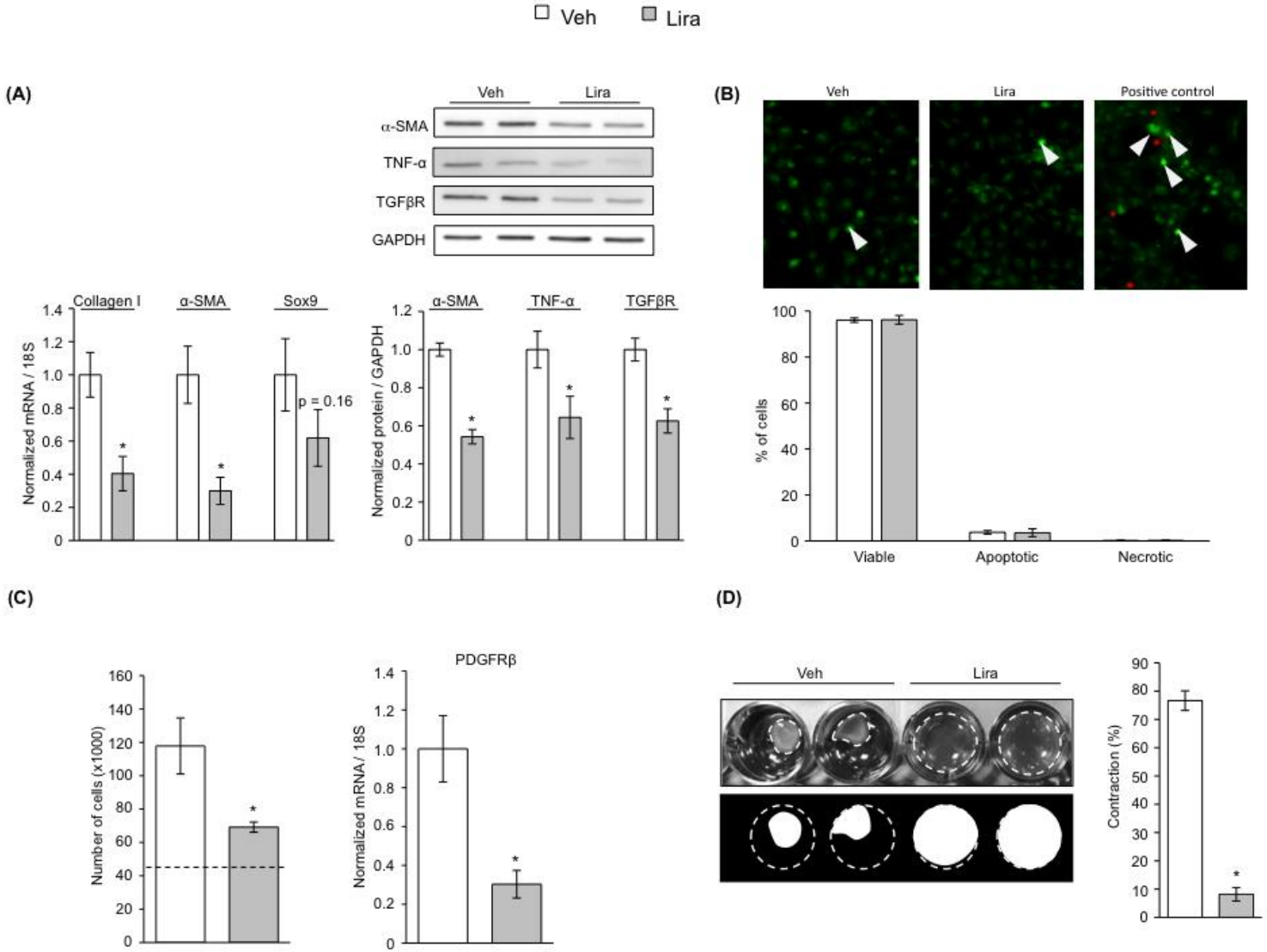
Veh
Lira
(A)
Veh
Lira
α-SMA
TNF-α
TGFβR
GAPDH
Collagen I
α-SMA
Sox9
Normalized mRNA / 18S
p = 0.16
α-SMA
TNF-α
TGFβR
Normalized protein / GAPDH
(B)
Veh
Lira
Positive control
% of cells
Viable
Apoptotic
Necrotic
(C)
Number of cells (x1000)
PDGFRβ
Normalized mRNA / 18S
(D)
Veh
Lira
Contraction (%)

Figure 3

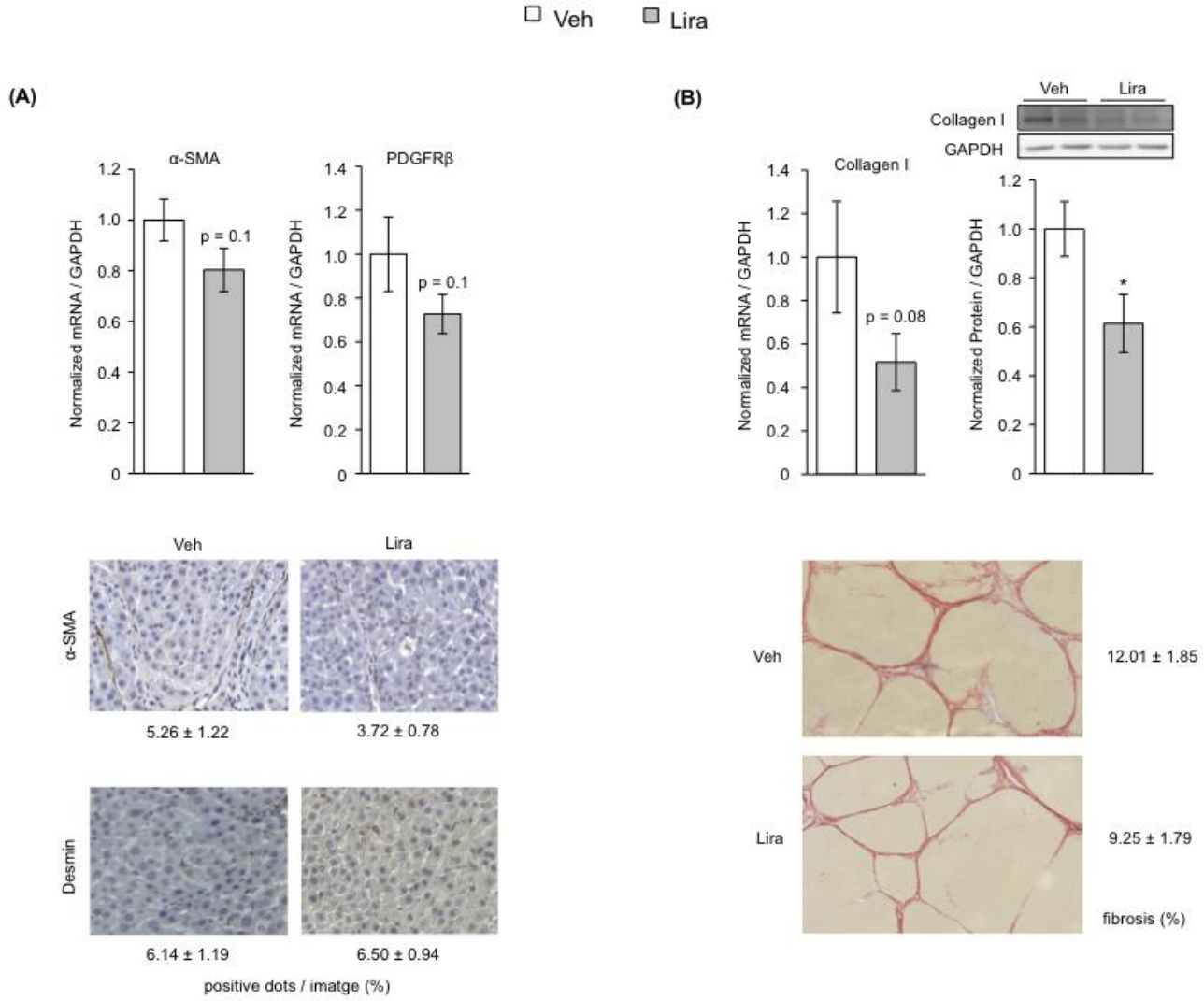
Veh
Lira
(A)
α-SMA
PDGFRβ
Normalized mRNA / GAPDH
p = 0.1
p = 0.1
Veh
Lira
α-SMA
Desmin
5.26 ± 1.22
3.72 ± 0.78
6.14 ± 1.19
6.50 ± 0.94
positive dots / imatge (%)
(B)
Veh
Lira
Collagen I
GAPDH
Collagen I
Normalized mRNA / GAPDH
p = 0.08
Normalized Protein / GAPDH
*
Veh
12.01 ± 1.85
Lira
9.25 ± 1.79
fibrosis (%)

Figure 3

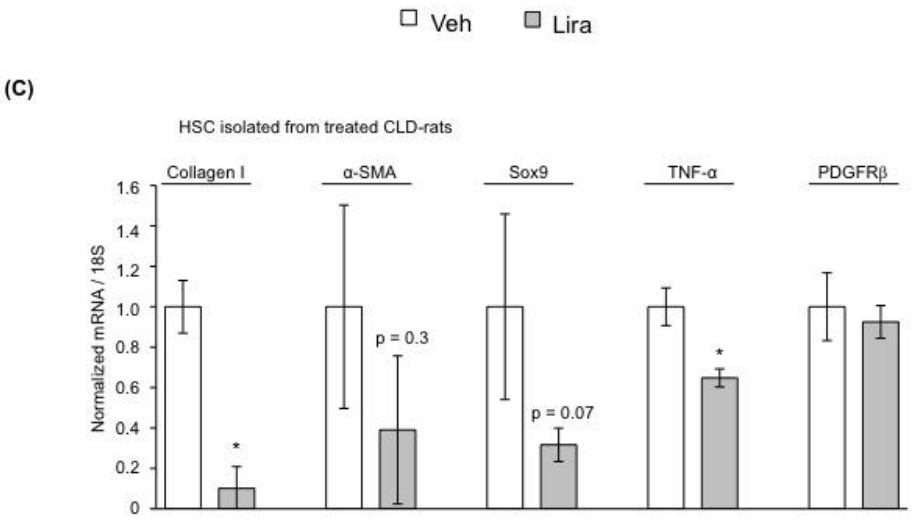
Veh
Lira
(C)
HSC isolated from treated CLD-rats
Collagen I
α-SMA
Sox9
TNF-α
PDGFRβ
Normalized mRNA / 18S
1.6
1.4
1.2
1.0
0.8
0.6
0.4
0.2
0
p = 0.3
p = 0.07
*
*

Figure 4

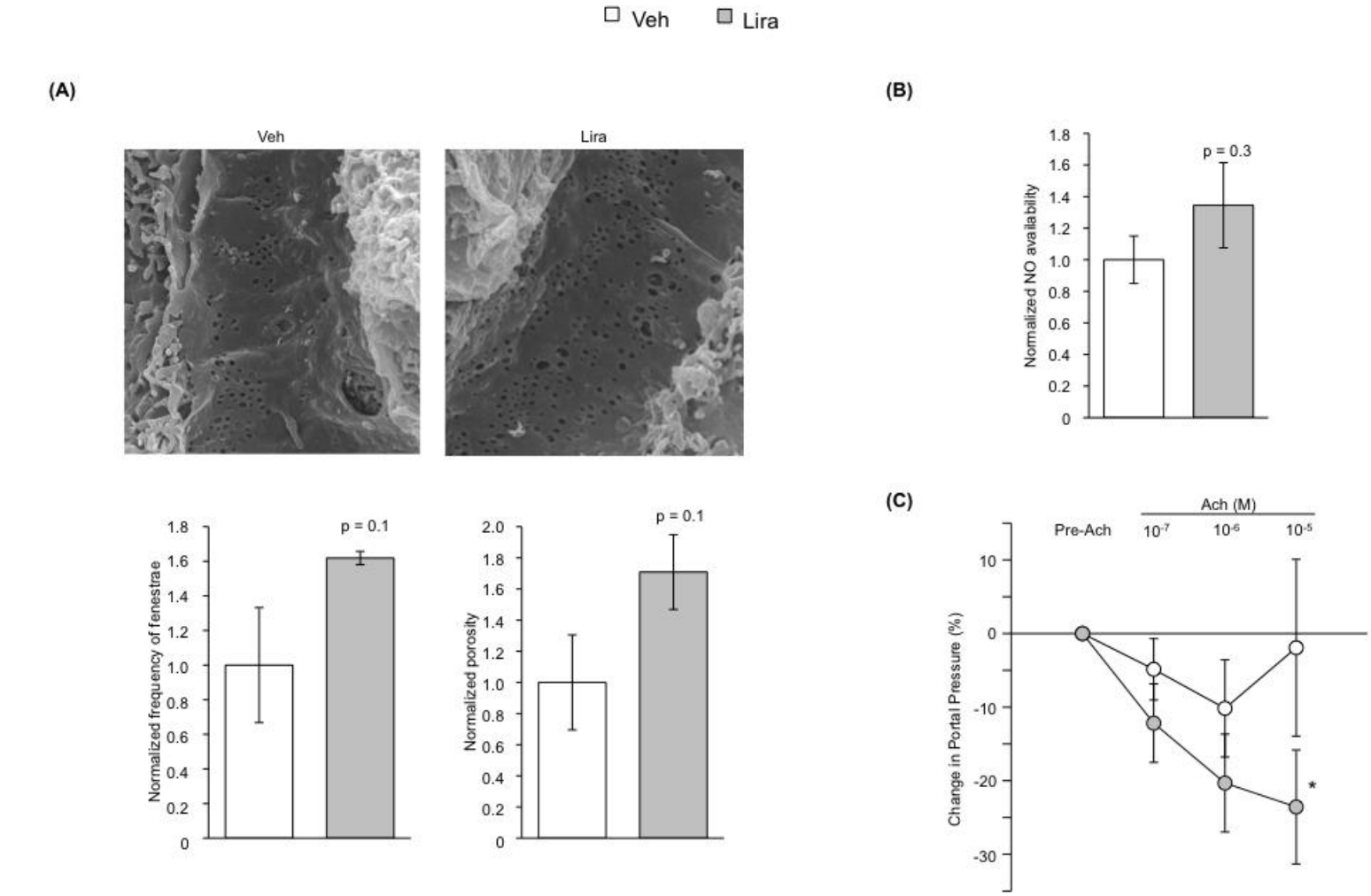
Veh
Lira
(A)
Veh
Lira
Normalized frequency of fenestrae
p = 0.1
Normalized porosity
p = 0.1
(B)
Normalized NO availability
p = 0.3
(C)
Ach (M)
Pre-Ach
10-7
10-6
10-5
Change in Portal Pressure (%)
*

Supplementary figure 1.

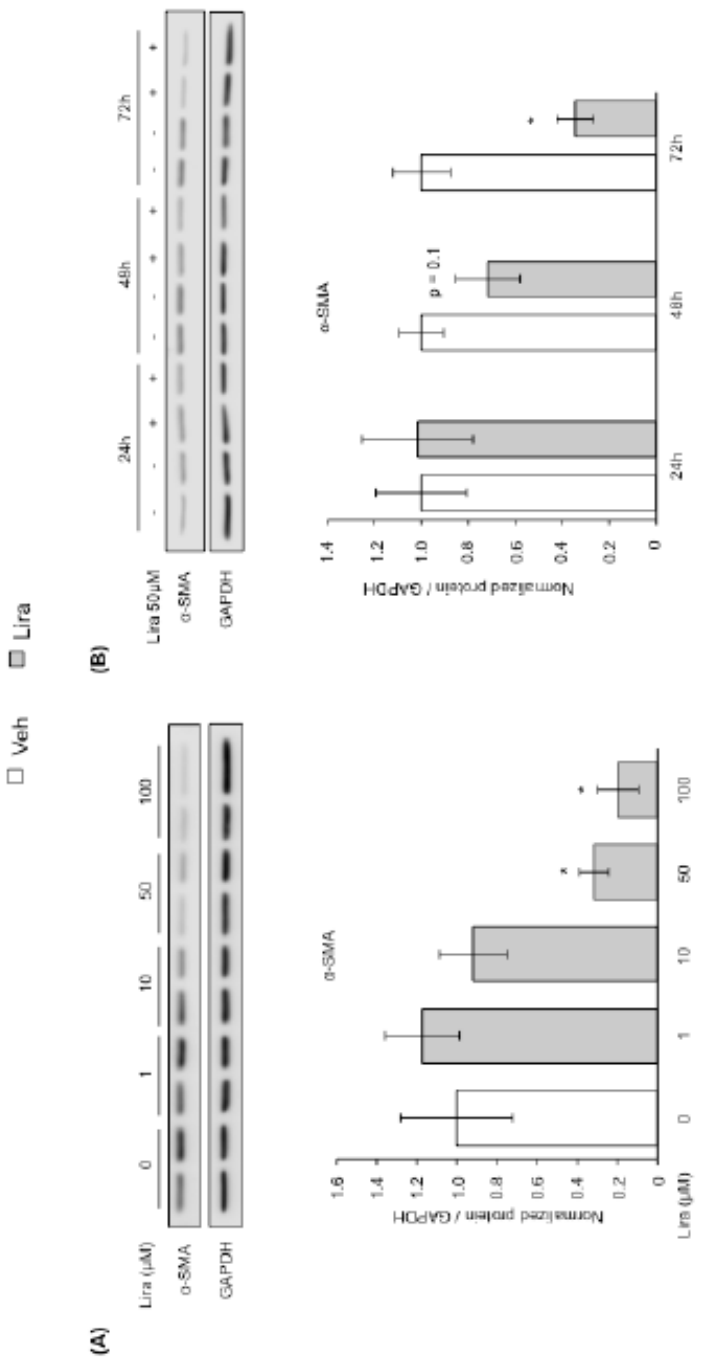

Supplementary figure 2.

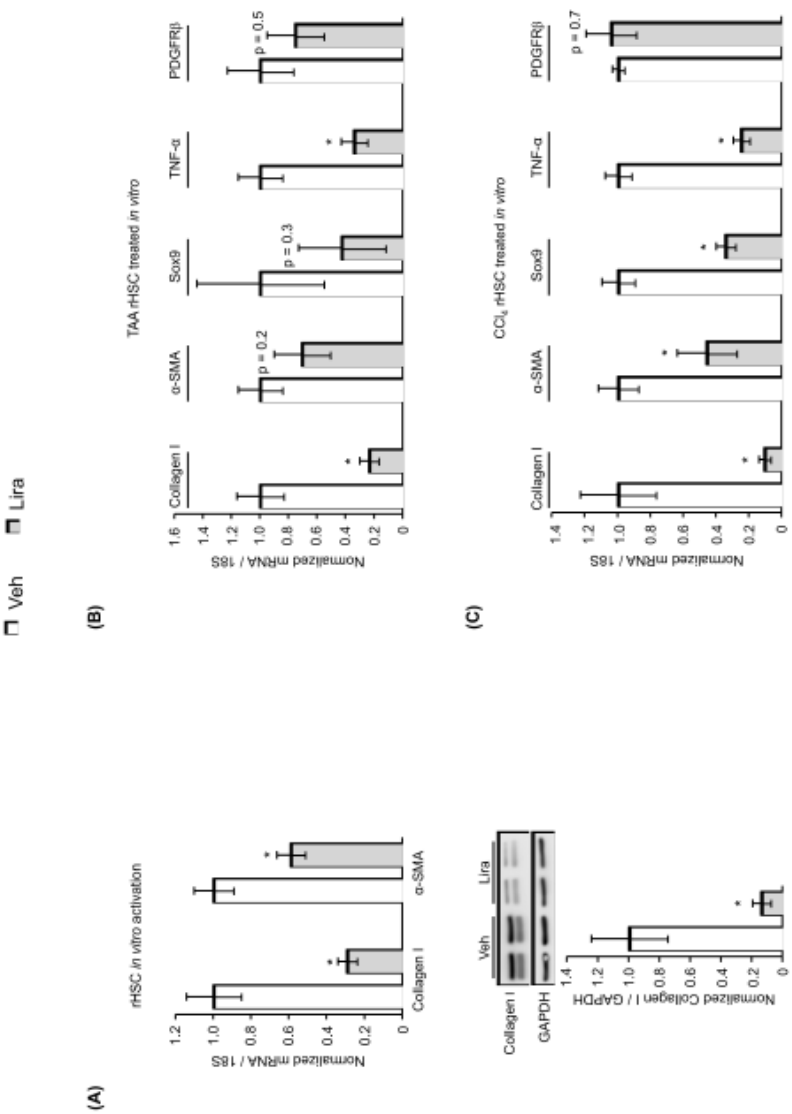

Supplementary figure 3.

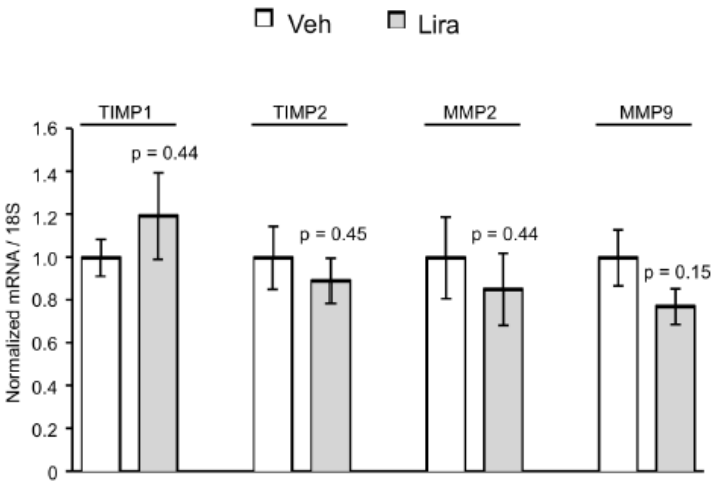

Supplementary figure 4.

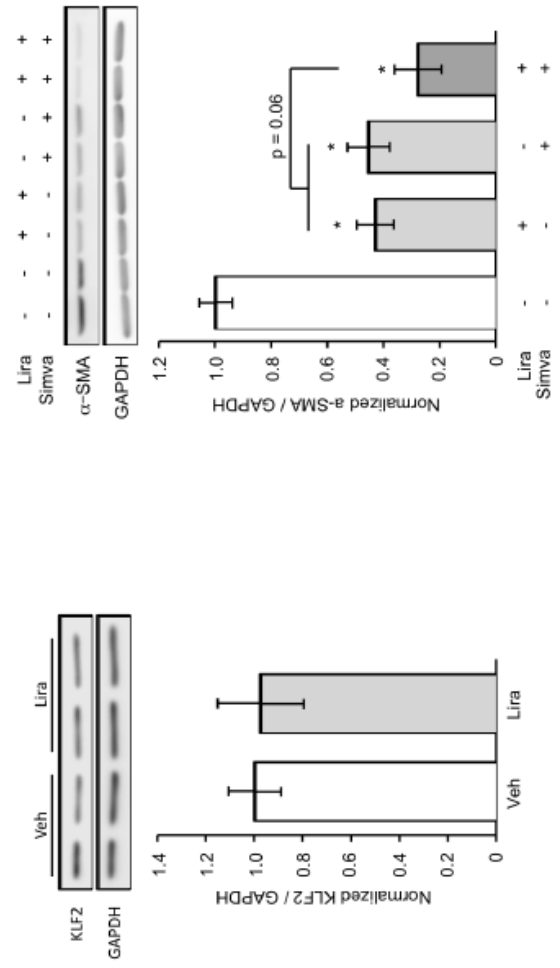

Supplementary figure 5.

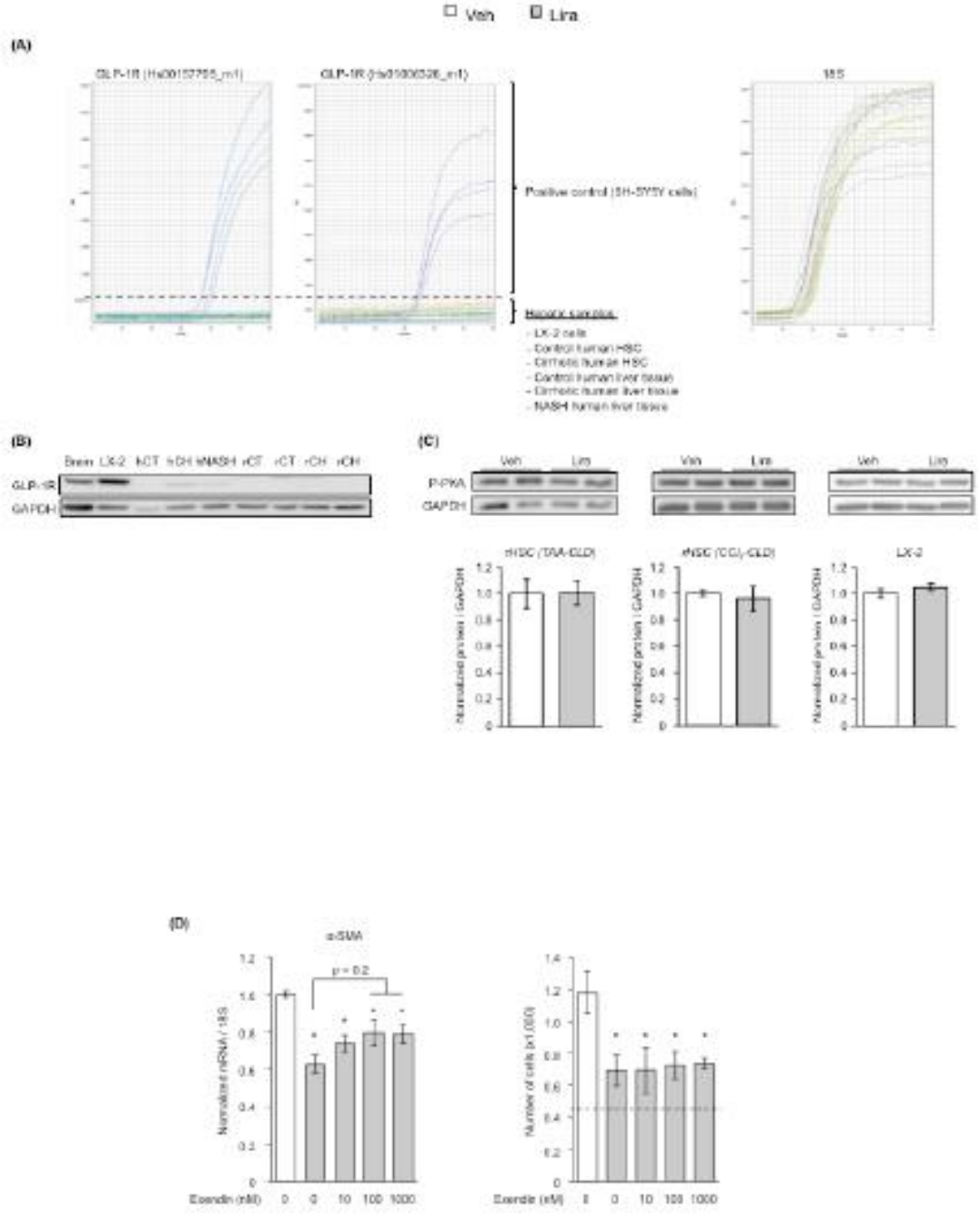

Supplementary figure 6.

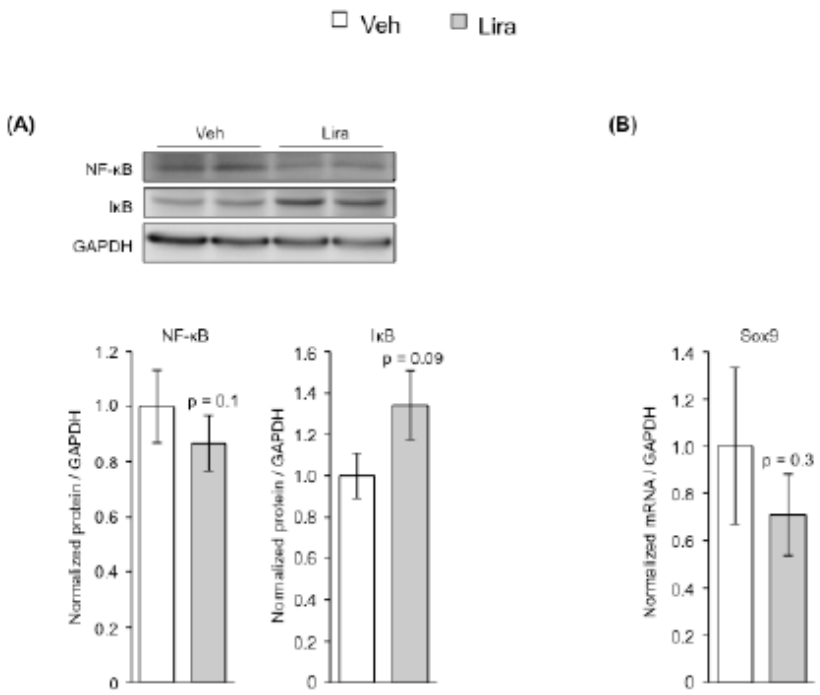

CAPÍTULO III

CONSIDERAÇÕES FINAIS

5. Considerações finais

A cirrose hepática é hoje um dos problemas mais graves de saúde pública e ocupa a oitava posição no ranking de mortalidade no Brasil, além do segundo lugar em casos de transplantes, perdendo somente para transplante renal, de acordo com o Registro Brasileiro de Transplantes de 2016. A busca por novos medicamentos que sejam capazes de tratar ou até mesmo reduzir a progressão da doença com efeitos colaterais reduzidos é de grande importância para o meio científico. Para isso, decidimos avaliar a ação da liraglutida como antifibrótico, já que este é um fármaco aprovado por EMA/FDA/ANVISA com comprovada segurança terapêutica e que possui efeitos anti-inflamatórios e antioxidantes. Estes efeitos são pontos chaves na inibição da progressão das doenças crônicas do fígado.

O primeiro objetivo deste trabalho foi realizar experimentos *in vitro* para avaliar se a liraglutida poderia ter alguma ação sob as células hepáticas estreladas, as quais estão diretamente envolvidas com o processo de iniciação e perpetuação da fibrose hepática. Iniciamos a pesquisa buscando concentrações não citotóxicas de liraglutida, através de uma curva de concentração nas células GRX (HSC murinas). Na figura 1 podemos ver que a liraglutida nas concentrações de 12,5, 25 e 50μM diminuiu significantemente a proliferação das células GRX. As concentrações escolhidas para os experimentos seguintes foram 12,5μM e 25μM, já que estas foram as mais baixas com ação efetiva.

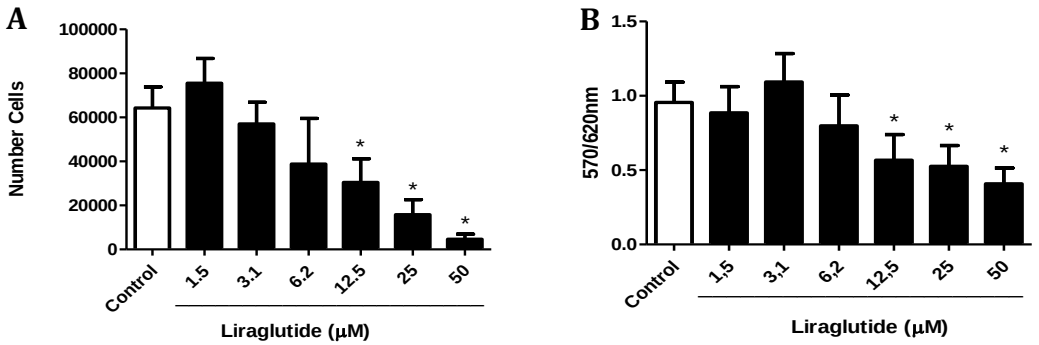

Figura 1 - Efeito da liraglutida sob as células GRX. Viabilidade celular por contagem através do método do Trypan Blue (A) e pelo método de Cristal Violeta (B). Dados apresentados pela média ± SD (n=3). *p<0,05 comparado ao controle.

Sabendo que as HSC quando ativadas perdem sua capacidade de acumular vitamina A, o próximo passo do trabalho foi analisar essas mudanças fenotípicas nas células GRX tratadas com liraglutida. Realizamos então, o experimento do *Oil Red O* (56) e obtivemos resultados consistentes que demonstravam o aparecimento de gotículas de gordura (figura 2A, B, C), com um importante aumento na quantidade de lipídios das células tratadas com liraglutida (figura 2D), associado a redução da proliferação celular, já mencionada anteriormente (figura 1). Estes resultados são fortes evidências da reversão do fenótipo ativado das HSC (característico das GRX), ao fenótipo de células quiescentes.

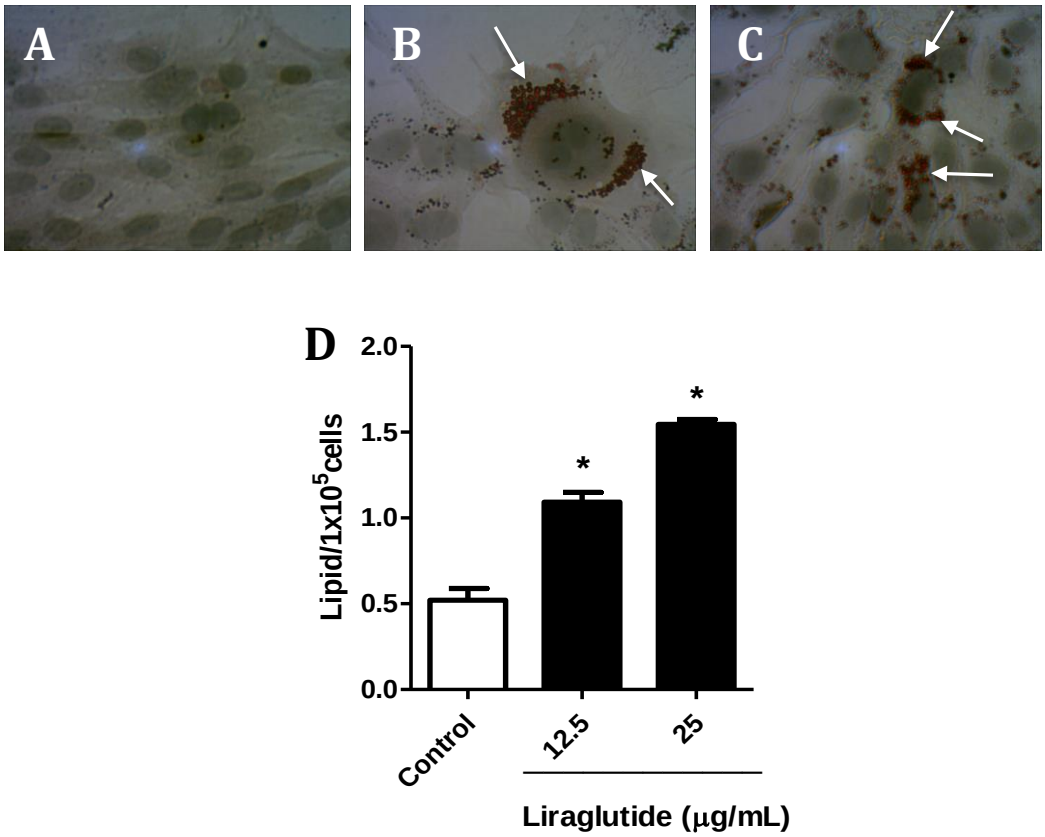

Figura 2 - Método do Oil Red-O (ORO) em células GRX sem tratamento (A) e tratadas com liraglutida 12.5µM (B) e 25µM (C). Avaliação do conteúdo lipídico em células GRX. Dados foram expressos espectrofotometricamente como a razão dos valores obtidos por ORO e Coomassie brilliant blue (D). Resultados expressos pela média ± SD. *p<0,05 comparado ao controle.

Seguimos buscando por mecanismos que fossem capazes de explicar e desvendar por quais rotas celulares a liraglutida estava promovendo os efeitos benéficos nessas células. Então, realizamos o experimento do DPPH (57) e

comprovamos por este método que a liraglutida não é uma molécula antioxidante (figura 3). Mesmo que alguns artigos mostrem diminuição de EROs em modelos experimentais tratados com liraglutida, com este dado, eliminamos a hipótese de que esses efeitos benéficos poderiam ser causados por uma ação antioxidante direta.

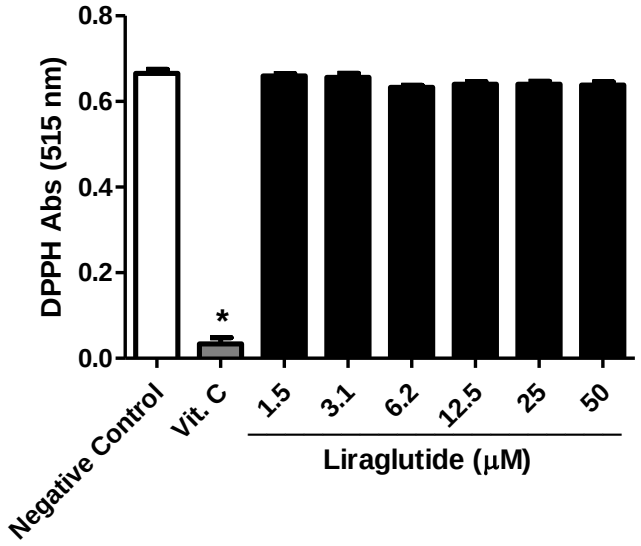

Figura 3 - Avaliação do potencial antioxidante através do método do DPPH. Resultados expressos pela média ± SD. *p<0,05 comparado ao controle.

O próximo passo seria a avaliação de mecanismos celulares envolvidos em rotas de proliferação celular e que seriam realizados durante o período de doutorado sanduiche na Espanha. Porém, a necessidade de outros tipos celulares de HSC que comprovassem os efeitos obtidos nas GRX, fez com que buscássemos por mais pesquisadores que trabalhassem com células hepáticas, permitindo assim um estudo mais completo e com comprovação efetiva dos efeitos antifibróticos da liraglutida. A colaboração com o laboratório na Espanha nos permitiu seguir o trabalho com um perfil mais clínico. E assim foi possível testar os efeitos da liraglutida em HSC isoladas de humanos e de ratos, além de experimentos com tecido fresco de fígado humano e estudos *in vivo* com ratos.

HSC quando se diferenciam em células ativadas apresentam elevados níveis de α-SMA e este marcador está diretamente relacionado com o desenvolvimento da fibrogenese experimental hepática, além da produção exarcebada de colágeno.

Então, para confirmar os efeitos de mudança de fenótipo das HSC tratadas com liraglutida avaliamos α-SMA e colágeno em oito modelos diferentes, incluindo tratamentos *in vitro* e *in vivo*. O tratamento com liraglutida foi capaz de reverter estes marcadores em todos os modelos, variando somente em intensidade:

Tratamento *in vitro:*

- Linhagem celular de HSC ativadas humanas (LX-2)
- HSC humanas → Pacientes com cirrose (hHSC ativadas)
  → Pacientes saudáveis com ativação in vitro das células
- HSC de ratos → Animais cirróticos (rHSC ativadas)
  → Animais saudáveis com ativação in vitro das células
- PCLS - Cortes precisos de fígado humano cirrótico posteriormente tratados com liraglutida

Tratamento *in vivo:*

- Tecido hepático de ratos que receberam liraglutida via subcutânea
- HSC ativadas isoladas de animais que receberam liraglutida via subcutânea

A análise de α-SMA em todas estas condições é de grande importância pois confirma que este efeito benéfico é independente do modelo experimental e não somente em um tipo celular.

A liraglutida também foi capaz de reduzir a proliferação das HSC ativadas, por consequência da redução de PDGFβR, sem ativar mecanismos de apoptose e/ou necrose. Além disso, reduziu a capacidade de contração celular das HSC, o que contribui para a melhoria do fenótipo das HSC. Estas células também apresentaram redução de marcadores fibróticos, como TGFβ e inflamatórios, como TNF-α. Estes dados corroboram com os primeiros resultados encontrados nas GRX já que a reversão do fenótipo dessas células, implica na redução da proliferação e de processos inflamatórios.

Seguimos com experimentos *in vivo* e tratamos os animais cirróticos com liraglutida ou solução fisiológica. Analisamos primeiramente a hemodinâmica

hepática, começando pela hipertensão portal que é uma grave consequência de pacientes cirróticos. Os animais apresentaram redução da pressão portal (PP) com manutenção do fluxo sanguíneo portal (PBF). Baseado na lei de Ohm, a diferença de pressão (ΔP) no sistema portal como em qualquer outro sistema vascular, é o resultado da interação entre o fluxo sanguíneo (Q) e a resistência vascular (R) que se opõe a esse fluxo e é representada matematicamente por ΔP= Q x R. Assim, sugerimos que a liraglutida pode ser capaz de reduzir a resistência hepática, em consequência da redução da pressão portal.

Nós também avaliamos a variação da pressão portal em resposta a diferentes doses de acetilcolina e é possível perceber que animais que receberam liraglutida possuem uma melhor capacidade vasodilatadora do que os animais tratados somente com o veículo do fármaco. Fizemos análise histológica do fígado que apresentou reduzida marcação de colágeno, porém sem diferença estatística nas metaloproteinases, inibidores das metaloproteinases e em desmina (marcador de HSC de ratos).

Observamos também uma redução significativa no peso destes animais, dado já descrito por muitos pesquisadores e que levou à industria farmacêutica a desenvolver uma nova formulação, com mesmo princípio ativo, para controle da obesidade. Marcadores bioquímicos como, AST, ALT, albumina, colesterol, triglicerídeos e ácidos graxos livres não apresentaram diferença estatística entre os animais tratados com liraglutida ou veículo.

O *crosstalk celular* entre HSC e LSEC tem sido recentemente descrito e é importante para manutenção das funções hepáticas normais e para que as células hepáticas sobrevivam. Na presença de lesão hepática, as LSEC tornam-se rapidamente desreguladas e iniciam a diferenciação para um fenótipo capilarizado. Sabendo disso, nós avaliamos a capilarização endotelial e percebemos que os animais tratados com liraglutida apresentam melhora dessa condição, pois possuem aumento na porosidade e na frequência das fenestras, além do aumento da biodisponibilidade de óxido nítrico (NO). Estudos sugerem que na cirrose ocorre diminuição intra-hepática de NO e que esse seria o principal fator responsável pelo aumento da resistência vascular intra-hepática.

Por fim, decidimos estudar por qual mecanismo a liraglutida possui estes efeitos benéficos. Como a liraglutida é um análogo do receptor do GLP-1, primeiramente tentamos inibir o receptor através da administração de Exendin9-39, um fragmento que se liga ao receptor e por mecanismo de competição impede a ligação da liraglutida. Porém, mesmo com doses altas de Exendin9-39 e administrando 10 minutos antes de liraglutida, não conseguimos impedir os efeitos da liraglutida.

A presença do receptor de GLP-1 no fígado ainda é uma informação controversa. A maioria dos artigos relatam sua ausência, porém em 2010 Gupta e colaboradores descrevem a presença do receptor em hepatócitos. Sabendo disso, decidimos avaliar a expressão do GLP1R nas nossas amostras e não encontramos este receptor em nenhuma amostra hepática, incluindo tecido hepático humano, mesmo utilizando duas sondas diferentes para real-time e estendendo a reação até 60 ciclos. Além disso quando a rota de GLP-1R é ativada, ocorre aumento de PKA (proteína quinase A, também chamada de proteína quinase dependente do AMP cíclico). Este aumento não foi observado nas amostras tratadas com liraglutida, portanto nós sugerimos que a liraglutida não atua através do receptor de GLP-1.

Após este resultado, buscamos outros possíveis mecanismos para esta ação da liraglutida. Gaspari e colaboradores em 2011 (58) descrevem que a liraglutida pode atuar via NFκB e portanto, decidimos analisar esta rota. De fato, a liraglutida aumenta a expressão de IκB e reduz NFκB e seu gene alvo Sox9, sugerindo que a liraglutida possa estar atuando por esta via. Para confirmar este resultado, tentamos avaliar a translocação do NFκB para o núcleo, porém por problemas técnicos não obtivemos êxito e decidimos não colocar este resultado no artigo científico. Ainda assim, sugerimos que no cenário específico de CLD a liraglutida melhora o fenótipo das HSC e a microcirculação hepática através de um mecanismo independente de GLP-1R e a via NF-κB-Sox9 é um forte candidato para mediar, pelo menos em parte, estes efeitos.

Após o término deste artigo e sabendo da ação antinflamatória em modelos de doenças neurodegenerativas, resolvemos avaliar o seu efeito no controle da apoptose e formação dos NETs de neutrófilos e na imunomodulação de células

mononucleares. Novos fármacos com poder de modular a resposta excessiva do hospedeiro estão sendo vistas como estratégias para mudar e melhorar os resultados dos tratamentos de doenças inflamatórias. Porém, nossos resultados demonstraram que a liraglutida não interfere no efeito do LPS em neutrófilos (figura 4) e só foi capaz de reduzir a proliferação dos linfócitos (figura 5) induzidos por PHA, em concentrações tóxicas. Portanto, concluímos que a liraglutida não impede a apoptose neutrofílica causada pelo LPS, nem possui efeito imunomodulador nos linfócitos. Por esta razão, não prosseguimos com esta linha de investigação.

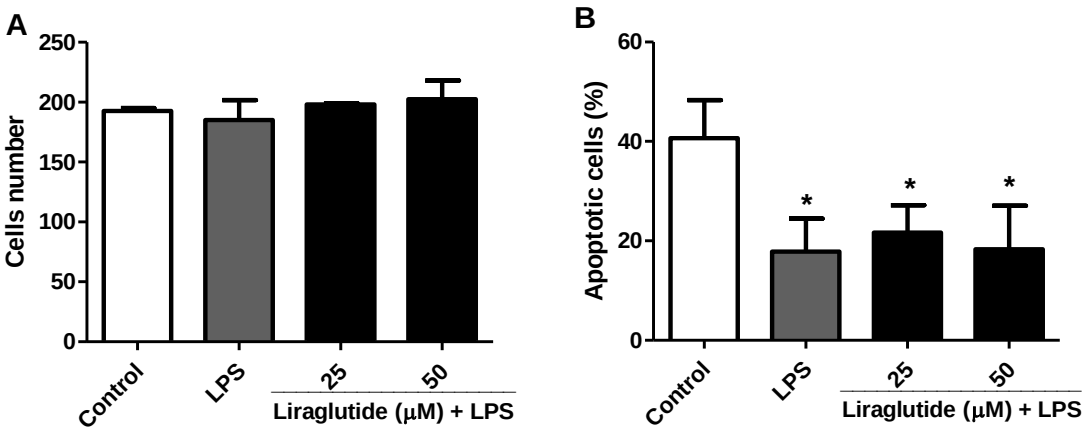

Figura 4 - Efeito da liraglutida, LPS e associação de ambos sob a viabilidade (A) e apoptose (B) de neutrófilos. Resultados expressos pela média ± SD. *p<0,05 comparado ao controle.

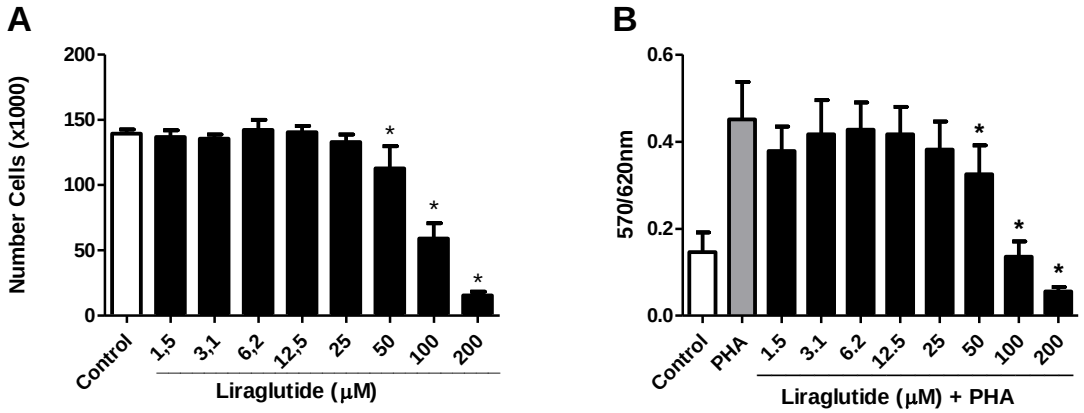

Figura 5 - Efeito da liraglutida sob a viabilidade de células mononucleares, predominantemente linfócitos (A) e linfoproliferação (B). Resultados expressos pela média ± SD. *p<0,05 comparado ao controle.

Com este trabalho concluímos que a liraglutida possui ação efetiva na redução da fibrose hepática, pela desativação das HSC, e que não possui ação direta como imunomodulador, nem impede a apoptose neutrofílica induzida por LPS. Na figura 6 mostramos o racional dos principais resultados obtidos.

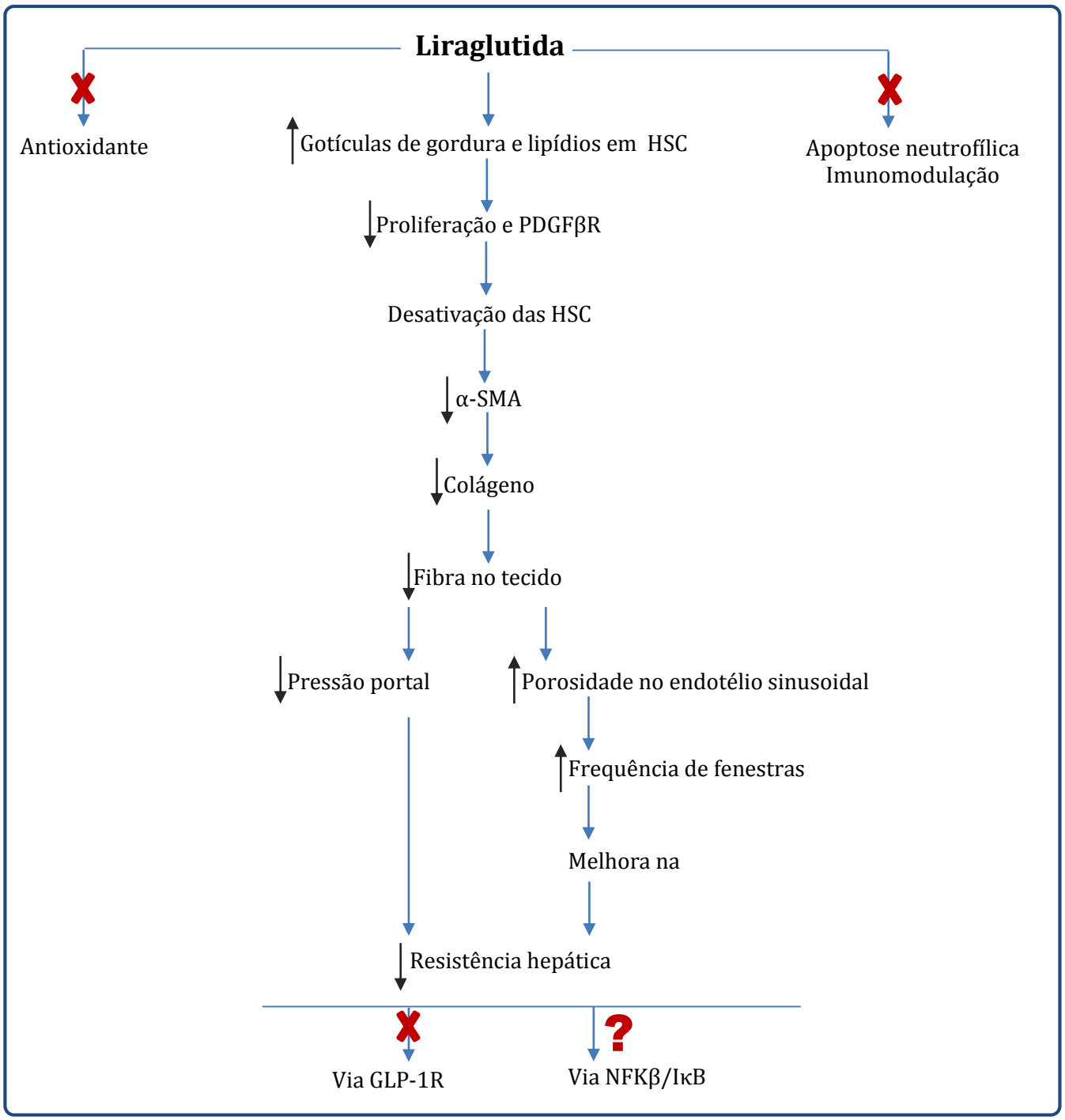

Figura 6 - Resumo esquemático das principais ações da Liraglutida estudadas. A Liraglutida desativa as HSC, o que leva a redução da fibrose, pressão portal e resistência hepática. Estes efeitos parecem ser através da redução de NFK β e independentes do receptor de GLP-1. A Liraglutida não demonstrou efeitos diretos como antioxidante, imunomodulador ou com capacidade de impedir a apoptose neutrofílica.

6. Referências

1. Friedman SL. Hepatic fibrosis -- overview. Toxicology. 2008;254(3):120-9. Epub 2008/07/30.
2. Friedman SL. Mechanisms of hepatic fibrogenesis. Gastroenterology. 2008;134(6):1655-69. Epub 2008/05/13.
3. Gressner AM. The cell biology of liver fibrogenesis - an imbalance of proliferation, growth arrest and apoptosis of myofibroblasts. Cell and tissue research. 1998;292(3):447-52. Epub 1998/06/24.
4. Hernandez-Gea V, Friedman SL. Pathogenesis of liver fibrosis. Annual review of pathology. 2011;6:425-56. Epub 2010/11/16.
5. Jang JY, Chung RT. Chronic hepatitis C. Gut and liver. 2011;5(2):117-32. Epub 2011/08/05.
6. Mormone E, George J, Nieto N. Molecular pathogenesis of hepatic fibrosis and current therapeutic approaches. Chemico-biological interactions. 2011;193(3):225-31. Epub 2011/08/02.
7. Krizhanovsky V, Yon M, Dickins RA, Hearn S, Simon J, Miething C, et al. Senescence of activated stellate cells limits liver fibrosis. Cell. 2008;134(4):657-67. Epub 2008/08/30.
8. Bosch J, Garcia-Pagan JC. Complications of cirrhosis. I. Portal hypertension. Journal of hepatology. 2000;32(1 Suppl):141-56. Epub 2000/03/23.
9. Fallowfield J, Hayes P. Pathogenesis and treatment of hepatic fibrosis: is cirrhosis reversible? Clin Med. 2011;11(2):179-83. Epub 2011/04/30.
10. Iredale J. Defining therapeutic targets for liver fibrosis: exploiting the biology of inflammation and repair. Pharmacological research. 2008;58(2):129-36. Epub 2008/07/26.
11. Sarem M, Znaidak R, Macias M, Rey R. [Hepatic stellate cells: it's role in normal and pathological conditions]. Gastroenterologia y hepatologia. 2006;29(2):93-101. Epub 2006/02/02. Las celulas estrelladas del higado: su importancia en condiciones normales y patologicas.
12. Senoo H. Structure and function of hepatic stellate cells. Medical electron microscopy : official journal of the Clinical Electron Microscopy Society of Japan. 2004;37(1):3-15. Epub 2004/04/02.
13. Winau F, Quack C, Darmoise A, Kaufmann SH. Starring stellate cells in liver immunology. Current opinion in immunology. 2008;20(1):68-74. Epub 2007/12/11.
14. Vicente CP, Fortuna VA, Margis R, Trugo L, Borojevic R. Retinol uptake and metabolism, and cellular retinol binding protein expression in an in vitro model of hepatic stellate cells. Molecular and cellular biochemistry. 1998;187(1-2):11-21. Epub 1998/10/27.
15. Li JT, Liao ZX, Ping J, Xu D, Wang H. Molecular mechanism of hepatic stellate cell activation and antifibrotic therapeutic strategies. Journal of gastroenterology. 2008;43(6):419-28. Epub 2008/07/05.
16. Lee UE, Friedman SL. Mechanisms of hepatic fibrogenesis. Best practice & research Clinical gastroenterology. 2011;25(2):195-206. Epub 2011/04/19.

17. Hinz B, Celetta G, Tomasek JJ, Gabbiani G, Chaponnier C. Alpha-smooth muscle actin expression upregulates fibroblast contractile activity. Molecular biology of the cell. 2001;12(9):2730-41. Epub 2001/09/13.
18. Marrone G, Shah VH, Gracia-Sancho J. Sinusoidal communication in liver fibrosis and regeneration. Journal of hepatology. 2016;65(3):608-17. Epub 2016/05/07.
19. DeLeve LD, Wang X, Hu L, McCuskey MK, McCuskey RS. Rat liver sinusoidal endothelial cell phenotype is maintained by paracrine and autocrine regulation. American journal of physiology Gastrointestinal and liver physiology. 2004;287(4):G757-63. Epub 2004/06/12.
20. Malhi H, Guicciardi ME, Gores GJ. Hepatocyte death: a clear and present danger. Physiological reviews. 2010;90(3):1165-94. Epub 2010/07/29.
21. Canbay A, Feldstein AE, Higuchi H, Werneburg N, Grambihler A, Bronk SF, et al. Kupffer cell engulfment of apoptotic bodies stimulates death ligand and cytokine expression. Hepatology. 2003;38(5):1188-98. Epub 2003/10/28.
22. Jiang JX, Mikami K, Venugopal S, Li Y, Torok NJ. Apoptotic body engulfment by hepatic stellate cells promotes their survival by the JAK/STAT and Akt/NF-kappaB-dependent pathways. Journal of hepatology. 2009;51(1):139-48. Epub 2009/05/22.
23. McGuire RF, Bissell DM, Boyles J, Roll FJ. Role of extracellular matrix in regulating fenestrations of sinusoidal endothelial cells isolated from normal rat liver. Hepatology. 1992;15(6):989-97. Epub 1992/06/01.
24. Gupta TK, Chen L, Groszmann RJ. Pathophysiology of portal hypertension. Clinics in liver disease. 1997;1(1):1-12. Epub 1997/05/01.
25. Reynaert H, Thompson MG, Thomas T, Geerts A. Hepatic stellate cells: role in microcirculation and pathophysiology of portal hypertension. Gut. 2002;50(4):571-81. Epub 2002/03/13.
26. Pinzani M. Hepatic stellate (ITO) cells: expanding roles for a liver-specific pericyte. Journal of hepatology. 1995;22(6):700-6. Epub 1995/06/01.
27. Friedman SL. Molecular regulation of hepatic fibrosis, an integrated cellular response to tissue injury. The Journal of biological chemistry. 2000;275(4):2247-50. Epub 2000/01/25.
28. Yoon YJ, Friedman SL, Lee YA. Antifibrotic Therapies: Where Are We Now? Seminars in liver disease. 2016;36(1):87-98. Epub 2016/02/13.
29. Lee YA, Wallace MC, Friedman SL. Pathobiology of liver fibrosis: a translational success story. Gut. 2015;64(5):830-41. Epub 2015/02/15.
30. Mihos CG, Pineda AM, Santana O. Cardiovascular effects of statins, beyond lipid-lowering properties. Pharmacological research. 2014;88:12-9. Epub 2014/03/19.
31. Marrone G, Maeso-Diaz R, Garcia-Cardena G, Abraldes JG, Garcia-Pagan JC, Bosch J, et al. KLF2 exerts antifibrotic and vasoprotective effects in cirrhotic rat livers: behind the molecular mechanisms of statins. Gut. 2015;64(9):1434-43. Epub 2014/12/17.
32. Trebicka J, Hennenberg M, Odenthal M, Shir K, Klein S, Granzow M, et al. Atorvastatin attenuates hepatic fibrosis in rats after bile duct ligation via decreased turnover of hepatic stellate cells. Journal of hepatology. 2010;53(4):702-12. Epub 2010/07/17.

33. Watts KL, Sampson EM, Schultz GS, Spiteri MA. Simvastatin inhibits growth factor expression and modulates profibrogenic markers in lung fibroblasts. American journal of respiratory cell and molecular biology. 2005;32(4):290-300. Epub 2005/01/29.
34. Reddy R, Chahoud G, Mehta JL. Modulation of cardiovascular remodeling with statins: fact or fiction? Current vascular pharmacology. 2005;3(1):69-79. Epub 2005/01/11.
35. Shiraki A, Oyama J, Komoda H, Asaka M, Komatsu A, Sakuma M, et al. The glucagon-like peptide 1 analog liraglutide reduces TNF-alpha-induced oxidative stress and inflammation in endothelial cells. Atherosclerosis. 2012;221(2):375-82. Epub 2012/01/31.
36. Vella A, Shah P, Reed AS, Adkins AS, Basu R, Rizza RA. Lack of effect of exendin-4 and glucagon-like peptide-1-(7,36)-amide on insulin action in non-diabetic humans. Diabetologia. 2002;45(10):1410-5. Epub 2002/10/16.
37. Agerso H, Vicini P. Pharmacodynamics of NN2211, a novel long acting GLP-1 derivative. European journal of pharmaceutical sciences : official journal of the European Federation for Pharmaceutical Sciences. 2003;19(2-3):141-50. Epub 2003/06/07.
38. Ishii H, Sato Y, Takei M, Nishio S, Komatsu M. Glucose-incretin interaction revisited. Endocrine journal. 2011;58(7):519-25. Epub 2011/06/28.
39. Holst JJ. The physiology of glucagon-like peptide 1. Physiological reviews. 2007;87(4):1409-39. Epub 2007/10/12.
40. Ceriello A, Esposito K, Testa R, Bonfigli AR, Marra M, Giugliano D. The possible protective role of glucagon-like peptide 1 on endothelium during the meal and evidence for an "endothelial resistance" to glucagon-like peptide 1 in diabetes. Diabetes care. 2011;34(3):697-702. Epub 2011/01/29.
41. Nystrom T, Gutniak MK, Zhang Q, Zhang F, Holst JJ, Ahren B, et al. Effects of glucagon-like peptide-1 on endothelial function in type 2 diabetes patients with stable coronary artery disease. American journal of physiology Endocrinology and metabolism. 2004;287(6):E1209-15. Epub 2004/09/09.
42. Noyan-Ashraf MH, Momen MA, Ban K, Sadi AM, Zhou YQ, Riazi AM, et al. GLP-1R agonist liraglutide activates cytoprotective pathways and improves outcomes after experimental myocardial infarction in mice. Diabetes. 2009;58(4):975-83. Epub 2009/01/20.
43. McClean PL, Holscher C. Liraglutide can reverse memory impairment, synaptic loss and reduce plaque load in aged APP/PS1 mice, a model of Alzheimer's disease. Neuropharmacology. 2013;76 Pt A:57-67. Epub 2013/08/27.
44. Parthsarathy V, Holscher C. The type 2 diabetes drug liraglutide reduces chronic inflammation induced by irradiation in the mouse brain. European journal of pharmacology. 2013;700(1-3):42-50. Epub 2013/01/02.
45. Iwai T, Ito S, Tanimitsu K, Udagawa S, Oka J. Glucagon-like peptide-1 inhibits LPS-induced IL-1beta production in cultured rat astrocytes. Neuroscience research. 2006;55(4):352-60. Epub 2006/05/25.
46. Gupta NA, Mells J, Dunham RM, Grakoui A, Handy J, Saxena NK, et al. Glucagon-like peptide-1 receptor is present on human hepatocytes and has a direct role in

decreasing hepatic steatosis in vitro by modulating elements of the insulin signaling pathway. Hepatology. 2010;51(5):1584-92. Epub 2010/03/13.
47. Pyke C, Heller RS, Kirk RK, Orskov C, Reedtz-Runge S, Kaastrup P, et al. GLP-1 receptor localization in monkey and human tissue: novel distribution revealed with extensively validated monoclonal antibody. Endocrinology. 2014;155(4):1280-90. Epub 2014/01/29.
48. Wang XC, Gusdon AM, Liu H, Qu S. Effects of glucagon-like peptide-1 receptor agonists on non-alcoholic fatty liver disease and inflammation. World journal of gastroenterology. 2014;20(40):14821-30. Epub 2014/10/31.
49. Armstrong MJ, Gaunt P, Aithal GP, Barton D, Hull D, Parker R, et al. Liraglutide safety and efficacy in patients with non-alcoholic steatohepatitis (LEAN): a multicentre, double-blind, randomised, placebo-controlled phase 2 study. Lancet. 2016;387(10019):679-90. Epub 2015/11/27.
50. Kieffer TJ, McIntosh CH, Pederson RA. Degradation of glucose-dependent insulinotropic polypeptide and truncated glucagon-like peptide 1 in vitro and in vivo by dipeptidyl peptidase IV. Endocrinology. 1995;136(8):3585-96. Epub 1995/08/01.
51. Deacon CF, Johnsen AH, Holst JJ. Degradation of glucagon-like peptide-1 by human plasma in vitro yields an N-terminally truncated peptide that is a major endogenous metabolite in vivo. The Journal of clinical endocrinology and metabolism. 1995;80(3):952-7. Epub 1995/03/01.
52. Ban K, Noyan-Ashraf MH, Hoefer J, Bolz SS, Drucker DJ, Husain M. Cardioprotective and vasodilatory actions of glucagon-like peptide 1 receptor are mediated through both glucagon-like peptide 1 receptor-dependent and -independent pathways. Circulation. 2008;117(18):2340-50. Epub 2008/04/23.
53. Gaspari T, Brdar M, Lee HW, Spizzo I, Hu Y, Widdop RE, et al. Molecular and cellular mechanisms of glucagon-like peptide-1 receptor agonist-mediated attenuation of cardiac fibrosis. Diabetes & vascular disease research. 2016;13(1):56-68. Epub 2015/09/27.
54. McClean PL, Jalewa J, Holscher C. Prophylactic liraglutide treatment prevents amyloid plaque deposition, chronic inflammation and memory impairment in APP/PS1 mice. Behavioural brain research. 2015;293:96-106. Epub 2015/07/25.
55. Gao H, Zeng Z, Zhang H, Zhou X, Guan L, Deng W, et al. The Glucagon-Like Peptide-1 Analogue Liraglutide Inhibits Oxidative Stress and Inflammatory Response in the Liver of Rats with Diet-Induced Non-alcoholic Fatty Liver Disease. Biological & pharmaceutical bulletin. 2015;38(5):694-702. Epub 2015/05/08.
56. Ramirez-Zacarias JL, Castro-Munozledo F, Kuri-Harcuch W. Quantitation of adipose conversion and triglycerides by staining intracytoplasmic lipids with Oil red O. Histochemistry. 1992;97(6):493-7. Epub 1992/07/01.
57. Kedare SB, Singh RP. Genesis and development of DPPH method of antioxidant assay. Journal of food science and technology. 2011;48(4):412-22. Epub 2011/08/01.
58. Gaspari T, Liu H, Welungoda I, Hu Y, Widdop RE, Knudsen LB, et al. A GLP-1 receptor agonist liraglutide inhibits endothelial cell dysfunction and vascular adhesion molecule expression in an ApoE-/- mouse model. Diabetes & vascular disease research. 2011;8(2):117-24. Epub 2011/05/13.

7. Anexo

Artigo original realizado durante o doutorado-sanduiche em Barcelona/Espanha em parceria com o laboratório de Hemodinâmica Hepática, IDIBAPS – Hospital Clinic – CIBEREHD. Publicado em janeiro de 2017, no periódico *Journal of Hepatology* com fator de impacto 10,590.

Research Article

JOURNAL OF HEPATOLOGY

Cross-talk between autophagy and KLF2 determines endothelial cell phenotype and microvascular function in acute liver injury

Sergi Guixé-Muntet[1], Fernanda Cristina de Mesquita[1,2], Sergi Vila[1], Virginia Hernández-Gea[1], Carmen Peralta[3], Juan Carlos García-Pagán[1], Jaime Bosch[1], Jordi Gracia-Sancho[1,*]

[1]Barcelona Hepatic Hemodynamic Lab., IDIBAPS – Hospital Clínic – CIBEREHD, University of Barcelona Medical School, Barcelona, Spain; [2]Laboratório de Biofísica Celular e Inflamação, Pontificia Universidade Católica do Rio Grande do Sul, PUCRS, Porto Alegre, RS, Brazil; [3]IDIBAPS & CIBEREHD, Spain

Background & Aims: The transcription factor Krüppel-like factor 2 (KLF2), inducible by simvastatin, confers endothelial vasoprotection. Considering recent data suggesting activation of autophagy by statins, we aimed to: 1) characterize the relationship between autophagy and KLF2 in the endothelium, 2) assess this relationship in acute liver injury (cold ischemia/reperfusion) and 3) study the effects of modulating KLF2-autophagy *in vitro* and *in vivo*.

Methods: Autophagic flux, the vasoprotective KLF2 pathway, cell viability and microvascular function were assessed in endothelial cells and in various pre-clinical models of acute liver injury (cold storage and warm reperfusion).

Results: Positive feedback between autophagy and KLF2 was observed in the endothelium: KLF2 inducers, pharmacological (statins, resveratrol, GGTI-298), biomechanical (shear stress) or genetic (adenovirus containing KLF2), caused endothelial KLF2 overexpression through a Rac1-rab7-autophagy dependent mechanism, both in the specialized liver sinusoidal endothelial cells (LSEC) and in human umbilical vein endothelial cells. In turn, KLF2 induction promoted further activation of autophagy.

Cold ischemia blunted autophagic flux. Upon reperfusion, LSEC stored in University of Wisconsin solution did not reactivate autophagy, which resulted in autophagosome accumulation probably due to impairment in autophagosome-lysosome fusion, ultimately leading to increased cell death and microvascular dysfunction.

Simvastatin pretreatment maintained autophagy (through the upregulation of rab7), resulting in increased KLF2, improved cell viability, and ameliorated hepatic damage and microvascular function.

Conclusions: We herein describe for the first time the complex autophagy-KLF2 relationship, modulating the phenotype and survival of the endothelium. These results help understanding the mechanisms of protection conferred by KLF2-inducers, such as simvastatin, in hepatic vascular disorders.

Keywords: Statins; Simvastatin; Ischemia/reperfusion; LSEC; HUVEC; Rab7; Rac1.
Received 21 December 2015; received in revised form 27 July 2016; accepted 30 July 2016; available online 18 August 2016

* Corresponding author. Address: Barcelona Hepatic Hemodynamic Lab., Rosselló 149, 4th floor, 08036 Barcelona, Spain. Tel.: +34 932275707x4306.
E-mail address: jordi.gracia@idibaps.org (J. Gracia-Sancho).

Lay summary: Autophagy and the transcription factor KLF2 share a common activation pathway in the endothelium, being able to regulate each other.

Statins maintain microvascular function through the inhibition of Rac1, which consequently liberates Rab7, activates autophagy and increments the expression of KLF2.

Introduction

Autophagy is a constitutive process that maintains cellular homeostasis in a wide variety of cell types through the encapsulation of damaged proteins or organelles in double-membrane vesicles called autophagosomes, which fusing with lysosomes allow degradation of the cargo. As a result, cells obtain amino-acids, lipids and other components that will serve as a source of energy and new building blocks for synthesis. Regulation of autophagy is complex since it shares molecular signaling with cell proliferation and apoptosis [1,2]. Cells activate autophagy as a mechanism of cellular recycling and survival in response to cellular stresses like low nutrients, low ATP or hypoxia [3,4].

Autophagy plays a role in the pathophysiology of diverse liver diseases, including non-alcoholic steatohepatitis, viral hepatitis, fibrosis, and hepatocellular carcinoma [5–7]. However, there is no consensus about the role of autophagy in ischemia and reperfusion injury, where autophagy may be differentially regulated, and have opposite effects, depending on type of ischemia (warm or cold) or the preservation solution used [7–11]. Moreover, the possible role of autophagy in the maintenance of liver sinusoidal endothelial cells (LSEC) phenotype is completely unknown.

The vasoprotective transcription factor Krüppel-like factor 2 (KLF2) is expressed in the liver endothelium in response to blood flow-derived shear stress and plays a key role in the pathophysiology of hepatic ischemia and reperfusion injury [12,13]. In fact, when the liver is ischemic due to cold preservation or to surgical procedures, the endothelium rapidly loses its KLF2 expression leading to the dysregulation of its specialized phenotype (capillarization), development of hepatic microvascular dysfunction, and ultimately hepatic injury.

Pharmacologically, KLF2 can be efficiently induced by statins. Although these FDA/EMA approved drugs were designed to reduce cholesterol synthesis, several reports demonstrated that statins are potent KLF2 activators independently of their lipid lowering effects but dependent on the geranylgeranyl-pyrophosphate (GGPP) pathway [14,15]. In the field of acute liver injury, previous studies demonstrated that simvastatin protects healthy and steatotic rat livers through the maintenance of LSEC vasoprotective phenotype [13.16.17].

Considering this background and recent studies suggesting that KLF2 activators such as simvastatin and resveratrol might be able to increase autophagic flux in the endothelium [18–20], and that autophagy is required for the endothelium to respond to shear stress [21], the present study aimed at: 1) characterizing the possible cross-link between autophagy and KLF2 in the endothelium; 2) defining endothelial autophagy in the context of liver ischemia/reperfusion; and 3) modulating hepatic autophagy *in vitro* and *ex vivo* to revert the negative effects of ischemia/reperfusion.

Materials and methods

Animals

Male Wistar rats (Charles River) weighting 300–350 g were kept in environmentally controlled facilities at the IDIBAPS. All experiments were approved by the Laboratory Animal Care and Use Committee of the University of Barcelona and were conducted in accordance with the European Community guidelines for the protection of animals used for experimental and other scientific purposes (European Economic Community (EEC) Directive 86/609).

Liver sinusoidal endothelial cells (LSEC) isolation

Rat LSEC were isolated as described in Supplementary methods. LSEC used in the present study showed average viability of 96% (by trypan blue exclusion) and 92% purity (by acetylated-low density lipoprotein (Ac-LDL) incorporation and Reca-1 staining) [22,23].

In vitro cold ischemia and warm reperfusion (I/R)

Freshly isolated LSEC were washed twice with warm phosphate balanced saline (PBS) and cultured at 4 °C in cold Celsior or University of Wisconsin (UWS) solutions. Using an oxygen microsensor (Unisense OX-NP), O_2 availability was measured demonstrating that cold storage solutions have a 35% reduction in O_2 saturation in comparison to standard culture conditions, therefore ensuring an appropriate hypoxic environment.

After ischemia time, cells were washed twice with cold PBS and *in vitro* reperfusion was mimicked incubating LSEC in complete media during 2 h at 37 °C in normoxic humid atmosphere.

Endothelial cells treatments

Primary rat LSEC or human umbilical vein endothelial cells (HUVEC) (Lonza) were treated with 5 μM simvastatin (Calbiochem), 5 μM mevastatin (Calbiochem), 10 μM GGPP (Sigma), 5 μM GGTI-298 (Sigma), 20 μM chloroquine (CQ; Sigma), 2 μM rapamycin (Santa Cruz), 1 μM resveratrol (Sigma), 50 μM NSC23766 (Sigma) or 50 nM bafilomycin (Baf; Sigma) when appropriate. Drugs concentrations derive from previously published reports [14,19,23,24] or from preliminary studies performed by our team.

For each experiment, culture medium was aliquoted and complemented with the corresponding drug or vehicle and added to the corresponding wells. Results from endothelial cells derive from at least n = 3 independent experiments (different isolations for LSEC; different commercial batches for HUVEC always below passage 6) with n = 2–3 replicates for each experimental condition.

Adenoviral overexpression of KLF2

Cells were seeded at a 60% confluence in complete medium. At the time of infection, plates were washed twice with PBS and were incubated with 10 MOI of adenovirus containing KLF2 (Ad*KLF2*) or adenovirus containing green fluorescent protein (AdGFP) (kindly provided by Prof Garcia-Cardena) for 2 h in culture medium containing 2% FBS. After infection, the medium containing the adenovirus was removed and cells were incubated for 24 h [25].

Endothelial shear stress

HUVEC were seeded in gelatin-coated μSlide flow chambers (IBIDI) at a confluence of 100,000 cells/chamber and maintained at the incubator for 12 h. Afterwards, culture media (Medium 199 with 20% FBS, 2 mM L-glutamine, 1% penicillin/streptomycin, 0.1 mg/ml heparin, 0.05 mg/ml endothelial mitogen and 2% dextran) was added and cells were cultured for 24 h in static or dynamic conditions (12 dyn/cm^2) [23].

Endothelial viability

Cell death was analyzed by double staining with acridine orange and propidium iodide (AO-PI) and by trypan blue exclusion assay, as previously described [25]. Briefly, for AO-PI staining, endothelial cells were incubated with 800 ng/ml acridine orange and 5 μg/ml propidium iodide for 10 min. Plates were washed twice with PBS and complete Roswell Park Memorial Institute (RPMI) without phenol red media was added. Cells were observed with a fluorescence microscope (Olympus BX51 with a U-LH100HG light source). Four fields were randomly selected per well and pictures of visible light, green light (488 nm emission) and red light (555 nm emission) were taken at 200x magnification. Images were merged using ImageJ software (NIH). Cells stained in plain green were counted as viable, cells with bright and green dotted nuclei were counted as apoptotic, and cells stained in red were counted as necrotic.

The trypan blue exclusion assay was performed on plate. Trypan blue (Fluka) was added to the medium at a final concentration of 0.04 mg/ml. Cells were incubated at 37 °C for 10 min and pictures were taken for further analysis.

Two independent researchers (SG-M and FM) performed the analysis of all pictures blindly.

Immunofluorescence

Endothelial cells were seeded onto 12 mm confocal coverglasses (Electron Microscopy Sciences). At the end of treatments, cells were fixed with 4% paraformaldehyde for 10 min, rinsed with PBS and permeabilized with 0.1% triton X-100 (Sigma) for 5 min. Cells were blocked for 30 min with 1% BSA in PBS and subsequently incubated with primary antibodies against LC3B (1:200, cell signaling) and Lamp2 (1:50, Santa Cruz) overnight at 4 °C. Incubation with secondary antibodies conjugated with Alexa Fluor 488/555 (1:300, Invitrogen) was performed at room temperature for 1 h along with DAPI (3 ng/ml, Invitrogen). Preparations were then mounted using Fluoromount-G (Bionovacientifica) and dried overnight. Six images per preparation and channel (visible; green, 488 nm; red, 555 nm) were obtained with a spectral confocal microscope (Leica TCS-SP5). Images were then analyzed with the ImageJ software (NIH).

Ex vivo model of ischemia/reperfusion

Male Wistar rats (250–300 g; n = 8 per experimental condition) were pretreated with the autophagy inhibitor CQ (60 mg/kg, i.p., t = −24 h and −2 h) [26], or its vehicle, followed by the KLF2 inducer simvastatin (1 mg/kg, i.v., t = −1 h) or vehicle. Afterwards, rats were anesthetized with ketamine (80 mg/kg i.p; Merial Laboratories, Barcelona, Spain) + midazolam (5 mg/kg i.p; Laboratorios Reig Jofré, Barcelona, Spain). Livers were exsanguinated with Krebs buffer, flushed through the portal vein with 10 ml of ice-cold UWS and explanted. Grafts were kept submerged in this solution for 16 h and reperfused for 2 h with warm Krebs buffer [13,16]. Then, liver microvascular function was evaluated analyzing endothelium-dependent vasorelaxation to incremental doses of acetylcholine (10^{-7}–10^{-5} M) after pre-constriction with methoxamine (10^{-4} M) [27].

Samples of perfusion buffer and liver tissue were stored for molecular analyses.

mRNA and protein analysis

Please see Supplementary methods for detailed information regarding RNA extraction, qPCR and Western blotting.

LC3 turnover assay

Autophagic flux was calculated as the accumulation of autophagosomes after inhibition of autophagosomes-lysosomes fusion with CQ or Baf for 2 h. Autophagic flux = LC3-II (CQ or Baf)/glyceraldehyde 3-phosphate dehydrogenase (GAPDH) − LC3-II (vehicle)/GAPDH for each experimental condition.

Transmission electron microscopy

Livers were perfused through portal vein with a fixation solution containing 2.5% glutaraldehyde and 2% paraformaldehyde and fixed overnight at 4 °C. Samples were washed 3 times with 0.1 M cacodylate buffer. Liver sections were fixed with 1% osmium in cacodylate buffer and, after dehydration in acetone gradients, embedded in Spurr resin. Ultrathin sections (50 nm) were counterstained with uranyl acetate and lead citrate [28]. Samples were analyzed using a JEOL J1010 microscope and an ORIUS camera (Gatan, Inc.; Roper Technologies, Inc.). Ultrastructural analysis derived from n = 3 rats per group, with 3 different tissue areas from each liver and at least 10 pictures of each one.

Statistical analysis

Statistics were performed using the SPSS V.19.0 software for Windows (IBM, Armonk, New York, USA). All results are expressed as mean ± SEM. Comparisons between groups were performed as follows: normality was assessed using the Kolmogorov-Smirnov test. For experimental data following a normal distribution we performed the one-way ANOVA test followed by least significant difference (LSD) and Bonferroni *post hoc* tests. Otherwise, non-parametric Kruskal-Wallis test followed by Mann-Whitney *U* test were performed when groups did not follow normality. Differences were considered significant at a p value <0.05.

Results

KLF2 upregulation induces autophagy in endothelial cells

Effects of KLF2 upregulation on the autophagy axis were analyzed using pharmacological, adenoviral and biomechanical strategies. Treatment of primary LSEC with the KLF2 activators simvastatin and resveratrol did not modify the protein expression of the autophagosome-formation mediator Atg7, or the ubiquitin-binding autophagic adaptor p62, but significantly upregulated autophagic flux as demonstrated by the LC3 turnover assay and autophagosome-lysosome colocalization (Fig. 1A, B and Supplementary Fig. 1). Rapamycin was used as positive control, showing comparable activation of autophagy. Simvastatin effects on autophagic flux were validated using a different statin formulation, mevastatin (Supplementary Fig. 2).

Modulation of the KLF2 protective pathway by inhibiting geranylgeranylation with GGTI-298 (activator of KLF2) mimicked the effects of simvastatin on autophagy (Fig. 1C left), while addition of the KLF2 inhibitor GGPP abrogated simvastatin effects (Fig. 1C right).

In addition, specific KLF2 overexpression using adenoviral constructs codifying for this transcription factor (Ad*KLF2*) (Fig. 1D) or biomechanical stimulation by shear stress (Fig. 1E) markedly increased autophagic flux, altogether demonstrating that KLF2 *per se* activates autophagy in the endothelium.

Effects of I/R on endothelial viability and autophagy

LSEC cultured under cold ischemia conditions, without reperfusion, did not exhibit significant changes in viability when compared to controls. However, cells that after cold preservation were subsequently warm reperfused displayed increased cell death, as observed with double staining with AO-PI and by trypan blue exclusion assay, and its magnitude was dependent on time of ischemia (Fig. 2A, B).

Analysis of autophagic flux in LSEC undergoing I/R revealed profound inhibition of autophagy in response to cold ischemia (both at 6 h, 12 h or 24 h of cold storage) using either Celsior or UW solutions. Upon reperfusion, LSEC stored in Celsior reactivated autophagy in an ischemia time-dependent manner. However, those cells kept in UWS failed to reactivate autophagic flux. In fact, they displayed marked accumulation of autophagosomes, suggesting that fusion of autophagosomes with lysosomes was impaired under these conditions (Fig. 2C). *In vitro* culture of LSEC did not modify autophagy as demonstrated analyzing cells cultured in standard conditions during the same periods of time.

Simvastatin stimulates the KLF2-autophagy axis and improves cell viability in endothelial cells undergoing I/R

LSEC pretreated with simvastatin 1 h before undergoing UWS cold ischemia showed proper upregulation of KLF2, activation of autophagy, and consequently preservation of cell viability (Fig. 3A–C). The beneficial effects of simvastatin were not observed when the simvastatin-KLF2 pathway was blocked with GGPP, or when autophagy was blocked with CQ, suggesting that simvastatin requires autophagy to induce KLF2 and confer vasoprotection. To note, endothelial cells preserved in Celsior solution did not show activation of autophagy in response to simvastatin (Fig. 3D), and was associated with no changes in cell viability (data not shown).

Simvastatin reactivates autophagic flux through Rab7 upregulation

Endothelial cells that underwent cold storage in UWS displayed lower levels of the autolysosome-formation mediating protein Rab7 in comparison to those cells stored in Celsior. Such decrease in Rab7 was prevented administering statins prior to cold ischemia (Fig. 4A and Supplementary Fig. 2).

Similarly, HUVEC and LSEC cultured under standard conditions and treated for 24 h with simvastatin exhibited significantly increased protein levels of Rab7 in comparison to vehicle-treated cells (Fig. 4B). This effect, together with activation of KLF2, was at least in part dependent on the small GTPase Rac1. Indeed, treatment of LSEC and HUVEC with the Rac1 inhibitor NSC23766 significantly upregulated Rab7, the KLF2 protective pathway (measured as KLF2 and its target gene eNOS), and autophagic flux (Fig. 5 and Supplementary Fig. 3).

A more detailed analysis of Rab7 upregulation in response to simvastatin revealed that statins do not promote *Rab7* transcription, measured as mRNA expression, nor inhibit its protein degradation, since Rab7 protein levels still increased in the presence of protease inhibitors (Supplementary Fig. 4). These data suggest that statins modulate Rab7 availability at its translational level.

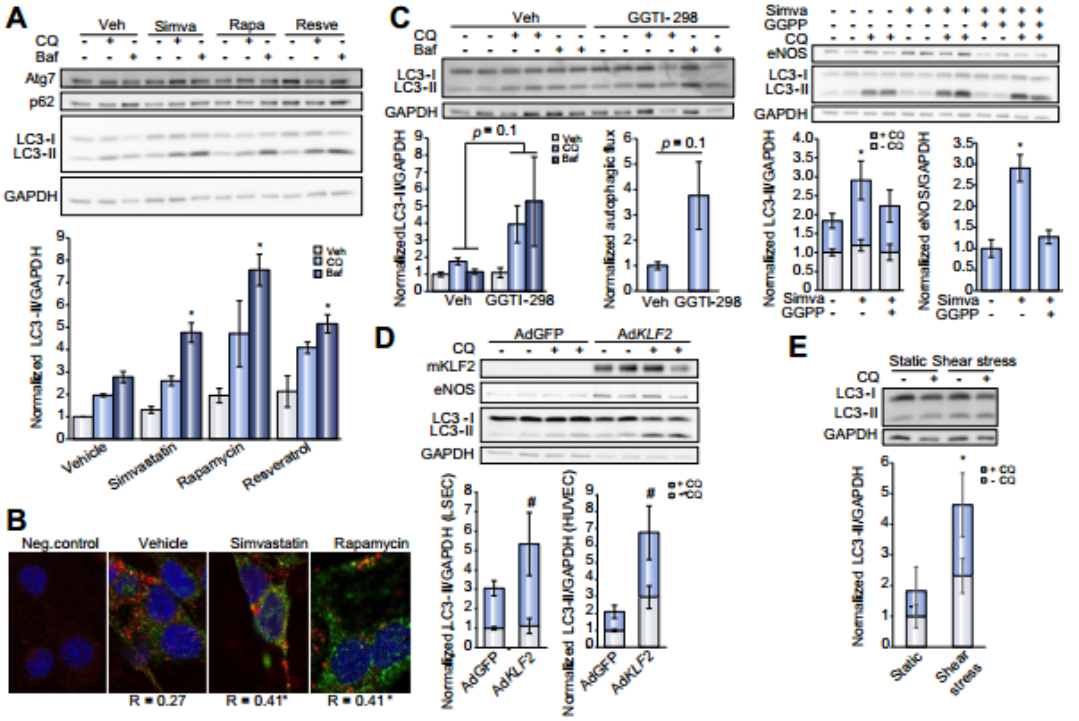

Fig. 1. KLF2 upregulates autophagy in the endothelium. (A) Protein expression of autophagy markers Atg7, p62 and LC3-II in primary liver sinusoidal endothelial cells (LSEC) treated with different vasoprotective drugs. The LC3 turnover is represented in the graph below (CQ: chloroquine, Baf: bafilomycin). (B) Representative images of autophagosomes (LC3, green) with lysosomes (Lamp2, red) colocalization in LSEC. Quantification of colocalization (R value representing autophagy) derives from n = 60–80 cells per condition from n = 3 independent experiments. (C) Autophagic flux in response to KLF2 modulators. Left, GGTI-298 as KLF2 inducer. Right, GGPP as KLF2 repressor. (D) Autophagic flux in response to genetic upregulation of KLF2 (mKLF2: transfected mouse KLF2) in LSEC and HUVEC. (E) Autophagic flux in HUVEC cultured under static conditions or biomechanical shear stress stimulation. *$p < 0.05$ *vs.* its corresponding control; #$p < 0.05$ *vs.* AdGFP.

Autophagy mediates the protective effects of simvastatin in livers undergoing I/R

Fig. 6 shows that livers undergoing UWS cold storage and warm reperfusion displayed marked accumulation of autophagosomes, both in the endothelium and in hepatocytes, that was accompanied by the development of acute microcirculatory dysfunction (Fig. 7). These detrimental effects of I/R were not observed in rats that received simvastatin prior to cold ischemia, which in fact exhibited increased autophagosome clearance and improved microcirculatory relaxation in response to acetylcholine. Importantly, pharmacological inhibition of hepatic autophagy using CQ completely abrogated the beneficial effects of simvastatin.

To denote, CQ had no effect in vehicle-treated animals, therefore suggesting that CQ specifically affected autophagy (which was indeed downregulated due to cold storage and warm reperfusion) and did not impair microcirculation independently of simvastatin action. Please find additional transmission electron microscopy (TEM) images at different magnifications in Supplementary Fig. 5.

Discussion

Different studies have recently reported that autophagy is inducible by simvastatin or resveratrol [18–20]. These drugs, in addition, are known to strongly activate KLF2 [14,29], a vasoprotective transcription factor determinant in the state and phenotype of the endothelium. Considering this background, we herein aimed to determine the possible link between KLF2 and autophagy in the unique liver sinusoidal endothelium. Interestingly, treatment of LSEC with pharmacological activators of KLF2 increased autophagic flux, demonstrated via two well-accepted techniques, which are the LC3 turnover assay using two different autophagy inhibitors (CQ and Baf) and the colocalization of autophagosomes with lysosomes using confocal microscopy. Moreover, precise upregulation of KLF2 using an adenovirus coding for KLF2 or due to biomechanical shear stress stimulation resulted in markedly increased autophagic flux not only in LSEC, but also in not so specialized endothelial cells (HUVEC), altogether demonstrating for the first time that KLF2 is able to activate autophagy. This finding is consistent with other results indicating that targets of

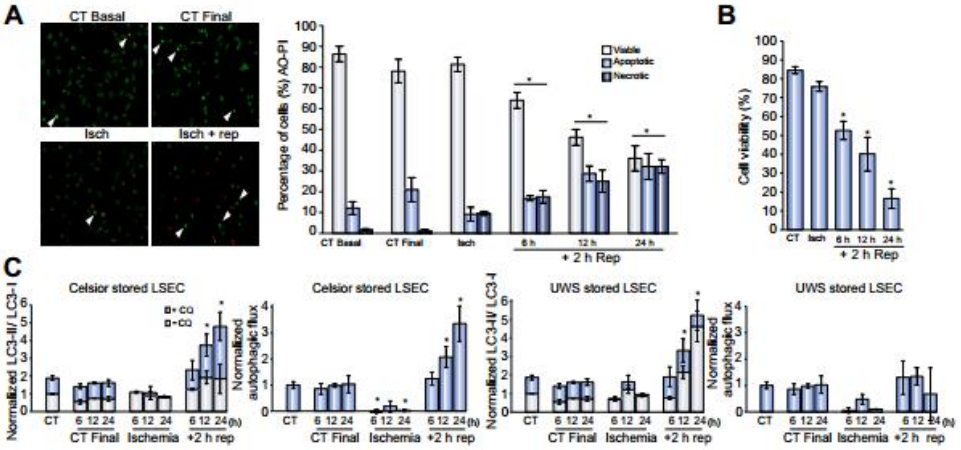

Fig. 2. Characterization of cell death and autophagy in *in vitro* acute liver injury. (A) Evaluation of cell death by double staining with acridine orange & propidium iodide in liver sinusoidal endothelial cells (LSEC) freshly isolated (control cells; CT basal), cultured in standard conditions for 24 h (CT final), cold stored for 24 h (Isch), or cold stored for 6 h, 12 h and 24 h and afterwards warm reperfused (Rep). Plain and tenuous green cells where counted as viable, cells with bright green nucleus (arrow heads) were considered apoptotic, and red cells, as necrotic. (B) Cell viability of cells described in A assessed by trypan blue exclusion assay. *p <0.05 *vs.* CT. (C) LC3 protein expression in LSEC described in A using Celsior or University of Wisconsin (UWS), as cold storage solutions. Autophagosomes are represented as white bars. Autophagic flux, i.e., autophagosomes accumulation after inhibition of autophagy with chloroquine (CQ), is represented as light blue bars. *p <0.05 *vs.* CT.

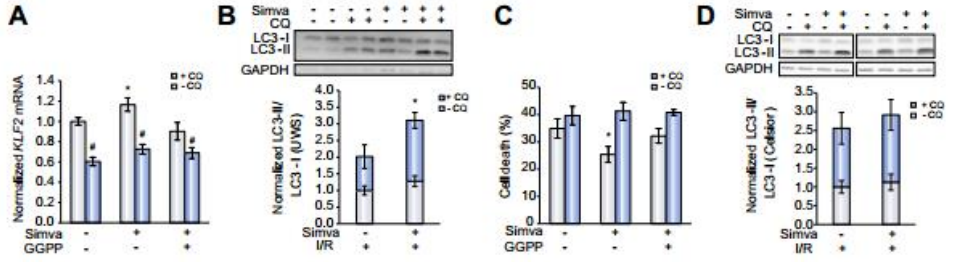

Fig. 3. Simvastatin reactivates the KLF2-autophagy vasoprotective pathway in UWS cold-stored endothelial cells. KLF2 levels (A), autophagic flux (B) and cell death (apoptotic + necrotic cells; C) in UWS cold stored/warm reperfused LSEC pretreated with simvastatin, the KLF2 inhibitor geranylgeranyl-pyrophosphate (GGPP), the autophagy inhibitor CQ, or their corresponding vehicles. (D) Autophagic flux in LSEC cold stored in Celsior solution and warm reperfused. *p <0.05 *vs.* corresponding vehicle; #p <0.05 *vs.* no-CQ.

KLF2 like HO-1 are associated with autophagy activation and liver protection [26].

Considering that autophagy is a general survival process that is involved in various types of liver injury and may confer opposite properties (i.e., protective or harmful) [7,30], we specifically characterized the viability status and the possible role of autophagy in endothelial cells suffering acute injury by means of cold ischemia and warm reperfusion. To properly evaluate cell viability, we performed a commonly used and well-described technique as is trypan blue exclusion assay, and a more specific fluorescent staining that allows to differentiate between apoptosis and necrosis (AO-PI) [25,31]. As expected, ischemia *per se* did not affect LSEC viability. However, LSEC survival dramatically decreased upon reperfusion depending on ischemia time, and independent of using Celsior or Wisconsin solutions. Upon reperfusion, cells that were stored in Celsior solution reactivated autophagy in an ischemia time-dependent manner. However, cells stored under UWS exhibited basal accumulation of autophagosomes and were unable to properly reactivate autoghagic flux, suggesting impairment of clearance of autophagosomes. It is intriguing how UWS may inhibit the fusion of autophagosomes and lysosomes, especially since its composition does not reveal known inhibitors of autophagy. However, it is important to denote that beyond its composition, previous studies reported significantly better maintenance of energy status (ATP levels) in cells preserved in UWS than in Celsior [32],

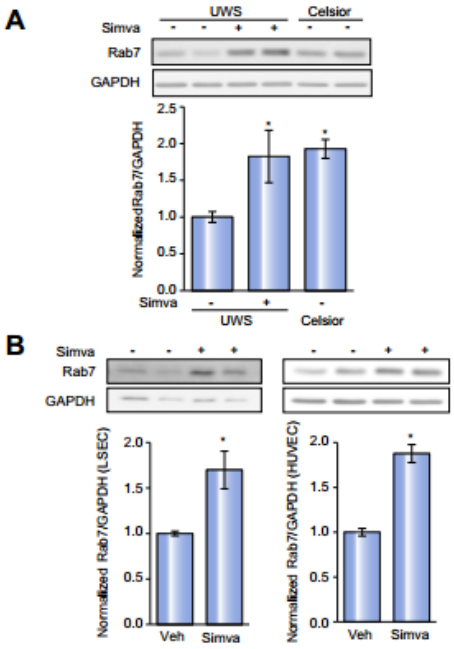

Fig. 4. Simvastatin upregulates Rab7 in endothelial cells. Rab7 protein expression in cold stored/warm reperfused endothelial cells (A), and endothelial cells cultured under standard conditions (B), in response to simvastatin or vehicle. *p <0.05 *vs.* vehicle.

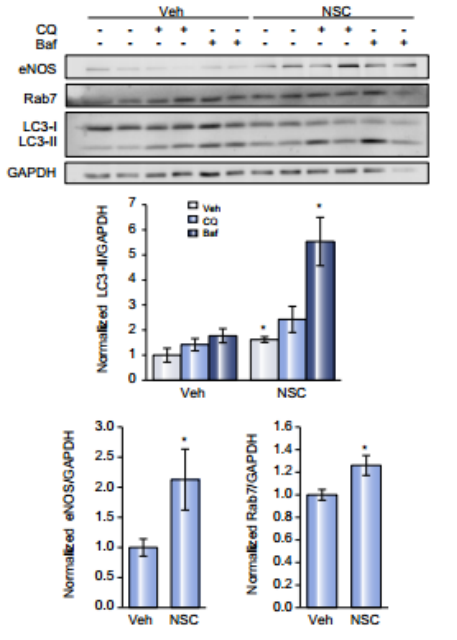

Fig. 5. Inhibition of Rac1 activates the Rab7-autophagy-KLF2 pathway. Protein expression, and relative quantification, of autophagic flux, eNOS (as major KLF2 target gene) and Rab7 in primary LSEC treated for 24 h with the Rac1 inhibitor NSC23766, or its vehicle. *p <0.05 *vs.* vehicle.

which may itself impair autophagic flux. Altogether suggests that UWS protective capability may be further potentiated through the exogenous addition of autophagy activators.

In order to better understand the underlying mechanism for this inhibited formation of autolysosomes, we analyzed the expression of Rab7, a small GTPase responsible for fusion of cellular vesicles that has been reported to mediate the fusion of autophagosomes with lysosomes [33]. These experiments revealed that endothelial cells stored in UWS displayed lower protein levels of Rab7 in comparison to Celsior stored cells.

Considering the above-described inter-relation between KLF2 and autophagy, we next evaluated the possible protective effects of simvastatin in the specific scenario of liver endothelial I/R injury. As expected, simvastatin significantly increased the expression of KLF2 in endothelial cells, which prevented cell damage. It is important to note that the maintenance of cell viability achieved with simvastatin was not observed when LSEC were pretreated with the KLF2 inhibitor GGPP, therefore confirming KLF2-mediated protection. However, when autophagosome-lysosome fusion was blocked using CQ, KLF2 levels and cell viability fell to a threshold level regardless of simvastatin pretreatment, suggesting that autophagy would be upstream of KLF2 in this case. As shear stress is the natural inducer of KLF2, our findings are in agreement with a recent report demonstrating that autophagy is required to transduce shear stress signaling to nitric oxide production [21].

In addition, regarding the underlying molecular mechanism on how KLF2 activators promote cell survival, we herein demonstrate for the first time that simvastatin activates autophagic flux in the cold stored sinusoidal endothelium, ultimately conferring vasoprotection. It is worth noting that this KLF2 activator did not increase autophagosomes, demonstrated by unchanged levels of Atg7 and basal LC3-II, but promoted their fusion with lysosomes probably through upregulation of Rab7. It is intriguing that p62 levels remain stable in response to simvastatin or rapamycin, however our results are in line with previous data demonstrating that p62 protein expression does not always correlate with autophagic flux, as it can be transcriptionally regulated during autophagy and also be degraded through the proteasomal pathway [33]. Accordingly, despite protein levels of p62 being invariant, autophagy activators increased transcription of p62, altogether suggesting enhanced p62 turnover and thus increased autophagic flux.

Importantly, the novel mechanism of protection of simvastatin was also confirmed in HUVEC and LSEC cultured under standard conditions, moreover validated using mevastatin, thus proposing a new pan-endothelial mechanism by which KLF2 activators may exert their vasoprotection.

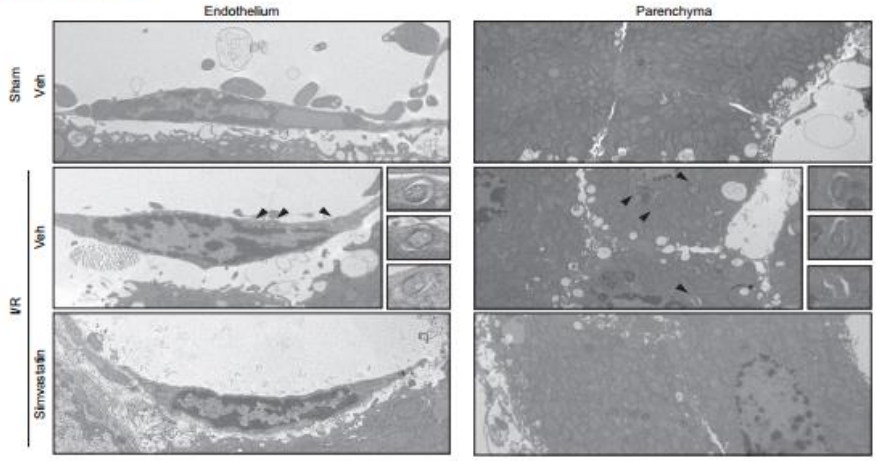

Fig. 6. Simvastatin prevents impairment of autophagosome clearance after I/R in rat livers. Representative TEM images of the endothelium (left panels, 12,000x magnification) and parenchyma (right panels, 6000x magnification) of livers from sham animals, and animals pretreated with simvastatin, or vehicle, and afterwards cold stored and warm reperfused (I/R). Autophagosomes are indicated with arrowheads and amplified on the right side of each image.

To ascertain the molecular link between autophagy activation and KLF2 upregulation, we focused on the GTPase Rac1. In fact, it has been shown that: 1) Rac1 represses autophagy [19], 2) its activity is modulated by geranylgeranylation [34], therefore representing a possible regulator of KLF2 expression, and 3) Rac1 regulates Rab7 protein availability [35]. Considering these data, we assessed whether Rac1 inhibition could have a crucial role in endothelial autophagy. Interestingly, we herein show that specific Rac1 inhibition using NSC23766 was associated with a significant activation of the Rab7-autophagy-KLF2 axis, both in LSEC and HUVEC. Although our results are consistent, it should be noted that previous studies showed opposed effects of statins on autophagy due to the inhibition of Rab11 [36], and that Rab GTPases may also be post-translationally modified by geranylgeranylation [37], so further desirable studies would clarify Rab7 activity and location under these circumstances. Nevertheless, our manuscript adds a significant piece of knowledge regarding the intermediaries involved in the molecular pathway activated by statins and ultimately leading to KLF2 expression. From the current studies it is clear that Rac1 should be now considered as the protein responsible for GGPP-mediated repression of KLF2 expression, either direct or indirectly, and therefore deserves further investigation.

The relevance of these results was also validated in *in vivo* and *ex vivo* models: Firstly, we confirmed the abrogation of autophagic flux in UWS cold stored livers. Indeed, transmission electron microscopy images revealed that rat livers cold stored using UWS showed marked accumulation of double-membraned structures, both in the sinusoidal endothelium and the parenchyma, compared to control rat livers. An increase in the number of autophagosomes after hepatic I/R in UWS was previously reported by others [8,38], but it was associated with an increase in autophagy. However, in the present study, the use of dynamic techniques to monitor autophagic flux *in vitro* suggests that this increase in autophagosomes after I/R in UWS is caused by a downstream impairment of autophagy also *ex vivo*. This is the reason why we investigated whether the microcirculatory protective effects of statins in the setting of hepatic I/R, previously shown by our group and others [13,16,39], may derive from the reactivation of autophagy. The results of these studies revealed that pretreatment of animals with simvastatin shortly before cold storage activated hepatic autophagic flux (demonstrated by ameliorated autophagosome clearance), leading to improvement of liver microvascular function upon reperfusion (measured as *ex vivo* vasodilatation in response to increasing concentrations of acetylcholine) in comparison to animals receiving vehicle. Moreover, the beneficial effects of simvastatin were dependent on autophagy, as they were not observed when autophagy was effectively blocked in the liver by administering CQ before statin. Aside from the protective effects of autophagy activation by simvastatin in the hepatic microcirculation, we didn't observe any other endothelial protective effects *in vivo*, such as improvement in endothelial cell phenotype (in terms of eNOS and vWF analysis; data not shown), suggesting that reactivation of endothelial autophagy by statins may also have KLF2-independent effects in the hepatic microcirculation, p.e. increased sinusoidal paracrine cross-talk due to rab7-mediated secretion of endothelial autophagic bodies [40–42]. It is also important to note that the *ex vivo* perfusion model used to mimic reperfusion injury reproduces only in part the detrimental effects of this process. Indeed, it lacks blood components such as polymorphonuclear neutrophils and platelets, which may also contribute to LSEC dysfunction and respond to statins.

Finally, and considering previous studies demonstrating simvastatin-mediated KLF2 upregulation in LSEC physiologically stimulated with shear stress [23], we herein propose that activation of autophagy through a simvastatin-KLF2-mediated mechanism may also confer protection in ischemia-independent

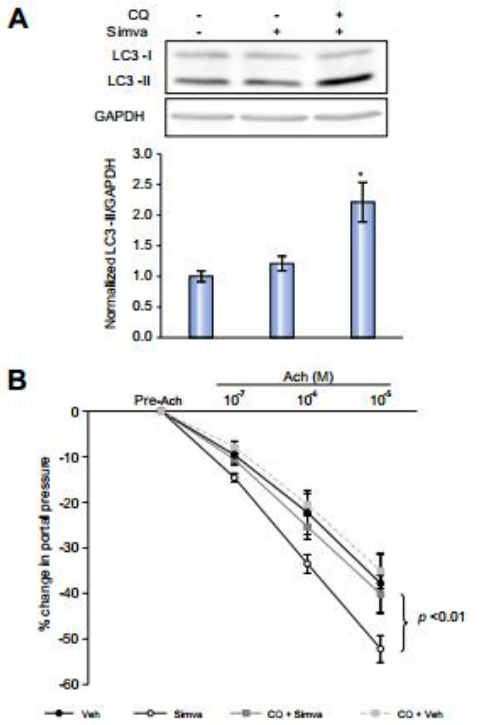

Fig. 7. Autophagy mediates simvastatin-protective effects on microvascular function of rat livers. (A) LC3-II Western blot and quantification in livers from rats pretreated with the autophagy inhibitor chloroquine (CQ), or vehicle, followed by simvastatin, or its vehicle, cold stored for 16 h and warm reperfused. (B) Hepatic microcirculatory function of livers described in A calculated as relaxation in response to increasing doses of acetylcholine (Ach) after pre-constriction with methoxamine. *p <0.05 *vs.* all.

situations, such as chronic liver disease or other types of acute liver injury.

In conclusion, we herein report for the first time the intimate cross-talk between autophagy and the transcription factor KLF2 in the endothelium. KLF2 *per se* is able to activate autophagy, but in an acute liver injury situation as is I/R, simvastatin would maintain proper autophagic flux through a Rac1-Rab7 pathway, which in turn would maintain KLF2 levels, ultimately conferring endothelial, microvascular and parenchymal protection. Our results help understanding the molecular mechanisms of statin-mediated vasoprotection and developing new therapeutic strategies for the treatment of hepatic and extrahepatic vascular diseases.

Financial support

This work was funded by the Ministerio de Economía y Competitividad – Instituto de Salud Carlos III, FIS (PI14/00029 and PI13/00341), and the European Union (Fondos FEDER, "una manera de hacer Europa"). SG-M has a Fellowship from the Fundació Catalana de Trasplantament. JG-S has a Ramón y Cajal contract from the Ministerio de Economía y Competitividad. CIBEREHD is funded by the Instituto de Salud Carlos III.

Conflict of interest

The authors who have taken part in this study declared that they do not have anything to disclose regarding funding or conflict of interest with respect to this manuscript.

Authors' contributions

S.G.-M. designed the research, conceived ideas, performed experiments, and wrote the manuscript. F.C.dM. and S.V. performed experiments and analyzed data. V.H.-G., C.P. and J.C.G.-P. critically revised the manuscript. J.B. critically revised the manuscript and obtained funding. JG-S. designed the research, conceived ideas, wrote the manuscript, obtained funding and directed the study. All authors edited and reviewed the final manuscript.

Acknowledgments

Authors are indebted to Diana Hide for her expert help in electron microscopy, and Martí Ortega-Ribera and Jose Yeste for their expertise in O_2 measurements.

Supplementary data

Supplementary data associated with this article can be found, in the online version, at http://dx.doi.org/10.1016/j.jhep.2016.07.051.

References

Author names in bold designate shared co-first authorship

[1] Tanida I. Autophagosome formation and molecular mechanism of autophagy. Antioxid Redox Signal 2011;14:2201–2214.
[2] Nikoletopoulou V, Markaki M, Palikaras K, Tavernarakis N. Crosstalk between apoptosis, necrosis and autophagy. Biochim Biophys Acta 2013;1833:3448–3459.
[3] Egan DF, Shackelford DB, Mihaylova MM, Gelino S, Kohnz RA, Mair W, et al. Phosphorylation of ULK1 (hATG1) by AMP-activated protein kinase connects energy sensing to mitophagy. Science 2011;331:456–461.
[4] Kim J, Kim YC, Fang C, Russell RC, Kim JH, Fan W, et al. Differential regulation of distinct Vps34 complexes by AMPK in nutrient stress and autophagy. Cell 2013;152:290–303.
[5] Amir M, Czaja MJ. Autophagy in nonalcoholic steatohepatitis. Expert Rev Gastroenterol Hepatol 2011;5:159–166.
[6] Schneider JL, Cuervo AM. Liver autophagy: much more than just taking out the trash. Nat Rev Gastroenterol Hepatol 2014;11:187–200.
[7] Gracia-Sancho J, Guixe-Muntet S, Hide D, Bosch J. Modulation of autophagy for the treatment of liver diseases. Expert Opin Investig Drugs 2014;23:967–977.
[8] Gotoh K, Lu Z, Morita M, Shibata M, Koike M, Waguri S, et al. Participation of autophagy in the initiation of graft dysfunction after rat liver transplantation. Autophagy 2009;5:351–360.
[9] Minor T, Stegemann J, Hirner A, Koetting M. Impaired autophagic clearance after cold preservation of fatty livers correlates with tissue necrosis upon

reperfusion and is reversed by hypothermic reconditioning. Liver Transpl 2009;15:798–805.
[10] Wang JH, Ahn IS, Fischer TD, Byeon JI, Dunn Jr WA, Behrns KE, et al. Autophagy suppresses age-dependent ischemia and reperfusion injury in livers of mice. Gastroenterology 2011;141:2188–2199.
[11] Cursio R, Colosetti P, Gugenheim J. Autophagy and liver ischemia-reperfusion injury. Biomed Res Int 2015;2015:417590.
[12] Gracia-Sancho J, Villarreal Jr G, Zhang Y, Yu JX, Liu Y, Tullius SG, et al. Flow cessation triggers endothelial dysfunction during organ cold storage conditions: strategies for pharmacologic intervention. Transplantation 2010;90:142–149.
[13] **Russo L, Gracia-Sancho J**, Garcia-Caldero H, Marrone G, Garcia-Pagan JC, Garcia-Cardena G, et al. Addition of simvastatin to cold storage solution prevents endothelial dysfunction in explanted rat livers. Hepatology 2012;55:921–930.
[14] Parmar KM, Nambudiri V, Dai G, Larman HB, Gimbrone Jr MA, Garcia-Cardena G. Statins exert endothelial atheroprotective effects via the KLF2 transcription factor. J Biol Chem 2005;280:26714–26719.
[15] **Sen-Banerjee S, Mir S**, Lin Z, Hamik A, Atkins GB, Das H, et al. Kruppel-like factor 2 as a novel mediator of statin effects in endothelial cells. Circulation 2005;112:720–726.
[16] Gracia-Sancho J, Garcia-Caldero H, Hide D, Marrone G, Guixe-Muntet S, Peralta C, et al. Simvastatin maintains function and viability of steatotic rat livers procured for transplantation. J Hepatol 2013;58:1140–1146.
[17] La Mura V, Pasarin M, Meireles CZ, Miquel R, Rodriguez-Vilarupla A, Hide D, et al. Effects of simvastatin administration on rodents with lipopolysaccharide-induced liver microvascular dysfunction. Hepatology 2013;57:1172–1181.
[18] Guo H, Chen Y, Liao L, Wu W. Resveratrol protects HUVECs from oxidized-LDL induced oxidative damage by autophagy upregulation via the AMPK/SIRT1 pathway. Cardiovasc Drugs Ther 2013;27:189–198.
[19] Wei YM, Li X, Xu M, Abais JM, Chen Y, Riebling CR, et al. Enhancement of autophagy by simvastatin through inhibition of Rac1-mTOR signaling pathway in coronary arterial myocytes. Cell Physiol Biochem 2013;31:925–937.
[20] Andres AM, Hernandez G, Lee P, Huang C, Ratliff EP, Sin J, et al. Mitophagy is required for acute cardioprotection by simvastatin. Antioxid Redox Signal 2014;21:1960–1973.
[21] Bharath LP, Mueller R, Li Y, Ruan T, Kunz D, Goodrich R, et al. Impairment of autophagy in endothelial cells prevents shear-stress-induced increases in nitric oxide bioavailability. Can J Physiol Pharmacol 2014;92:605–612.
[22] Gracia-Sancho J, Lavina B, Rodriguez-Vilarrupla A, Garcia-Caldero H, Bosch J, Garcia-Pagan JC. Enhanced vasoconstrictor prostanoid production by sinusoidal endothelial cells increases portal perfusion pressure in cirrhotic rat livers. J Hepatol 2007;47:220–227.
[23] **Marrone G, Russo L**, Rosado E, Hide D, Garcia-Cardena G, Garcia-Pagan JC, et al. The transcription factor KLF2 mediates hepatic endothelial protection and paracrine endothelial-stellate cell deactivation induced by statins. J Hepatol 2013;58:98–103.
[24] Dutting S, Heidenreich J, Cherpokova D, Amin E, Zhang SC, Ahmadian MR, et al. Critical off-target effects of the widely used Rac1 inhibitors NSC23766 and EHT1864 in mouse platelets. J Thromb Haemost 2015;13:827–838.
[25] **Marrone G, Maeso-Diaz R**, Garcia-Cardena G, Garcia-Pagan JC, Bosch J, Gracia-Sancho J. KLF2 exerts anti-fibrotic and vasoprotective effects in cirrhotic rat livers: behind the molecular mechanisms of statins. Gut 2015;64:1434–1443.
[26] Yun N, Cho HI, Lee SM. Impaired autophagy contributes to hepatocellular damage during ischemia/reperfusion: heme oxygenase-1 as a possible regulator. Free Radic Biol Med 2014;68:168–177.
[27] Gupta TK, Toruner M, Chung MK, Groszmann RJ. Endothelial dysfunction and decreased production of nitric oxide in the intrahepatic microcirculation of cirrhotic rats. Hepatology 1998;28:926–931.
[28] McLean AJ, Cogger VC, Chong GC, Warren A, Markus AM, Dahlstrom JE, et al. Age-related pseudocapillarization of the human liver. J Pathol 2003;200:112–117.
[29] **Gracia-Sancho J, Villarreal Jr G**, Zhang Y, Garcia-Cardena G. Activation of SIRT1 by resveratrol induces KLF2 expression conferring an endothelial vasoprotective phenotype. Cardiovasc Res 2010;85:514–519.
[30] Rautou PE, Mansouri A, Lebrec D, Durand F, Valla D, Moreau R. Autophagy in liver diseases. J Hepatol 2010;53:1123–1134.
[31] Foglieni C, Meoni C, Davalli AM. Fluorescent dyes for cell viability: an application on prefixed conditions. Histochem Cell Biol 2001;115:223–229.
[32] Janssen H, Janssen PH, Broelsch CE. UW is superior to Celsior and HTK in the protection of human liver endothelial cells against preservation injury. Liver Transpl 2004;10:1514–1523.
[33] Mizushima N, Yoshimori T, Levine B. Methods in mammalian autophagy research. Cell 2010;140:313–326.
[34] Roberts PJ, Mitin N, Keller PJ, Chenette EJ, Madigan JP, Currin RO, et al. Rho Family GTPase modification and dependence on CAAX motif-signaled posttranslational modification. J Biol Chem 2008;283:25150–25163.
[35] Carroll B, Mohd-Naim N, Maximiano F, Frasa MA, McCormack J, Finelli M, et al. The TBC/RabGAP Armus coordinates Rac1 and Rab7 functions during autophagy. Dev Cell 2013;25:15–28.
[36] Miettinen TP, Bjorklund M. Mevalonate pathway regulates cell size homeostasis and proteostasis through autophagy. Cell Rep 2015;13:2610–2620.
[37] Coxon FP, Ebetino FH, Mules EH, Seabra MC, McKenna CE, Rogers MJ. Phosphonocarboxylate inhibitors of Rab geranylgeranyl transferase disrupt the prenylation and membrane localization of Rab proteins in osteoclasts in vitro and in vivo. Bone 2005;37:349–358.
[38] Lu Z, Dono K, Gotoh K, Shibata M, Koike M, Marubashi S, et al. Participation of autophagy in the degeneration process of rat hepatocytes after transplantation following prolonged cold preservation. Arch Histol Cytol 2005;68:71–80.
[39] Trocha M, Merwid-Lad A, Szuba A, Chlebda E, Piesniewska M, Sozanski T, et al. Effect of simvastatin on nitric oxide synthases (eNOS, iNOS) and arginine and its derivatives (ADMA, SDMA) in ischemia/reperfusion injury in rat liver. Pharmacol Rep 2010;62:343–351.
[40] Nilsson P, Saido TC. Dual roles for autophagy: degradation and secretion of Alzheimer's disease Abeta peptide. Bioessays 2014;36:570–578.
[41] **Baietti MF, Zhang Z, Mortier E**, Melchior A, Degeest G, Geeraerts A, et al. Syndecan-syntenin-ALIX regulates the biogenesis of exosomes. Nat Cell Biol 2012;14:677–685.
[42] **Jae N**, McEwan DG, Manavski Y, Boon RA, Dimmeler S. Rab7a and Rab27b control secretion of endothelial microRNA through extracellular vesicles. FEBS Lett 2015;589:3182–3188.

Pontifícia Universidade Católica do Rio Grande do Sul
Pró-Reitoria Acadêmica
Av. Ipiranga, 6681 - Prédio 1 - 3º. andar
Porto Alegre - RS - Brasil
Fone: (51) 3320-3500 - Fax: (51) 3339-1564
E-mail: proacad@pucrs.br
Site: www.pucrs.br/proacad